LOCKHEED MARTIN ENERGY RESEARCH LIBRARIES

3 4456 0509633 9

ORNL/TM-5446

Cy 3

Biochemical Technology Program Progress Report for the Period January 1–June 30, 1976

OAK RIDGE NATIONAL LABORATORY
CENTRAL RESEARCH LIBRARY
CIRCULATION SECTION
4500N ROOM 175
LIBRARY LOAN COPY
DO NOT TRANSFER TO ANOTHER PERSON.
If you wish someone else to see this report, send in name with report and the library will arrange a loan.
ORNL-118 (6-97)

LIBRARY
REFERENCE COPY

OAK RIDGE NATIONAL LABORATORY
OPERATED BY UNION CARBIDE CORPORATION FOR THE ENERGY RESEARCH AND DEVELOPMENT ADMINISTRATION

Printed in the United States of America. Available from
National Technical Information Service
U.S. Department of Commerce
5285 Port Royal Road, Springfield, Virginia 22161
Price: Printed Copy $7.50; Microfiche $2.25

This report was prepared as an account of work sponsored by the United States Government. Neither the United States nor the Energy Research and Development Administration/United States Nuclear Regulatory Commission, nor any of their employees, nor any of their contractors, subcontractors, or their employees, makes any warranty, express or implied, or assumes any legal liability or responsibility for the accuracy, completeness or usefulness of any information, apparatus, product or process disclosed, or represents that its use would not infringe privately owned rights.

ORNL/TM-5446

Contract No. W-7405-eng-26

CHEMICAL TECHNOLOGY DIVISION

BIOCHEMICAL TECHNOLOGY PROGRAM PROGRESS REPORT FOR THE PERIOD JANUARY 1-JUNE 30, 1976*

Compiled by:

John E. Mrochek, Carl A. Burtis**
and Charles D. Scott

Other Contributors:

Martin L. Bauer†
William D. Bostick
Stanley R. Dinsmore
James L. Fasching††
Richard K. Genung
Wayne F. Johnson†
Dale G. Lakomy§
Norman E. Lee
Roy C. Lovelace
James B. Overton
L. H. Thacker†

---

*Activities of this program are supported by the National Institute of General Medical Sciences, National Aeronautics and Space Administration, National Center for Toxicological Research, National Cancer Institute, and Energy Research and Development Administration.

**Present address: Center for Disease Control, Atlanta, Georgia.

†Instrumentation and Controls Division.

††Visiting scientist, University of Rhode Island, Kingston.

§Present address: University of Rochester, Rochester, New York.

NOTICE This document contains information of a preliminary nature and was prepared primarily for internal use at the Oak Ridge National Laboratory. It is subject to revision or correction and therefore does not represent a final report.

SEPTEMBER 1976

OAK RIDGE NATIONAL LABORATORY
Oak Ridge, Tennessee 37830
operated by
UNION CARBIDE CORPORATION
for the
ENERGY RESEARCH AND DEVELOPMENT ADMINISTRATION

LOCKHEED MARTIN ENERGY RESEARCH LIBRARIES

3 4456 0509633 9

This report is submitted to fulfill the reporting requirements of the Energy Research and Development Administration and interagency agreements:

(1) Joint ERDA-NIH/NIGMS Interagency Agreement 40-95-66, "Advanced Analytical Techniques for the Clinical Laboratory"

(2) Joint ERDA-NIH/NIGMS Interagency Agreement 40-173-69, "Fast Clinical Analyzers"

(3) Joint ERDA-NASA Interagency Agreement 40-259-71, "Development of a Miniaturized Analytical Clinical Laboratory System"

(4) Joint ERDA-FDA-NCTR Interagency Agreement 40-449-73, "Centrifugal Fast Analyzer Systems for Animal Toxicological Studies"

(5) Joint ERDA-NIH/NCI Interagency Agreement NCI-CR-(71)-60, "Chemical Profile of Body Fluids"

CONTENTS

	Page
SUMMARY	vii
1. INTRODUCTION	1
2. CENTRIFUGAL ANALYZER DEVELOPMENT	2
2.1 Evaluation and Utilization in Bioanalytical Laboratories	3
2.1.1 ORNL evaluation	4
2.1.2 NIH evaluation	4
2.1.3 NASA evaluation	11
2.1.4 NCTR evaluation	11
2.1.5 University of Michigan evaluation	13
2.1.6 NIH-2 system	15
2.2 Development of Portable Centrifugal Analyzer	15
2.2.1 Description of system	15
2.2.2 Rapid transfer and mixing	17
2.2.3 Temperature control	25
2.2.4 Evaluation of the portable Centrifugal Fast Analyzer	30
2.2.5 Fabrication of Microprocessor-II	34
2.2.6 Software development	34
2.3 Applications	43
2.3.1 Environmental analysis	43
2.3.2 Development of CFA rotors preloaded with reagent	69
2.3.3 Adaptation of Coombs test	79
2.3.4 Measurement of kinetic parameters	97
2.3.5 Isoenzyme measurement	105
2.3.6 Biochemical markers of cancer - kinetic analysis for serum gamma-glutamyl transpeptidase	119
2.4 References for Section 2	129

Page

3. ADVANCED ANALYTICAL SYSTEMS 135

3.1 High-Resolution Liquid Chromatographic Systems 135

3.1.1 Chromatographic analysis for protein-bound sialic acid 135

3.1.2 Variation in protein-bound carbohydrates with changes in clinical status of breast cancer 137

3.1.3 Development of a liquid chromatographic monitor for optically active substances 139

3.2 Blood Sample Preparation System 145

3.2.1 Summary of experience with original prototype 145

3.2.2 Design and fabrication of new prototype 146

3.3 Automated Elution Electrophoresis 153

3.3.1 Electrophoretic mobility studies 153

3.3.2 Zone elution studies 160

3.3.3 Alternate concepts for automated electrophoresis systems 163

3.3.4 Summary 164

3.4 References for Section 3 169

4. PUBLICATIONS AND ORAL PRESENTATIONS 170

4.1 Publications 170

4.2 Oral Presentations 171

BIOCHEMICAL TECHNOLOGY PROGRAM PROGRESS REPORT FOR THE PERIOD JANUARY 1-JUNE 30, 1976

SUMMARY

Centrifugal Analyzer Development

Five miniature Centrifugal Fast Analyzer (CFA) systems are being routinely operated and/or evaluated in laboratories of the ORNL Health Division; the NASA Johnson Space Center, Houston, Texas; the National Institutes of Health, Bethesda, Maryland; the National Center for Toxicological Research, Jefferson, Arkansas; and the Department of Human Genetics, University of Michigan, Ann Arbor. A sixth CFA system has been completed and was delivered to the Albert Einstein College of Medicine, Bronx, New York, for evaluation in their clinical laboratory. Initial testing of a third-generation CFA with a number of innovative capabilities is currently under way. Innovations include temperature control by means of a heat pump, the ability to monitor chemical or enzymatic reactions within 100 to 150 msec of their initiation, microprocessor control of the analyzer, and mobility and portability with either battery pack or AC power supplies. A state-of-the-art microprocessor based on the Intel 8080 microprocessor chip is included in this prototype, and an extensive software package that includes capabilities for both instrument control and data processing has been developed and tested. Using a new parallel-channel rotor design, transfer of solutions was demonstrated within one revolution (less than 100 msec) on the new prototype system. The development of rotors preloaded with reagents is continuing using reagents in tablet form. A ten-week stability study using tablets for the enzymatic assay of glucose has been successfully completed and a similar study is under way for enzymatic assay of SGOT. A new substrate, L-glutamyl-2-amino-5-nitrobenzoate, has been successfully tested for the assay of gamma-glutamyl transpeptidase. This substrate overcomes low solubility and reagent stability problems associated with L-glutamyl-*p*-nitroaniline, the original substrate used for this assay. Initial tests attempting to adapt the Coombs test for foreign antibodies to the CFA have been partially successful; however, low-level agglutination reactions were not distinguishable from negatives by light transmission.

Advanced Analytical Techniques

High-resolution liquid chromatographic analyses for protein-bound carbohydrates and their evaluation as potential biochemical markers of breast cancer are continuing. An assay was developed and tested for protein-bound *n*-acetylneuraminic (sialic) acid. Assay of protein-bound fucose, mannose, galactose, and sialic acid in sera from patients whose malignancy was categorized clinically as either stable, responsive, or progressive revealed that variations in fucose reflected patient status in every case; i.e., decreases were observed for responsive disease,

increases for progressive disease, and little change was noted for patients with stable disease.

A new concept for a liquid chromatographic monitor based on the detection of optical activity was designed and tested. Initial testing on a mocked-up detector demonstrated the feasibility of the concept which employs plane-polarized ultraviolet light. Sensitivity to 0.003 M sugar solutions was demonstrated in a pathlength of 1 cm.

An epoxy resin formulation, resistant to organic solutions, was fabricated into a 30-chamber rotor for use on the automated blood sample preparation system. Evaluation of this rotor is currently under way. Testing of hemolysates, prepared using the second-generation 16-place rotor by means of acrylamide gel and starch gel electrophoresis, revealed no significant differences between samples taken directly from the system and those that had undergone an additional high-speed centrifugation.

Fundamental studies are continuing on the use of elution electrophoresis as an analytical tool for the separation of proteins. Peak dispersion was shown to be strongly dependent on the type of packing material used. Dye studies revealed that backmixing at the column exit was excessive and contributed greatly to low resolution. Design changes to minimize this problem while retaining a high conductive path are under consideration. The use of a gel plug was tried with some success; however, gel casting would contribute to system complexity.

1. INTRODUCTION

This is the fourth in a series of semiannual progress reports which will cover the development of programs funded at the Oak Ridge National Laboratory by the National Institute of General Medical Sciences (NIGMS), National Aeronautics and Space Administration (NASA), National Center for Toxicological Research (NCTR), National Cancer Institute (NCI), and Energy Research and Development Administration (ERDA). In general, these reports will simply document basic experimental results. However, topical reports and open-literature publications will be used to further correlate these results and to present conclusions based on them.

This document, which covers the period January 1-June 30, 1976, describes progress in the following areas: (1) Advanced Analytical Techniques for the Clinical Laboratory, (2) Fast Clinical Analyzers, (3) Development of a Miniaturized Analytical Clinical Laboratory System, (4) Centrifugal Fast Analyzers for Animal Toxicological Studies, and (5) Chemical Profile of Body Fluids.

2. CENTRIFUGAL ANALYZER DEVELOPMENT

C. A. Burtis,* M. L. Bauer,** W. D. Bostick, J. L. Fasching,†
R. K. Genung, W. F. Johnson,** D. G. Lakomy,†† N. E. Lee,
J. E. Mrochek, C. D. Scott, J. B. Overton, and R. C. Lovelace

A continued developmental effort at the Oak Ridge National Laboratory has demonstrated that the Centrifugal Fast Analyzer (CFA) is a sophisticated and versatile analytical tool that has broad utility in a variety of analytical situations. Because of these significant qualities, this effort has received funding from many agencies, including the Energy Research and Development Administration (ERDA), the U.S. Environmental Protection Agency (EPA), the National Aeronautics and Space Administration (NASA), the National Center for Toxicological Research (NCTR), the National Cancer Institute (NCI), and the National Institute of General Medical Sciences (NIGMS).

During this report period, the development of both miniature and portable centrifugal systems has continued. To expose such systems to a variety of laboratory situations, prototypes are being evaluated in laboratories in the following locations: Oak Ridge, Tennessee; Houston, Texas; Bethesda, Maryland; Jefferson, Arkansas; and Ann Arbor, Michigan. An additional system has been fabricated and tested; it will be evaluated in the clinical laboratory of the Albert Einstein College of Medicine, Bronx, New York. Fabrication of a third-generation prototype of the portable CFA

---

*Present address: Center for Disease Control, Atlanta, Georgia.

**Instrumentation and Controls Division.

†Visiting scientist, University of Rhode Island, Kingston.

††Present address: University of Rochester, Rochester, New York.

is nearing completion, and several of its components have been individually tested. A state-of-the-art microprocessor is included in this prototype, and an extensive software package that contains routines for both control and data processing has been developed for use with it. This system will be assessed for possible use in on-site water analysis as well as for blood grouping.

A varied applications program has continued in the general areas of chemistry, immunology, hematology, and environmental analysis. In addition, Centrifugal Fast Analyzers are being utilized in various programs involving the study of potential biochemical markers for cancer and genetic screening. Development of a rotor that contains preloaded reagents and is capable of receiving, processing, and analyzing the constituents of a whole-blood sample is continuing.

2.1 Evaluation and Utilization in Bioanalytical Laboratories

As part of a program to appraise the performance and broaden the utility of analytical systems which have a miniature CFA as their basic component, several prototype systems have been fabricated and are being routinely used and evaluated in a variety of analytical situations. These include laboratories of the ORNL Health Division; the NASA Johnson Space Center, Houston, Texas; the National Institutes of Health (NIH), Bethesda, Maryland; the National Center for Toxicological Research, Jefferson, Arkansas; and the Department of Human Genetics, University of Michigan, Ann Arbor. An additional system has been fabricated and will be evaluated in the clinical laboratory of Albert Einstein College of Medicine, Bronx, New York.

2.1.1 ORNL evaluation

A miniature analytical system was installed in the clinical laboratory of the ORNL Health Division on April 1, 1973. After an initial evaluation, this system has been utilized to routinely analyze the samples that are obtained from ORNL employees during their periodic physical examinations. During the last three years, approximately 100,000 assays have been performed. The performance of this analytical system has been excellent; very little downtime has been experienced with it. As a result of the evaporation study[1] that indicated minimal evaporation occurred when Micro-Tube sample cups were used, consideration is being given to modifying the system's sample-reagent loader to utilize these cups.

2.1.2 NIH evaluation

A complete analytical system was installed in the clinical laboratory of the NIH, Bethesda, Maryland, on June 20, 1974. After an initial assessment by both NIH and ORNL personnel, the system was utilized to determine the blood groups (A, B, AB, O, Rh) of more than 300 NIH patients. Two manuscripts, describing the concept, system, and evaluation, are being prepared in a joint effort by NIH and ORNL personnel.

On February 6, 1976, the analyzer from the NIH system was returned to Oak Ridge for the installation of a multipurpose optical system which will provide it with transmittance, fluorescence, chemiluminescence, and light scattering measurement capabilities.[2] The multiple-purpose optical system (Fig. 2.1) consists of the following components:

Light sources. Two light sources are used. One is the quartz-iodine-tungsten light that was an original component and is located in a movable housing mounted above the rotor. The second is external and

PHOTO 0724-76

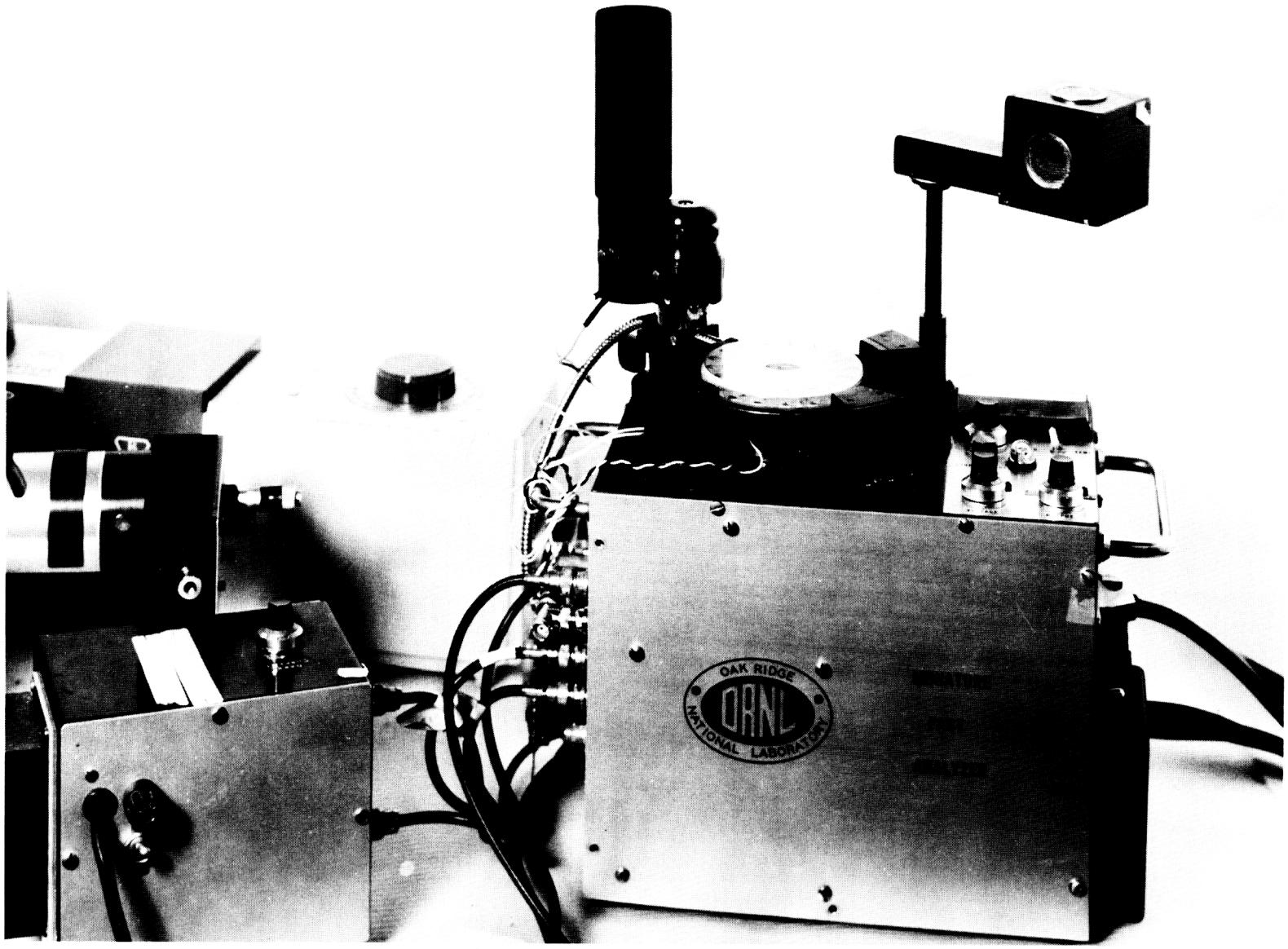

Fig. 2.1. Photograph of the multipurpose optical system.

consists of a 200-W xenon-mercury lamp coupled with a small monochromator and a stabilized dc power supply (Schoeffel Instrument Co., Westwood, New Jersey 07675).

Optical path. The optical output from the tungsten source is focused downward through the rotating cuvets in a 180° orientation. As shown in Fig. 2.2, the monochromatic output from the xenon source is directed in a 90° orientation via a quartz optical fiber bundle (Schott Optical Glass, Inc., Duryea, Pennsylvania 18642).

Filters. The output from the tungsten lamp as it exits from the cuvet is filtered using either interference or narrow bandpass filters (Ditric Optics, Inc., Marlboro, Massachusetts 01752). Additionally, in the fluorescence or chemiluminescence mode, the emitted light is isolated by the use of these filters.

Photodetector. The multipurpose optical system utilizes the same photomultiplier tube (Type HTV R-300, Hamamatsu Corp., Lake Success, New York 11040) as did the original analyzer. The multipurpose optical system, in the fluorescence mode, requires a 100-fold amplification of the output from the photomultiplier tube before it is processed by the on-line data system. This is obtained by means of an external switch.

Rotors. Both clear-body and quartz-insert rotors[2] will be provided with the multipurpose optical system.

Prior to receipt of the NIH analyzer for retrofitting of its multipurpose optical system, the conceptual design was separately evaluated on one of the earlier prototype analyzers. A Bausch and Lomb tungsten source with a slit width of 2 mm was used for the excitation of fluorescein at 490 nm (grating monochromator). The emission was measured using two

PHOTO 0723-76

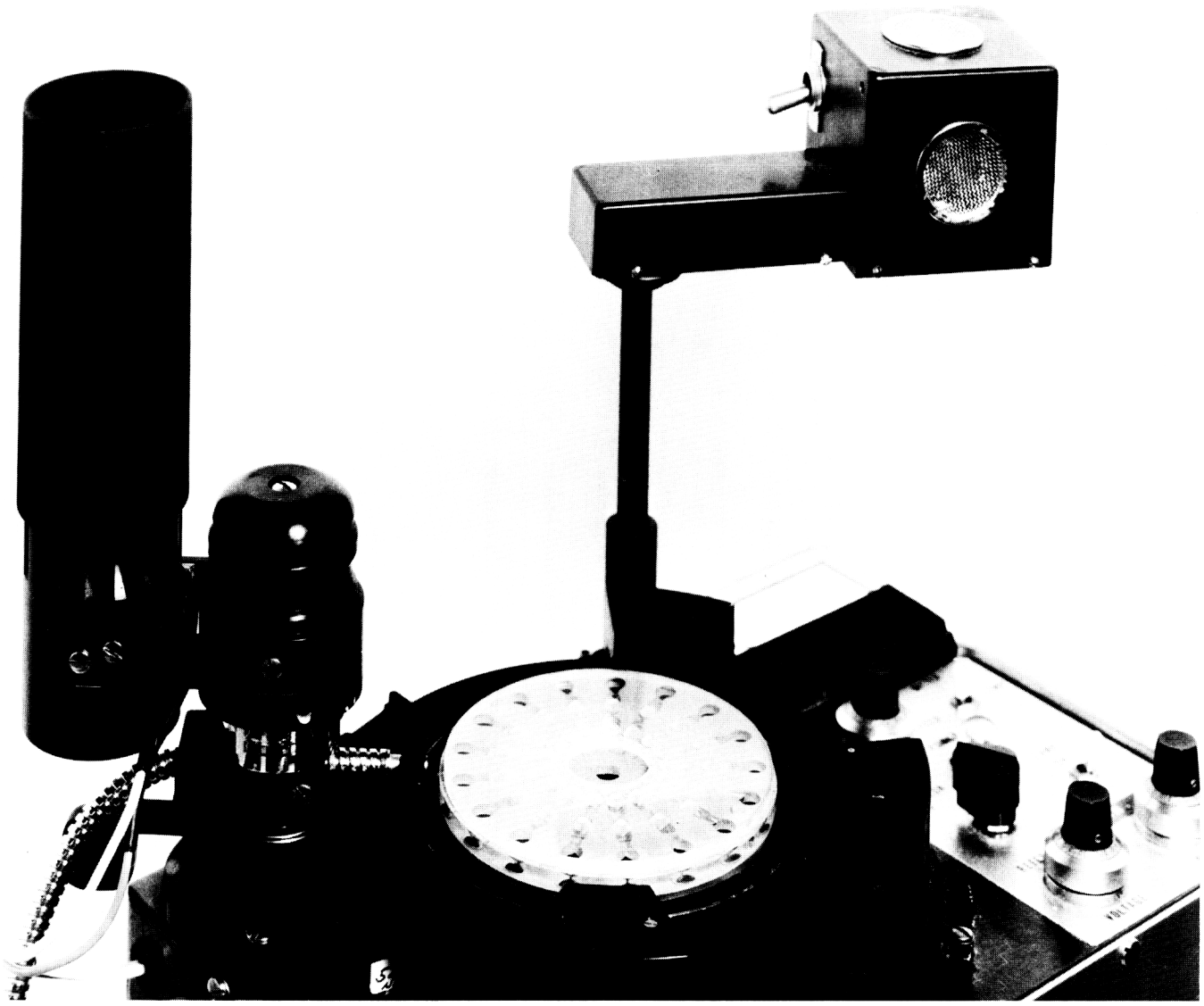

Fig. 2.2. The multipurpose optical system shown with the fiber optical bundle directing the excitation source in the 90° orientation.

filters: (1) a narrow bandpass interference filter (520 nm peak transmission, 8.2 nm half bandwidth), and (2) a 520-nm "cut-on" filter (approximately 1% transmission at 490 nm, >50% transmission for λ >520 nm). A clear-body rotor design was employed. The data obtained for the fluorescence intensity vs fluorescein concentration are linear for either filter; however, there is a larger positive intercept for the cut-on filter due to the greater amount of scattered incident radiation passed (Fig. 2.3).

In Fig. 2.4, a 200-W xenon-mercury source coupled with a small monochromator and a stabilized dc power supply (Schoeffel Instrument Co., Westwood, New Jersey) was employed to excite the fluorescence of a 4-methylumbelliferone at 360 nm. The relative fluorescence intensity was identical (λem = 440 nm) for both the clear-body and quartz-insert rotor designs. The sensitivity for the fluorimetric determination of 4-methylumbelliferone with the present configuration is estimated at approximately 1.4×10^{-7} M, compared to approximately 0.3×10^{-7} M for the original multiple-purpose optical system under similar conditions. Further optimization of the orientation of the fiber optic bundle and lens assembly with respect to the photomultiplier aperture of the analyzer may improve the sensitivity of the retro-fit assembly.

A lens assembly is employed with the secondary emission filter, as previously described (see Ref. 2). With the lens, a gain in intensity of approximately tenfold is realized. The lens assembly has also been of value in transmission measurements. The additional signal intensity permits operation of the analyzer with decreased electrical gain (and thus decreased noise) in spectral regions where the sensitivity of the photomultiplier tube (PMT) is limited. In addition, since the lens focuses to the center

ORNL DWG. 76-242R1

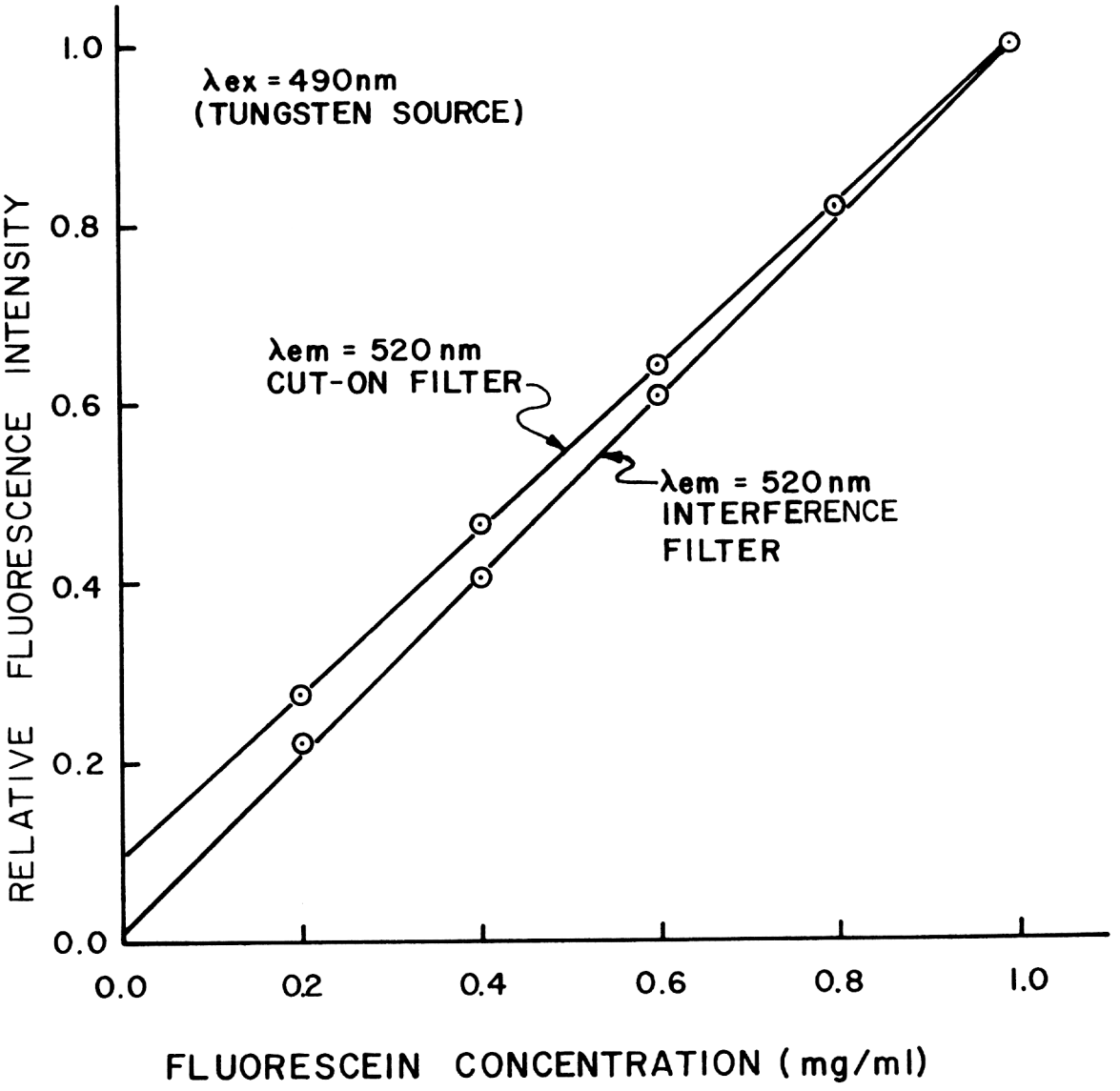

Fig. 2.3. Evaluation of the multipurpose optical system installed on the NIH analyzer: Fluorescence intensity as a function of fluorescein concentration.

ORNL DWG. 76-241

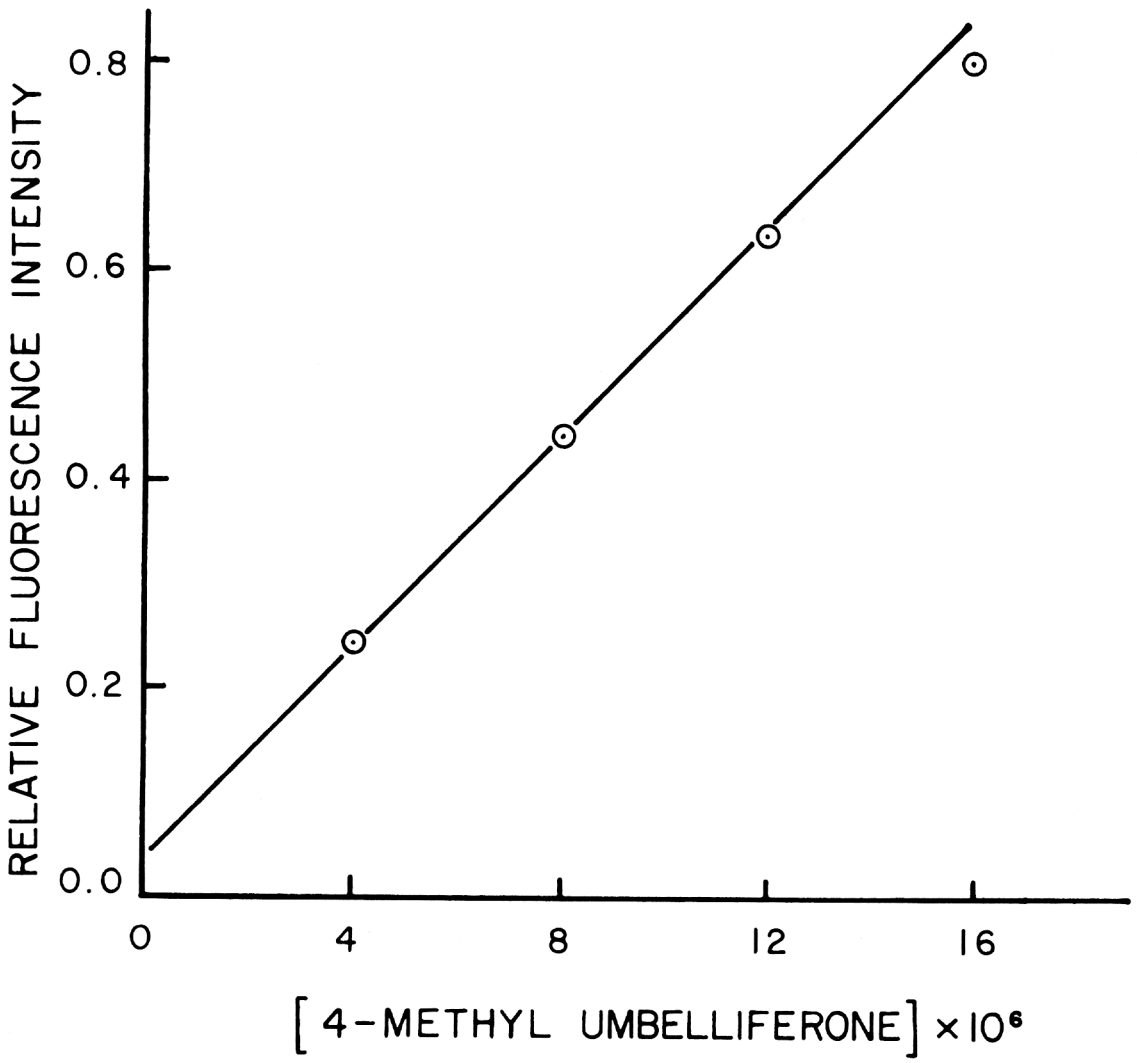

Fig. 2.4. Evaluation of multipurpose optical system installed on the NIH analyzer: Fluorescence intensity as a function of 4-methylumbelliferone concentration.

of the cuvet, inhomogeneities in the baseplate and the rotor windows are decreased. For example, a rotor that has been used extensively for Coombs testing was found to calibrate at 620 nm with a cuvet-to-cuvet variation of 0.98% (PMT voltage = 365 V) using the lens assembly compared to a variation of 6.52% (PMT voltage = 450 V) without the lens.

2.1.3 NASA evaluation

An analytical system has been undergoing evaluation in the clinical laboratory of the NASA Johnson Space Center, Houston, Texas, since February 1, 1973. In April 1975 this system was further updated by the delivery and installation of a computerized data system.

Two types of evaluation are being performed with the NASA system. In one, the results of clinical assays obtained from the miniature analyzer were compared with those obtained from conventional clinical analyzers or ion-specific electrodes. In the other, the system is undergoing evaluation as an on-board analyzer in the forthcoming flights of the Space Shuttle. In September 1974 it performed satisfactorily in a certified verification test (CVT) at Houston (Fig. 2.5). A second CVT was conducted at the Marshall Space Center, Huntsville, Alabama, during the week of August 11-15, 1975. A third CVT was conducted during January 1976 at the Manned Space Center at Houston. In this CVT, rotors preloaded with glucose tablets (see Sect. 2.3.2) were used and evaluated by NASA personnel. Both the performance of the system and the results obtained under the conditions of the test were quite satisfactory.

2.1.4 NCTR evaluation

One of the major objectives of the National Center for Toxicological Research, Jefferson, Arkansas, is the development of techniques and methods

NASA
S- 74- 31319

Fig. 2.5. The miniature Centrifugal Fast Analyzer system as it was used in a Space Shuttle mockup test conducted at the NASA Johnson Space Center in September 1974.

to determine the detrimental biological effects induced by various chemicals and other types of environmental insults to genetically defined mice. Since small animals will often be used as model test systems, assays that require very small quantities of sample are imperative. Obviously, the analytical system should also be highly automated and require a limited amount of sample preparation. The development of the miniature CFA has resulted in an analyzer that meets the requirements of the NCTR situation. Consequently, a collaborative program has been initiated with NCTR in which a miniature CFA system will be evaluated in the NCTR laboratory. The system, which has been fabricated and installed in the NCTR laboratory in Jefferson, Arkansas, consists of the following: (1) two miniature analyzers (NCTR-1, which will operate at 30°C, and NCTR-2, which will operate at either 30° or 37°C, (2) two automated sample-reagent loaders (modified to use microsample cups), (3) two rotor-cleaning stations, (4) 50 rotors, and (5) a computer.

After an initial evaluation at NCTR, 27 different enzyme assays were adapted and optimized for use with this system. These enzyme assays plus 23 additional ones that are currently being developed are listed in Tables 2.1 and 2.2, respectively. During this report period, a procedure that provides for enzyme activity to be expressed as activity per milligrams of protein or hemoglobin was developed and placed into routine use. In addition, one of the analyzers (NCTR-2) was returned to Oak Ridge and modified by the addition of a multipurpose optical system (see Sect. 2.1.2).

2.1.5 University of Michigan evaluation

An analytical system was delivered and installed during the week of September 29, 1975, in the laboratory of the Department of Human Genetics

Table 2.1. List of enzymes which are routinely assayed with the NCTR miniature Centrifugal Fast Analyzer

1.	Malic dehydrogenase	14.	Isocitrate dehydrogenase
2.	Glutathione reductase	15.	Sorbitol dehydrogenase
3.	Glutamic-pyruvate transaminase	16.	Creatine phosphokinase
4.	Glutamic-oxalacetic transaminase	17.	Fatty acid synthetase
		18.	Adenylate kinase
5.	Adenosine triphosphatase	19.	UDP glucose epimerase
6.	Alcohol dehydrogenase	20.	Glucokinase
7.	Serine dehydratase	21.	Hexokinase
8.	Malic enzyme	22.	Glucose 6-P dehydrogenase
9.	Fructose diphosphatase	23.	6-P gluconate dehydrogenase
10.	Lactic dehydrogenase	24.	Cytochrome C reductase
11.	Pyruvate kinase	25.	B galactosidase
12.	Alcolase-FIP	26.	B glucuronidase
13.	Aldolase-FDP	27.	Catalase

Table 2.2. Enzymes for which assays are being adapted and optimized for use with the NCTR Centrifugal Fast Analyzer

1.	Glutathione peroxidase	12.	Phosphoglucomutase
2.	Indophenol oxidase	13.	Galactose 6-P dehydrogenase
3.	Glycerol kinase	14.	Glucuronyl transferase
4.	Serine-pyruvate transaminase	15.	Adenosine deaminase
5.	Glycerol dehydrogenase	16.	Galactose 1-P uridyl transferase
6.	Hydroxy butyric dehydrogenase	17.	Galactokinase
7.	Glucose phosphate isomerase	18.	Triosephosphate isomerase
8.	Glyceraldehyde phosphate dehydrogenase	19.	Glyoxalase I
		20.	Glyoxalase II
9.	Phosphoglucerate kinase	21.	Transulferase
10.	Monophosphoglyceromutase	22.	Acetyl choline esterase
11.	Enolase	23.	Diphosphoglyceromutase

at the University of Michigan. After a period of familiarization and evaluation, the system is being used to develop procedures which will enable isoenzymes to be measured. Currently, the enzyme malic dehydrogenase and its isoenzymes are being studied. In November 1975, a computer program that has been developed for use with an isoenzyme stripping routine (see Sect. 2.3.5) was supplied for use with the Michigan system.

2.1.6 NIH-2 system

A second analytical system has been fabricated using funds provided by the National Institute of General Medical Sciences (NIGMS). It will be used in the Department of Laboratory Medicine at the Albert Einstein College of Medicine. The system has been evaluated by ORNL personnel and was delivered to the New York site on June 28, 1976.

2.2 Development of Portable Centrifugal Analyzer

During this report period, the majority of the subsystems of the third-generation prototype of the portable CFA have been evaluated as parts of the overall system. Extensive software development has permitted operation of the system under control of the microprocessor, and this has permitted the initial testing of the system's rapid transfer and mixing capabilities.

2.2.1 Description of system

A prototype of the portable Centrifugal Fast Analyzer is being developed which incorporates both the analytical, data reduction, and analyzer control modules all in one 14" x 14" x 8" package (Fig. 2.6). This prototype has the capability of performing transmission, light-scatter,

Fig. 2.6. Prototype of the portable Centrifugal Fast Analyzer.

or luminescence measurements all in the same rotor. It utilizes a unique clutch-brake and flywheel mechanism (Fig. 2.7) to rapidly accelerate the rotor to 4000 rpm from a rest position. With a properly designed rotor, this rapid acceleration transfers and mixes the samples and reagents and allows the first data points to be obtained within the first 135 msec of the reaction.

The majority of the subsystems of this prototype have been fabricated and are currently being tested as a part of the larger analyzer system. During this developmental phase, a teletype has been interfaced to the data-reduction and analyzer-control module of the analyzer to allow program optimization and debugging. This also provides communication with the analyzer while the printer interface is being checked.

Most of the parts of the analyzer are operational, but development work remains to be done on the rotor temperature control system and a check-out must be performed on the filter bar drive and printer systems. Some additional power supply isolation is also required in the analog circuit, which consists of the photomultiplier preamplifier, sample-and-hold, and analog-to-digital converter. This is necessary due to an excessive amount of high-frequency noise picked up on the power supply leads and apparently originating in the digital data system.

2.2.2 Rapid transfer and mixing

One of the unique features of the portable analyzer is the clutch-brake mechanism utilized in its rotor drive assembly (see Fig. 2.7). A flywheel, coupled to the motor by a belt drive, serves to maintain the momentum of the drive assembly. With the clutch disengaged, the motor and flywheel assembly may be accelerated to run speed while the rotor itself

ORNL DWG 76-317

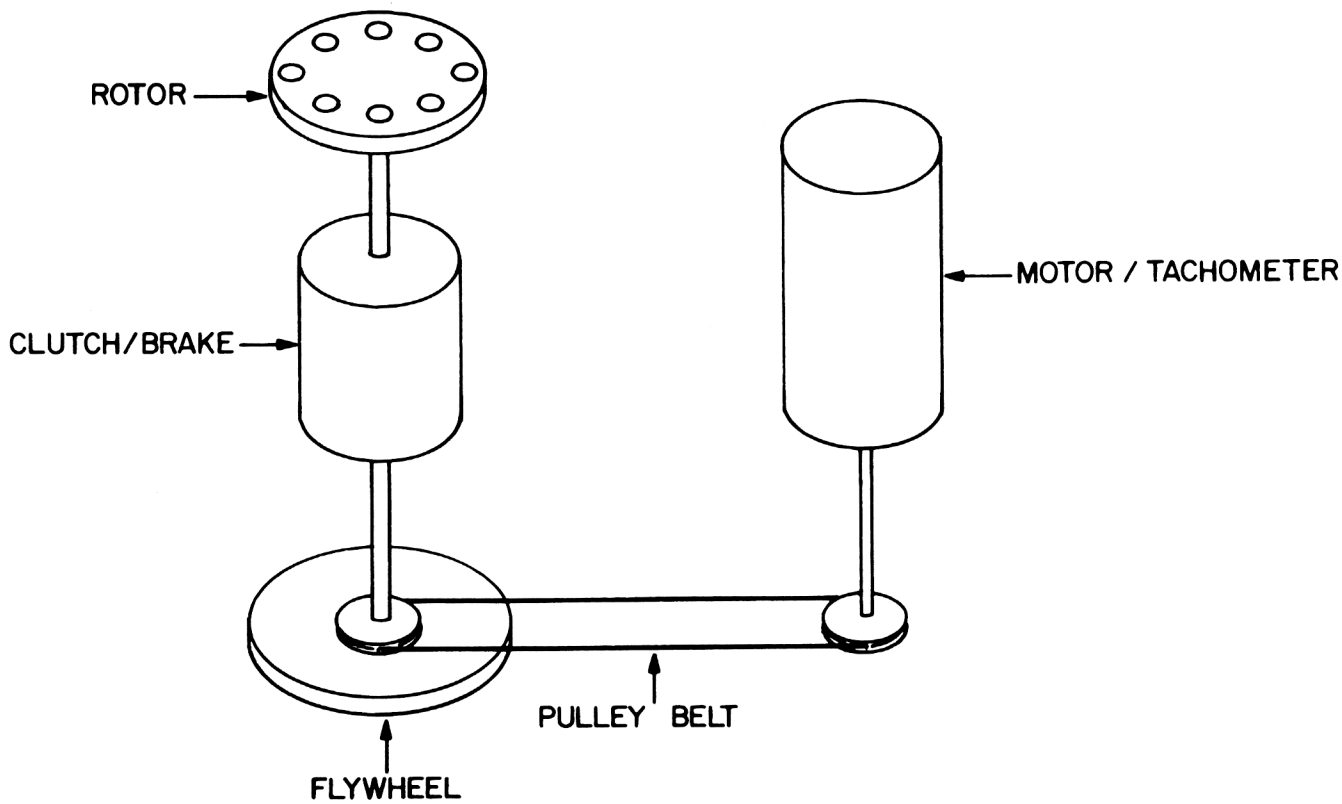

Fig. 2.7. Schematic of the clutch-brake and flywheel assembly used in the portable Centrifugal Fast Analyzer.

remains stationary. When the clutch is engaged, the rotor is rapidly accelerated from "rest" to its final run speed. Using specially designed rotors that have parallel sample and reagent chambers plus transfer channels, it is proposed that mixing and transfer will occur simultaneously as the solutions jet into their respective cuvets.

Preliminary experiments involving the mixing of homogeneous dye solutions have indicated that transfer of samples and reagents occurs during the first revolution of the rotor when it is rapidly accelerated to a run speed of 3800 rpm. As shown in Fig. 2.8, transfer of liquid commences about 22.5 msec after the rotor begins to move. By the end of the first revolution, transfer of liquid appears to have been completed indicated by the stabilization of absorbance measurements, as shown in Fig. 2.8. At this point, sample and reagent solutions have been in contact for about 40 msec (these measurements are not intended to demonstrate that effective mixing has occurred within this interval), and the rotor has accelerated to 49% of its final run speed of 3820 rpm. By the end of the third revolution, the rotor has achieved 88% of its final run speed and, by the end of the fourth revolution, it has reached 97%. Thus 102 msec after initial contact of samples and reagents, the rotor has achieved 97% of its final run speed. Table 2.3 illustrates some of the important events before and during the initial movement of the rotor on the new portable analyzer, their respective times of occurrence, and rotor speeds during acceleration to run speed. Thus we have the potential of monitoring ensuing reactions much earlier than is possible with either the original or miniature versions of the Centrifugal Fast Analyzers.

To utilize this capability, it is mandatory that the solutions be quantitatively transferred and mixed. Due to the small volumes and very

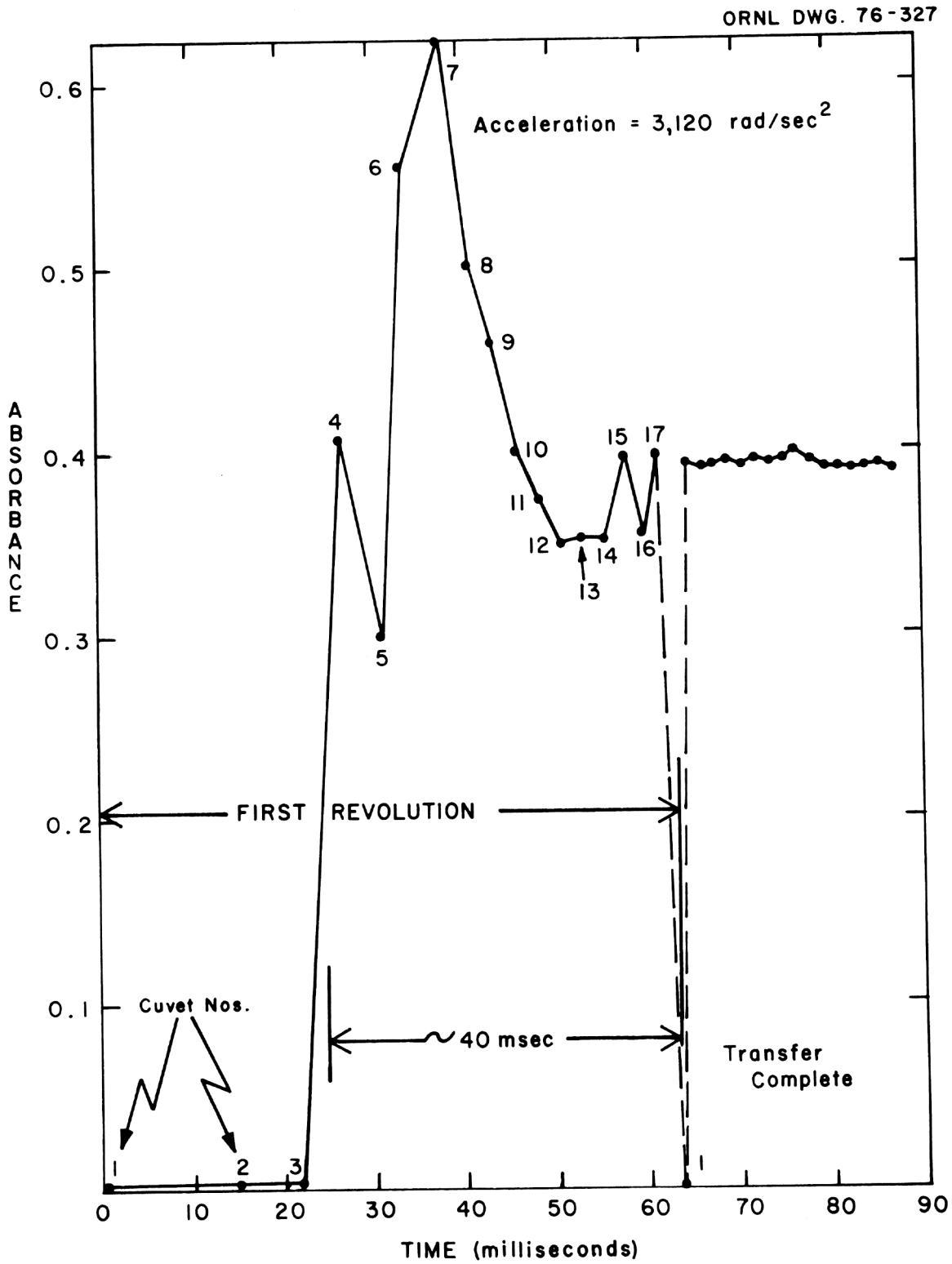

Fig. 2.8. Absorbance measurements for individual cuvets during the first two revolutions of the rotor showing liquid transfer was completed within one revolution.

Table 2.3. Time and rotor-speed measurements for rapid transfer of a homogeneous dye solution from sample and reagent cavities of a parallel chamber rotor

Event	Time (msec)	Rotor speed
Clutch engagement	0	-
Rotor starts to move[a]	44	-
Solutions start to transfer	66	-
Cuvet 1, 2nd revolution	109	1860[b]
Cuvet 1, 3rd revolution	134	2700[c]
Cuvet 1, 4th revolution	153	3360[c]
Cuvet 1, 5th revolution	169	3715[c]
Cuvet 1, 6th revolution	185	3820[c]

[a]Signal for cuvet 1 is acquired.

[b]Based on the time measurement between cuvet 16, 1st revolution and cuvet 1, 2nd revolution.

[c]Based on the time measurement between cuvet 16, 2nd revolution and cuvet 1, 3rd revolution; etc.

rapid times involved, verifying this experimentally becomes a difficult task. Previously, we have used an optical technique in which equal aliquots of water and dye of known absorbance were transferred into their respective cuvets. If transfer and mixing were quantitative, the resulting absorbance would be one-half the undiluted dye. We have now expanded this technique to include two dyes of known absorbances and variable volumes. In the new protocol, variable volumes of these two dyes are transferred and mixed and the resulting absorbances compared to the calculated absorbances. For example, the absorbance of the resulting mixture can be expressed as follows:

$$A_{cal} = \frac{V_1}{V_T} * A_1 + \frac{V_2}{V_T} * A_2 , \qquad (1)$$

where

A_{cal} = calculated absorbance of a mixture of the two dyes,

V_1 = volume of dye 1,

V_2 = volume of dye 2,

V_T = total volume,

A_1 = absorbance of dye 1, and

A_2 = absorbance of dye 2.

The efficiency of transfer and mixing can then be assessed by the ratio of calculated-to-measured absorbance with a ratio of 1.00 indicating quantitative transfer and mixing. This procedure has now been incorporated into a FOCAL program (Fig. 2.9); a typical output is shown in Fig. 2.10. This procedure will be utilized to study the time and efficiency of mixing for parallel transfer of both sample and reagent during rapid acceleration on the new portable analyzer. Experiments are also planned where one of the dye-containing liquids will simulate the viscosity and density of serum.

ORNL DWG 76-629

```
 W
C-GEMSAEC 2A 741163W

01.01 C-MIXING EFFICIENCY-SET FORMAT-MANUAL ENTRY OF DATA
01.02 E
01.03 T !!!
01.10 S DY=FDAY(0);S T=FTIM(0);S HR=FITR(T/3600)
01.11 S MN=FITR((T-3600*HR)/60);S SC=FITR(T-3600*HR-60*MN)
01.12 T !"DAY"%3,DY,"  TIME"%2,HR," :"MN," :"SC
01.20 A !"PROCEDURE"D
01.22 G 1.8
01.30 A !"GEMSAEC UNIT"UN;S NC=FITR(UN);S IM=FITR(968/[2*FITR(NC/2+1)])
01.32 S ST=(FITR((UN-NC)*10+0.05)-1)*64
01.40 A !"FILTER"XF
01.50 A !"DELAY INTERVAL--SEC"DI;I (600-DI)1.5
01.51 A !"OBS. INTERVAL--SEC"SE;I (60-SE)1.51;I (SE-1)1.51;S S1=SE
01.52 S MD=FITR(DI/60);S CD=60*(DI-60*MD);S MI=0;S CY=60*SE
01.60 A !"NUM OF SETS OF OBS."NI;I (NI-1)1.6;I (IM-NI)1.6
01.70 A !"READINGS PER CUVET"SC
01.80 A !"RUN NUMBER"RN
01.88 D 2.8

02.10 S A1=(AV(14)+AV(15))/2
02.20 S A2=(AV(16)+AV(17))/2
02.30 F J=2,4;S V1(J)=75;S V2(J)=50
02.31 F J=5,7;S V1(J)=50;S V2(J)=75
02.32 F J=8,10;S V1(J)=25;S V2(J)=100
02.33 F J=11,13;S V1(J)=100;S V2(J)=25
02.34 F J=14,15;S V1(J)=150;S V2(J)=0
02.35 F J=16,17;S V1(J)=0;S V2(J)=150
02.70 D 10
02.71 T !!,Q
02.80 T !,"ENTER ABS. FOR EACH CUVET";F J=2,17;T !,%3,J;A AV(J)

05.05 S D=FDIS(,,);S D=FDIS(,,2);S D=1↑300;S D=FCLK(,,,,)
05.10 S D=FTAK(,,);S D=FTAK(SC,NI,NC);S ZZ=FCNI(2);T !"READY!"
05.30 I (FCNI(2))5.3,5.5;Q
05.50 S D=FCLK(MD,CD,MI,CY,1)

06.03 T !!"CUVET      MEAN ABS.       SIGMA      C.V."
06.40 F J=2,NC;D 8
06.42 D 2.1;D 2.2;D 10
06.45 T !!"QUIT"!;Q
06.50 T !!"  ";F J=J1,J2;T %8,J
06.60 T !,%3,DI+(N-1)*SI;F J=J1,J2;D 7;T "  ",%5.04,AB(J)
06.70 I (PL)6.9;F J=2,NC;D 7;D 15
06.80 S J2=J1+6;I (J2-NC)6.9;S J2=NC
06.90 R

08.05 S T=0
08.10 F N=1,NI;D 7;S T=T+AB(J)
08.24 S AV(J)=T/NI;S SU=0
08.30 F N=1,NI;D 7;S SU=SU+[(AV(J)-AB(J))↑2]
08.32 S SM=FSQT[SU/(NI-1)]
08.40 S P=SM*100/AV(J)
08.45 T !,%3,J,"   ",%8.04,AV(J),"     ",SM," ",%6.02,P
08.46 R

10.01 C-CACULATIONS AND DATA OUTPUT
10.10 T !!"CUVET    VOLUME (UL)            "
10.12 T "ABSORBANCE          ERROR     RATIO"
10.14 T !,"         DYE-1    DYE-2     CALCULATED   "
10.16 T "MEASURED      (%)       (C/M)"
10.40 F J=2,17;S AC(J)=(V1(J)/(V1(J)+V2(J)))*A1+(V2(J)/(V1(J)+V2(J)))*A2
10.45 F J=2,17;S RE(J)=((AC(J)-AV(J))/AC(J))*100
10.46 F J=2,17;S RA(J)=AC(J)/AV(J)
10.50 F J=2,17;D 11

11.10 T !,%3,J,"   ",%4,V1(J),"   ",V2(J),"     "
11.20 T %6.04,AC(J),"     ",AV(J),"    ",%4.02,RE(J),"   ",
11.30 T %5.04,RA(J)
11.90 R
*
```

Fig. 2.9. FOCAL text of computer program used to assess transfer and mixing efficiency of the portable Centrifugal Fast Analyzer.

DAY 104 TIME 13 : 14 : 28 ORNL DWG 76-634
PROCEDURE:PCFA

RUN NUMBER:12

ENTER ABS. FOR EACH CUVET
2:.4693
3:.4674
4:.4723
5:.4093
6:.4134
7:.4089
8:.3524
9:.3540
10:.3528
11:.5249
12:.5244
13:.5232
14:.5797
15:.5788
16:.2941
17:.2940

CUVET	VOLUME (UL) DYE-1	VOLUME (UL) DYE-2	ABSORBANCE CALCULATED	ABSORBANCE MEASURED	ERROR (%)	RATIO (C/M)
2	75	50	0.4652	0.4693	- 0.89	0.9912
3	75	50	0.4652	0.4674	- 0.48	0.9952
4	75	50	0.4652	0.4723	- 1.53	0.9849
5	50	75	0.4081	0.4093	- 0.29	0.9972
6	50	75	0.4081	0.4134	- 1.29	0.9873
7	50	75	0.4081	0.4089	- 0.19	0.9981
8	25	100	0.3511	0.3524	- 0.37	0.9963
9	25	100	0.3511	0.3540	- 0.83	0.9918
10	25	100	0.3511	0.3528	- 0.49	0.9952
11	100	25	0.5222	0.5249	- 0.52	0.9949
12	100	25	0.5222	0.5244	- 0.42	0.9958
13	100	25	0.5222	0.5232	- 0.19	0.9981
14	150	0	0.5793	0.5797	- 0.08	0.9992
15	150	0	0.5793	0.5788	0.08	1.0008
16	0	150	0.2941	0.2941	- 0.02	0.9998
17	0	150	0.2941	0.2940	0.02	1.0002

Fig. 2.10. Typical computer output from transfer and mixing program.

2.2.3 Temperature control

In the portable CFA, temperature control in the rotor is achieved by adding or removing heat from the rotor's lower surface by conduction into the thin copper baseplate that also serves to support the rotor during analysis. The driving force (temperature difference) for this heat transfer is provided by a low-current, low-capacity thermoelectric module (heat pump) which pumps heat to or from an aluminum plate (heat sink). Heat is dissipated from the aluminum plate by free convection.

In the prototype system, the heat pump was chosen subject to three constraints:

(1) that it have the capacity to pump heat at any rate required to maintain a designated average rotor temperature (in the range of 20 to 37°C) in a given ambient-temperature environment (in the range of 15 to 35°C);

(2) that it preheat to a steady-state at the designated temperature in a reasonable period of time (arbitrarily less than 10 min); and

(3) that it be suited for direct dc battery operation.

A three-mode (proportional-integral-derivative) controller was designed to regulate heat transfer within the system; the controller response was determined by an "error signal" generated by comparing the temperature set point with the temperature read from a thermistor sealed in a copper pin at the outer radius of the baseplate (corresponding to radial cuvet position). Early experience demonstrated a requirement that the pin be thermally isolated from the baseplate, receiving heat only from the rotor so that it might reflect cuvet temperature more accurately. This controller was tuned at 20°C in order to maintain the rotor temperature at

30°C; the capacity and dynamic response of the system were then evaluated with special attention given to its sensitivity to ambient temperature changes.

During the tests, temperature was monitored by both the thermistor in the rotor-holder pin and by a thermistor placed in a cuvet. The preheating stage (which required approximately 10 min) was monitored, as well as the system response during and after transfer. Rotor acceleration for transfer of liquids was initiated manually and was based on the temperature indicated by the pin thermistor; transfer routinely began at 0.1°C below the desired set point temperature. Test results demonstrated that temperature control as indicated by the cuvet thermistor was reproducibly maintained within ±0.1°C under tuning conditions.

The dynamic response of the system was good under tuning conditions. The overshoot was approximately 1°C, and steady-state was achieved in approximately 1 min. Part of the overshoot was attributable to a radial temperature gradient that developed in the baseplate as a result of construction characteristics; the radial gradient caused the fluid near the center of the rotor to be preheated to a temperature greater than the temperature sensed at the rotor's edge. Thus the cuvet thermistor recorded an overshoot attributable to this slight overheating, as well as to the heat input caused by the controller.

The radial temperature gradient in the baseplate and on the rotor surface (with reagent chambers carrying water) was investigated by applying a step input to the heat pump and allowing steady-state to be reached (for a stationary rotor) without control action. The results as shown in Figs. 2.11 and 2.12 indicate radial temperature gradients of approximately

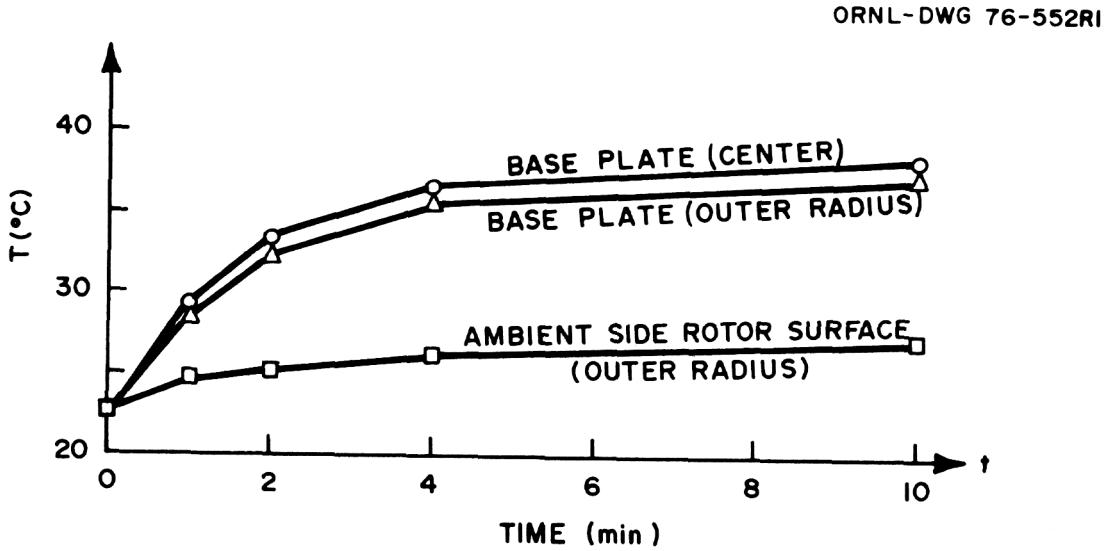

Fig. 2.11. Development of radial temperature profiles in the baseplate and rotor surface after a 2-V step input to the heat pump.

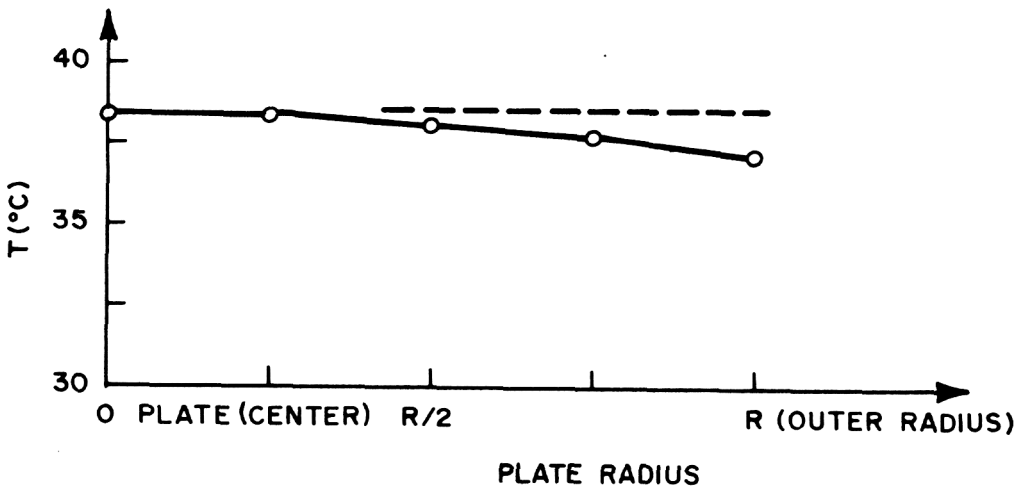

Fig. 2.12. Radial temperature profile for the baseplate under steady-state conditions.

1°C on each surface. The apparent temperature drop across the rotor thickness was approximately 10°C (see Fig. 2.11); however, the uneven thermal contact between the rotor and the baseplate surface probably caused most of this temperature drop. When the surface thermometer was used to measure the inner surface temperature of the plastic layer adjacent to the copper plate (via the opening in the upper rotor face), the temperature differed from the upper rotor face by only 1°C. The magnitude of gradients discussed above remained the same when the step input to the heat pump was 1 V, and when cooling rather than heating was performed (the step inputs corresponded to those required during the initial tuning procedure).

Steady-state control, as indicated, was within 0.1°C of the set point under tuning conditions. However, as ambient conditions varied from tuning conditions, oscillation in the transient response of the system increased. An offset between the steady-state control temperature and the desired set point was also observed to increase with increasing variations in ambient conditions (see Fig. 2.13). The offset was traced to a hardware failure in the control circuit which eliminated the integral action of the controller.

Design limitation of the voltage input to the heat pump resulted in an apparent lack of capacity for both heating and cooling during the tests; at an ambient of 15°C, the system could not preheat the rotor to 30°C; at an ambient of 35°C, the system failed to cool the rotor to 30°C. Two steps are being taken to overcome this system limitation. First, the voltage limit for input to the heat pump is being expanded to take greater advantage of the pump's capacity. Second, improvements in the heat sink design involve developing its capacity to adsorb heat by increasing its effective surface area (beyond the increase accompanying the mass increase) with fins;

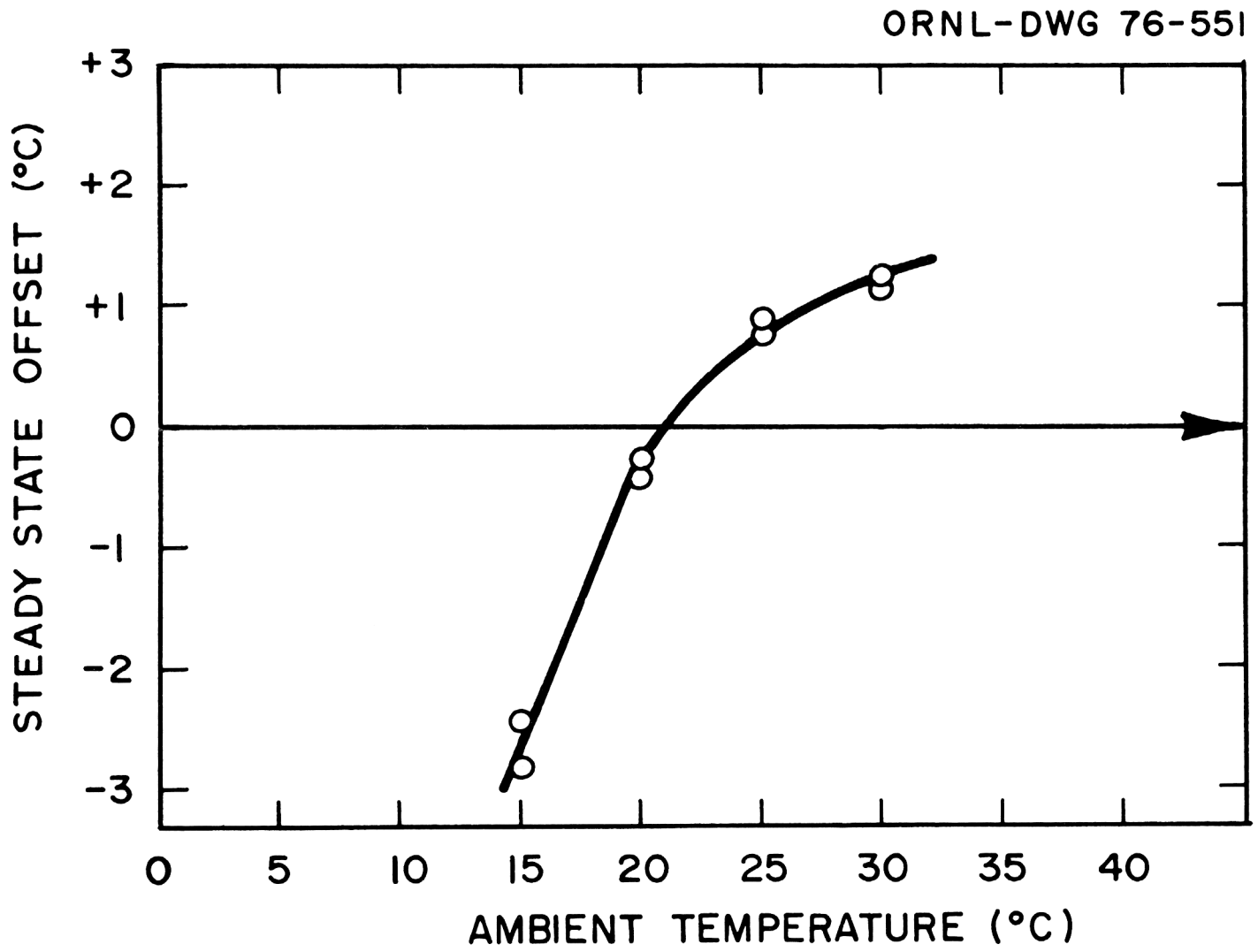

Fig. 2.13. Effect of changes in ambient temperature on the offset between control temperature and desired set point temperature under steady-state conditions.

the rotor cover was also repositioned to provide cooling by forced rather than free convection.

In summary, both the controller and the heat sink are being modified to improve overall system performance in temperature control. Additional tuning and testing are planned to evaluate performance after modifications are made.

2.2.4 Evaluation of the portable Centrifugal Fast Analyzer

Enzymatic determination of glucose. The ATP-hexokinase enzymatic assay for the determination of glucose has been evaluated in detail on both the original GeMSAEC[3] and the miniature[4] prototype Centrifugal Fast Analyzers. We have employed this assay to evaluate the performance of the new portable analyzer and microprocessor unit.

Sample (2 λ) and reagent (20 λ) were loaded via the ORNL sample-reagent loader[5] into a conventional sequential transfer rotor (total volume = 122 λ). Data acquisition parameters were: delay time, 0.2 sec (this does not include a time interval of approximately 0.28 sec during which the rotor and its contents were accelerated to 4000 rpm, dynamic braking was applied with subsequent re-acceleration of the rotor; run speed, 3500 rpm (17 msec/revolution); observation interval, 0.3 sec; and 5 readings averaged per data point. Data were acquired and all computations performed by the microprocessor unit (see Ref. 4) of the portable analyzer. The first 30 measurements obtained by the analyzer (corresponding to approximately 0.5 to 9.5 sec after the rotor first began to accelerate) are illustrated in Fig. 2.14; data are shown for a reagent blank and a 200-mg glucose/dl aqueous sample -- both versus a water reference. A final measurement was obtained on the samples after equilibrium had been attained (approximately 30 min at 25°C).

ORNL DWG 76-299R1

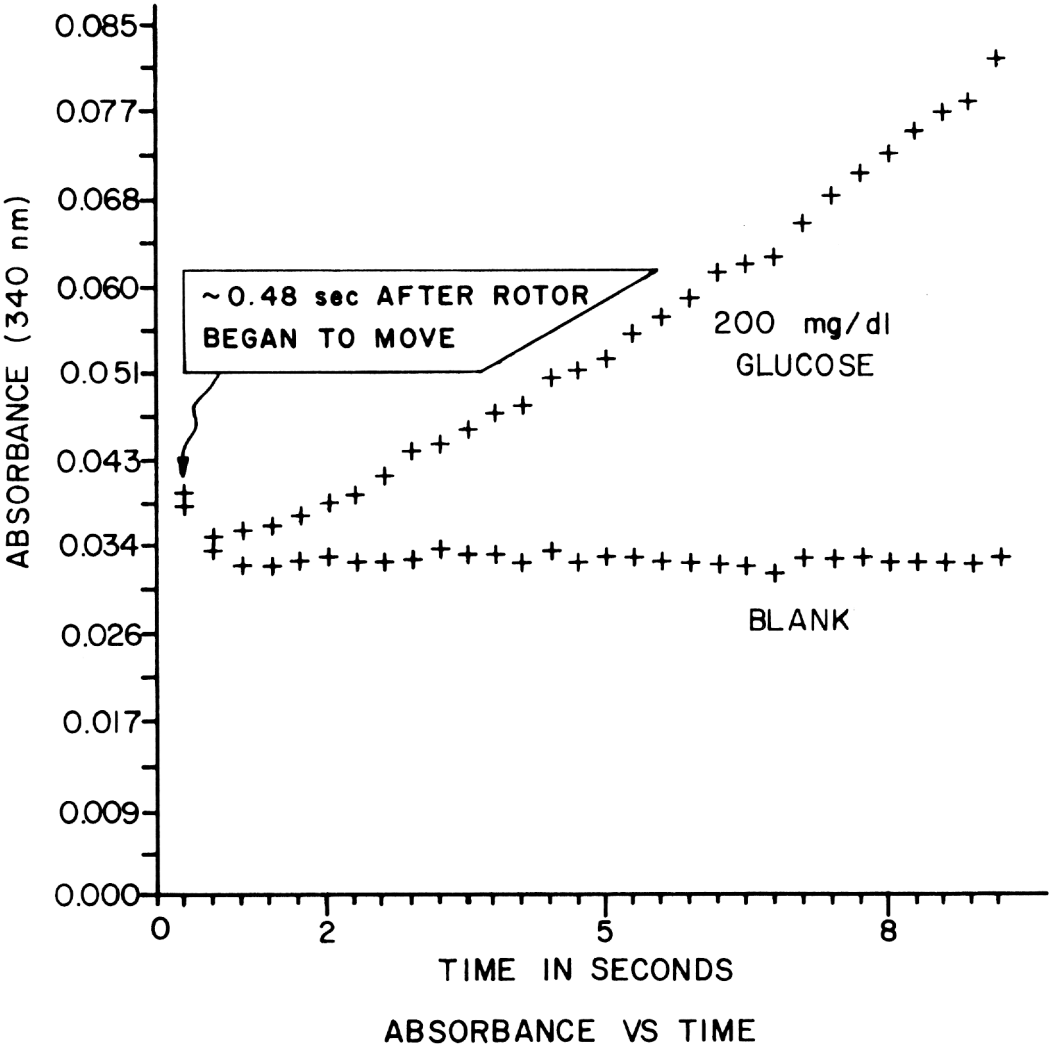

Fig. 2.14. Progress curve for the hexokinase-glucose reaction monitored by the portable Centrifugal Fast Analyzer. Total time elapsed ≈9.2 sec.

The data of Fig. 2.14 are summarized in Table 2.4. In this figure, the first data points appear to be high; this may be due to a transient power drain on the system from the mixing sequence and can thus be corrected. The first few data points were omitted in calculating the data of Table 2.4. The optical precision of the system is shown in the measurement of the reagent blank. The measurement precision within cuvet was <1%, and the average blank (n=5, $\bar{A}$=0.0323 ODU) was precise to within ±1.4 to 1.8%; at higher absorbances (e.g., the final absorbance of the 400 mg/dl sample), the overall precision was approximately 0.2% (n=5, $\bar{A}$=1.2132 ODU). The ratio of the change in absorbance of the 400 mg/dl sample to that of the 200 mg/dl sample was 1.995 (theoretical = 2.0). The linear least-squares analysis subroutine of the microprocessor unit (see Ref. 4) was used to estimate the initial absorbance (A_o) of the reactions, and this was used, together with the measured final absorbance (A_f), to estimate the change in absorbance. The results of this analysis agreed very well with the average change in absorbance measured at equilibrium (see Table 2.4).

In summary, the optical performance of the analyzer was excellent. The microprocessor unit performed faultlessly for the data acquisition and manipulation, and the feasibility of performing moderately fast kinetic analyses with great sensitivity was established (note in Fig. 2.14 that 30 data points representing an absorbance change of 47 milliabsorbance units were obtained in 9.2 sec, with a standard deviation of the slope of only 1.7%).

Table 2.4. Enzymatic determination of glucose on the portable Centrifugal Fast Analyzer

Cuvet number	Glucose concentration (mg/dl)	A_o [a] (extrapolation)	A_f [b]	A_f [c] (average)	$A_f - A_o$	$A_f - A_o$ [c] (average)	$\bar{A}_f - \bar{A}_f$ (blank)
2		0.0325	0.0323	0.0323	-0.0002		
3		0.0328	0.0328	±0.0004	0.0000	0.0001	
4	0	0.0313	0.0317	(1.36%)	0.0004		0.0000
5		0.0323	0.0327		0.0004		
6		0.0325	0.0322		-0.0003		
7		0.0257	0.6203	0.6243	0.5946		
8		0.0267	0.6280	±0.0045	0.6013	0.5960	
9	200	0.0279	0.6203	(0.72%)	0.5924	±0.0034	0.5920
10		0.0283	0.6230		0.5947	(0.57%)	
11		0.0331	0.6301		0.5970		
12		0.0240	1.2177		1.1937		
13		0.0247	1.2100	1.2132	1.1853	1.1893	
14	400	0.0206	1.2127	±0.0028	1.1921	±0.0035	1.1809
15		0.0245	1.2122	(0.23%)	1.1877	(0.29%)	
16		0.0257	1.2133		1.1876		

[a] y-Intercept for linear least-squares analysis of absorbance (y) vs time (x) for the time interval 1.9-9.2 sec.

[b] Data taken after 30-min reaction time at 25°C.

[c] Data reported as mean ± standard deviation (coefficient of variation given in parentheses).

2.2.5 Fabrication of Microprocessor-II

Microprocessor-II is completely checked out and operable at this time. Two aspects of interest in this computer are the memory size and the clock. The computer has a 12K byte capacity for program storage (PROM devices). This is enough storage to accommodate the data acquisition software (time-based and counts-based) and all the data analysis tables (see Sect. 2.2.6). Approximately 3K of memory is unused and, therefore, available for future program expansion. In addition, the computer has 8K byte capacity for data storage (RAM devices). This storage capacity will allow 99 observations (17 cuvet readings = 1 observation) and 99 sets (1 set = 2 time measurements) of time measurements. A new computer clock, included in the microprocessor, measures time with a resolution of 100 μsec and with better than 0.1% accuracy. The resolution figure is particularly important because at 4000 rpm, only 880 μsec elapse between successive cuvets.

A brief mention of how the computer hardware and software were debugged is of interest. A second processor was built which incorporated special software and a teletype output. Figure 2.15 shows the schematic system configuration for troubleshooting.

The diagnostic processor has the capability to exercise the hardware in the portable analyzer (e.g., the clutch, motor, filters, lamps, etc.). Also, the diagnostic processor can control execution of program readout in the portable CFA processor. This system configuration has proved very satisfactory and of great value.

2.2.6 Software development

The software for Microprocessor-II has been substantially checked and is operable for the portable CFA. Figure 2.16 depicts a flow diagram for its sequential operation when interfaced to a portable CFA. With the

ORNL DWG 76-335

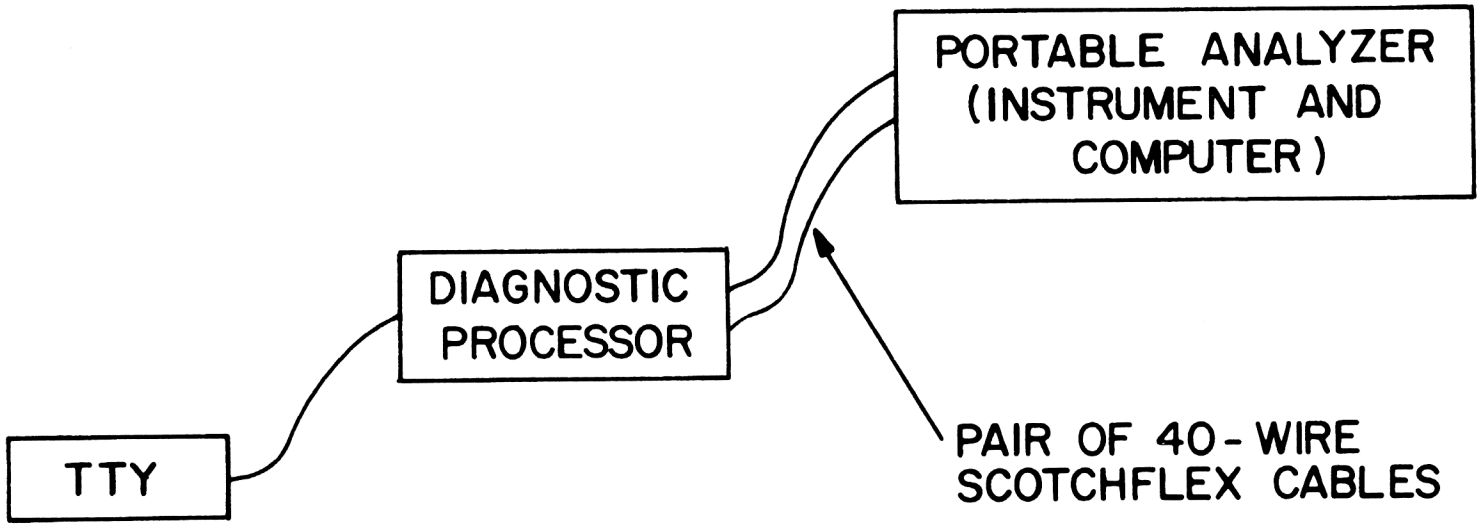

Fig. 2.15. Schematic diagram to show the system configuration for troubleshooting Microprocessor II with a second microprocessor.

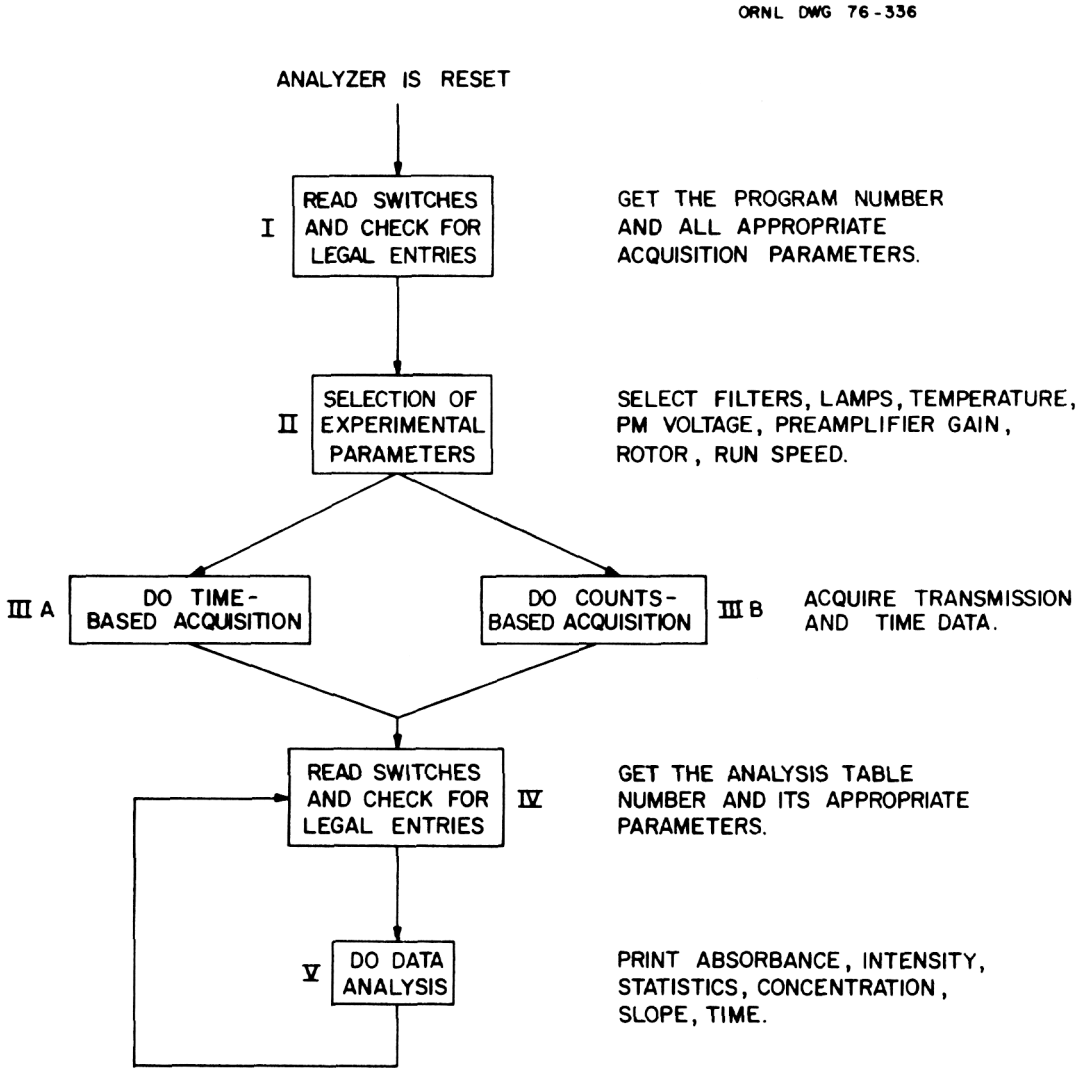

Fig. 2.16. Operational sequence for the software of Microprocessor II interfaced to the portable Centrifugal Fast Analyzer.

analyzer reset, the operator enters the program number and the appropriate acquisition parameters on 12 decimal-coded switches on the front panel. When he is satisfied with his entries, he depresses a "continue" switch (also on the front panel). The computer immediately reads all switch settings (I). In the next step, the computer accomplishes all the process control that a particular program number asks for (II) - filters, lamps, PM voltage, temperature, etc. When all of these are accomplished, the computer decides which acquisition type is required (IIIA or IIIB), performs the necessary acceleration sequence, and then acquires the data. When completed, the computer prints a flag on the printer device and halts. The operator then selects the data analysis table number and all its appropriate parameters by means of the thumbwheel switches. When he is satisfied with the switch settings, he depresses the "continue" switch. The computer reads the switches (IV) and then performs the requested analysis (V). When finished, the computer waits for another table request (IV). The data acquisition software has been expanded to include not only a time-based acquisition (same acquisition type as the miniature analyzer), but also a counts-based acquisition.

Counts-based data acquisition. This type of data acquisition was designed specifically to accurately record fast kinetics reactions that are complete in less than 1 sec.

The important parameters of this acquisition type are as follows:

(1) delay revolutions,

(2) number of observations,

(3) revolutions between observations, and

(4) revolutions per observation.

Two parameters that are unique to this acquisition type are the delay revolutions and the revolutions between observations. Delay revolutions are the revolutions counted before the first observation is recorded. Revolutions between observations are the revolutions counted between successive observations. A value of zero for this latter parameter directs the acquisition to record data on every successive revolution.

When the counts-based acquisition is in progress, both transmission data and time data are recorded. For a given observation, time is recorded twice - at cuvet 1 on the first revolution and again at cuvet 16 on the last revolution. These time data can be displayed on the printer device once the acquisition is complete. In addition, the time data are used with the transmission data in the calculation of linear variable statistics (slope, variance of slope, intercept, variance of intercept, and correlation coefficient).

An exciting aspect of this counts-based acquisition is that a given acquisition can run under more than one set of data-gathering parameters. For example, it is possible to record the first n observations under the following parameters:

(1) delay revolutions = 0,

(2) revolutions between observations = 0,

(3) revolutions per observation = 1, and

(4) rotor speed approximately = 4000 rpm.

The next (99-n) observations (99 total observations maximum) will be recorded under a second set of parameters:

(1) delay revolutions = 99,

(2) revolutions between observations = 250,

(3) revolutions per observation = 10, and

(4) rotor speed approximately = 1000 rpm.

For the first n observations of this particular acquisition run, the computer will record data on every revolution for the first n revolutions. On each of these observations, the computer will do no averaging of the transmission data. The rotor speed dictates that data for the nth cuvet will be recorded once every 16 msec, typically (62 observations per minute at 4000 rpm).

For the final observations of this particular acquisition run, the computer will record data only once every 250 revolutions. On each of these observations, the computer will do 10 revolutions of averaging on the transmission data. The rotor speed dictates that data for the nth cuvet will be recorded once every 15 sec, typically. ([250 rev bet obs] * [60 sec/min]/[1000 rpm]). For example, if n=50, the first 50 observations will be recorded in under 1 sec, and the last 49 observations will be recorded in 13 min.

This discontinuity in the acquisition parameters will not complicate the data analysis tables in any way. The reason for this is that the internal clock will continue to give a "true" time as the acquisition parameters shift from the first kind to the second kind. This is particularly important in the statistical evaluation of slope and intercept, where both transmission data and time data are used.

Time-based data acquisition. A description of the time-based acquisition was given in detail in an earlier report.[4] One important aspect of this acquisition that was not previously described is the mixing sequence at the start of the acquisition. Before data are acquired in a time-based

acquisition, the rotor will undergo an acceleration-brake-acceleration sequence to transfer and mix samples and reagents. This is the same sequence used with the miniaturized CFA.

The time sequence in which the rotor and its assembly are operated is as follows:

(1) Initially, the brake is applied and the entire assembly is at a standstill.

(2) The motor is energized to a predetermined speed indicated by the setting of the acceleration speed dial on the instrument's front panel. Typically, this speed is adjusted for 4000 rpm, and approximately 6 sec is allowed for the motor to attain this speed. The rotor remains motionless.

(3) The clutch is energized for a time period of 150 msec. The rotor will accelerate to an instantaneous speed of approximately 3500 rpm by the end of the time period.

(4) The brake is again applied but only for a time period of 120 msec. The rotor decelerates and completely halts for approximately 100 msec.

(5) The motor is now energized for a new speed, as determined by the run speed dial on the instrument's front panel. Typically, this speed might be adjusted for 1000 rpm.

(6) The clutch is again energized and will remain energized for the duration of the data-gathering period. A typical profile of rotor speed versus time for this sequence of events is shown in Fig. 2.17.

The rotor speed is guaranteed to be at an instantaneous speed of at least the run speed value 400 msec after the clutch is initially energized. This implies that the data acquisition itself can begin 400 msec after initial mixing. Notice that rotor speed at the 400 msec time actually

ORNL DWG 76-337RI

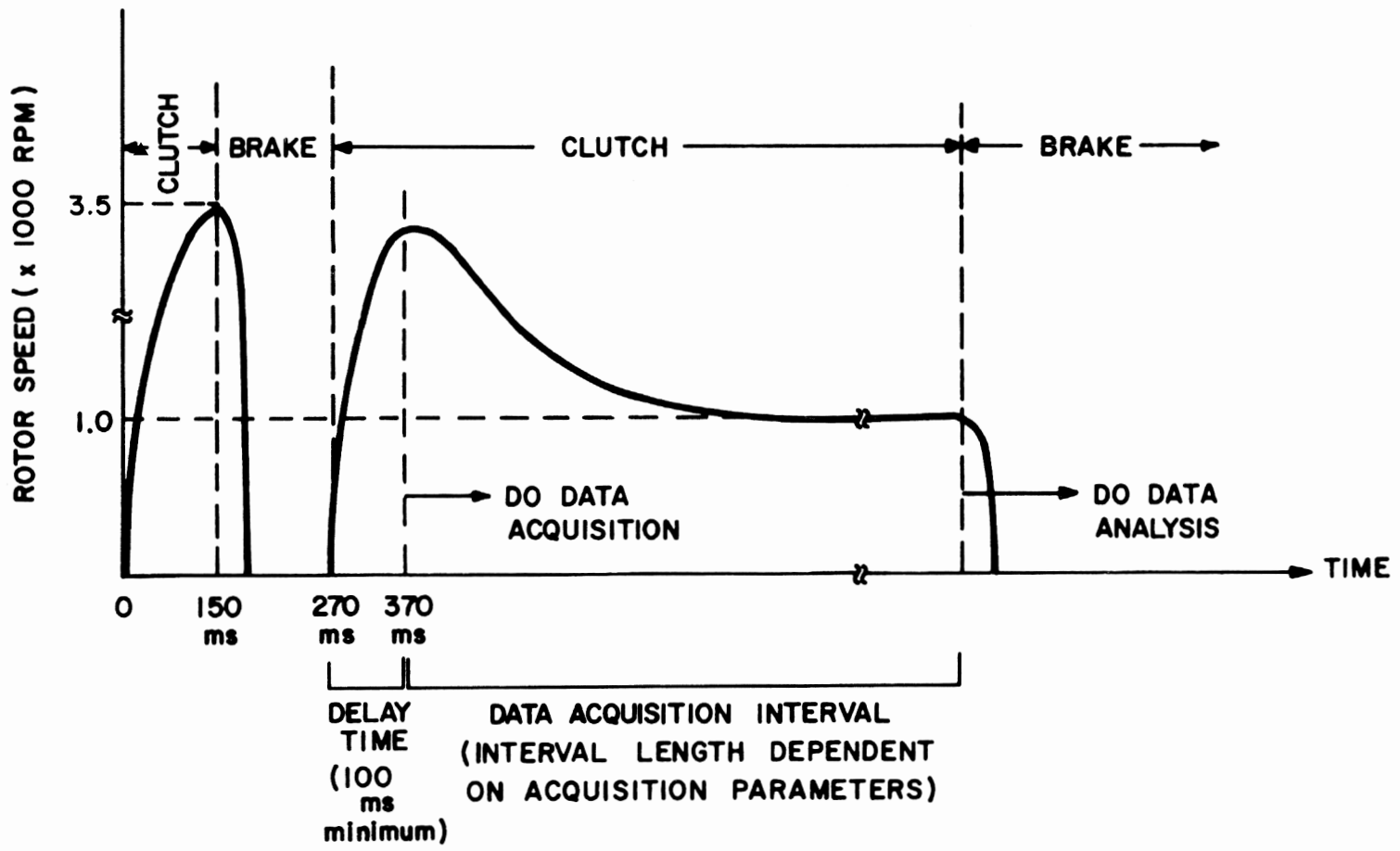

Fig. 2.17. Time and speed profile for the accelerate-brake-accelerate sequence used in time-based data acquisition on the portable Centrifugal Fast Analyzer.

exceeds the desired run speed for a time. This speed overshoot is due to the inertia stored in the flywheel during the acceleration period. Special algorithms were experimentally implemented that eliminated this overshoot characteristic. However, it doesn't appear as if this overshoot will be detrimental to the accuracy of data obtained. For the present, the overshoot will be allowed.

The counts-based acquisition, of course, has no mixing sequence. At the start of the acquisition, the rotor is synchronized to the position of cuvet 1; with the brake applied, the motor is then energized to run speed; and finally, the clutch is energized.

The last point to be considered in regard to acquisition is how much, how fast, and how accurately can data be stored in computer memory. The amount of data that can be stored is solely a function of the random-access memory (RAM) size. Presently, the computer can store 99 observations (an observation is 17 cuvet transmission readings). Also, 99 pairs of time data can be stored in the counts-based acquisition. The maximum rotor speed at which the computer can collect data is 4500 revolutions per minute. This means that the nth cuvet is sampled once every 13.3 msec. Either time-based or counts-based acquisition is capable of this speed. The accuracy of the transmission data collected is approximately three decimal digits. The determining factors here are the 14-bit analog-to-digital converter (ADC), sample and hold circuit offset and drift, and general system noise. The accuracy of the time data collected is better than 0.1%, with a resolution of 100 μsec.

2.3 Applications

A number of diverse applications of Centrifugal Fast Analyzer technology are being investigated. These include the analysis of environmental pollutants using rotors preloaded with reagents and the development of assay procedures for a number of enzymes having clinical importance. Further applications useful in blood-banking procedures are being studied by assaying for the presence of antibodies by an adaptation of the direct Coombs test to the CFA. New computer programming concepts are being developed and tested in the measurement of kinetic parameters of enzymes and in the detection and assay of isoenzymes. Finally, the enzyme gamma-glutamyl transpeptidase is being evaluated as a potential biochemical marker for detecting metastatic malignancy.

2.3.1 Environmental analysis

Several chemical methodologies are currently being developed for use with the miniature and the portable Centrifugal Fast Analyzers. Initially, efforts have been concentrated on the analysis for inorganic nutrients commonly found in water with an aim toward a possible "nutrient rotor," whereby a number of constituents may be determined simultaneously from different aliquots of a water sample. Previously, we have discussed the development of methods for silica and phosphate.[4] During this report period, we have continued to investigate methods for determining ammonia and nitrate in waste waters.

Enzymatic determination of ammonia. The enzymatic determination of ammonia in water using the miniature CFA was introduced in a previous report.[4] The advantages of this method include speed of analysis (up to 16 samples may be analyzed in a run time of 8 min) and the fact that,

when a "2-point stoichiometric" approach is employed, the assay is an absolute method not requiring multiple standards to establish an empirical calibration curve. Rather, a control sample will suffice to verify the integrity of the reaction. In this report, the effect of chemical interferents on the enzyme reaction, the stability of the enzyme reagent, and the correlation of the method with a reference method, the direct Nessler reaction, are investigated. In addition, since either an initial rate or a "2-point stoichiometric" approach to determine ammonia is possible using the enzyme reagent,[4] the relative merits of the two approaches are considered.

Reagent preparation and stability. L-glutamate dehydrogenase, ADP, α-ketoglutarate, and NADH were combined as a single reagent in 0.30 M Tris buffer, pH 8.6. The combined reagent was found to be stable for at least 3 days when stored at 2 to 4°C. Since the procedure requires the monitoring of a decrease in absorbance at 340 nm (due to consumption of NADH), the initial concentration of NADH determines the substrate range that can be examined. The sensitivity of the assay may be optimized for other ranges of substrate concentration by adjusting the initial concentration of NADH and the ratio of sample volume to total volume.

As indicated in Table 2.5, the combined reagent for enzymatic analysis is stable to storage at 2 to 4°C for at least 3 days. To test the feasibility of preparing preloaded rotors with this reagent, its stability to lyophilization was examined. Aliquots of the reagent were lyophilized and stored desiccated at 2 to 4°C. The remainder of the combined reagent was also stored at the same temperature. Although glutamate dehydrogenase has been reported to be inactivated by freezing, the presence of high concentrations of ADP and phosphate ion in this reagent apparently enabled

Table 2.5. Effect of storage on activity of glutamate dehydrogenase reagent for the determination of ammonia

NH_3-N (ppm)	Initial reaction velocity, A_{340}/min		
	Fresh reagent[a]	Stored reagent[b]	Lyophilized reagent[c]
2	0.0251	0.0319	0.0275
4	0.0569	0.0560	0.0550
6	0.0829	0.0842	0.0804
Slope[d]	0.0145	0.0131	0.0132
Intercept	-0.0028	0.0051	0.0014
Correlation coefficient	0.9983	0.9989	0.9997
Relative standard error	2.49%	1.68%	0.91%

[a]Reagent tested on day of preparation. Initial absorbance of reaction mixture approximately 1.06 ODU.

[b]Reagent stored 4 days at 2-4°C. Initial absorbance of reaction mixture approximately 0.50 ODU (some degradation of NADPH upon storage).

[c]Reagent lyophilized on day of preparation and stored 4 days at 2-4°C prior to reconstitution. Initial absorbance of reaction mixture approximately 0.98 ODU.

[d]$(A_{340}$nm/min)/(NH_3-N, ppm), calculated from linear least-squares analysis.

it to survive lyophilization. Note that when the reagent is stored in liquid form, much of the NADH is degraded (compare footnotes a and b of Table 2.5). This could result in error if higher concentrations of ammonia are analyzed. However, NADH appears stable in the lyophilized reagent. Thus the lyophilized reagent should be amenable to the "preloaded rotor" concept.[4]

Analytical methods. For direct measurement using Nessler's reagent (Hach Chemical Company, Ames, Iowa), samples (35 µl plus 50 µl of diluent) and reagent (7.5 µl plus 45 µl of diluent) are loaded into a rotor by means of the rotor loading station.[5] The rotor is placed on the analyzer and is brought to 30°C; the reaction is initiated by acceleration of the rotor to 4000 rpm, followed by dynamic braking and adjustment to run speed (1000 rpm). After 60 sec, the absorbance at 400 nm is determined vs a reagent blank.

For enzymatic measurement of ammonia, 30 µl of reagent (plus 25 µl of diluent) and 45 µl of sample (plus 30 µl of diluent) are loaded into the appropriate chambers of the rotor. The rotor temperature is brought to 30°C and the transfer and mixing of samples and reagents is initiated. The reaction is monitored by determining the absorbance at 340 nm as a function of time.

Interferences. The specificity of the enzyme reaction for ammonia, with respect to organic nitrogen-containing compounds, has been demonstrated by Verdouw.[6] Some of these compounds were examined under our reaction conditions, and the data are given in Table 2.6. The effect of several cations known to produce interferences in the Nessler reaction[7] was examined for the 2-point stoichiometric and initial rate enzymatic methods

Table 2.6. Effect of selected chemical interferents on the determination of a 5-ppm NH_3-N standard

	Direct Nesslerization		Enzymatic method: 2-Point stoichiometric		Enzymatic method: Initial rate	
Interferent	NH_3-N[a] found (ppm)	Percent error	NH_3-N[b] found (ppm)	Percent error	NH_3-N[a] found (ppm)	Percent error
100 ppm Mg^{2+} [c]	3.96	-20.8	4.51	-9.8	1.84	-63.2
10 ppm Fe^{3+} [d]	5.83	+16.6	5.07	+1.4	4.91	-1.9
10 ppm Mn^{2+} [e]	15.04	+200	4.98	-0.4	5.21	+4.2
10 ppm hydroxylamine·HCL	8.70	+74.0	5.10	+2.0	5.09	+1.8
10 ppm urea	5.09	+1.8	4.94	-1.2	4.99	-0.2
10 ppm glycine	5.10	+2.0	5.04	+0.8	5.04	+0.8

[a]Calculated from linear least-squares regression analysis.

[b]Calculated from the equation $C = SF \times \Delta A$ (see text).

[c]Prepared from $Mg(C_2H_3O_2)_2 \cdot 4H_2O$.

[d]Prepared from $FeCl_3 \cdot 6H_2O$.

[e]Prepared from $MnCl_2 \cdot 4H_2O$.

and also for the Nessler method. The levels of interferents examined were approximately 3 to 20 times the upper limits normally encountered in surface waters.[8] The ions examined interfere by formation of insoluble hydroxy complexes with the strongly alkaline Nessler's reagent, whereas the enzymatic reaction occurs in mildly alkaline solution (pH 8.6). Comparative results indicate that interference is greatest for the Nessler's reagent and is least for the 2-point stoichiometric assay (see Table 2.6). The presence of magnesium in large quantities apparently inhibited the enzyme reaction (low initial reaction rate), and results were also low for the 2-point stoichiometric approach when the run time was only 8 min (the run time used for the 2-point stoichiometric data in Table 2.6). Increasing the run time to 10 min decreased this interference, apparently because equilibrium was more nearly achieved.

Results. In Table 2.7 the 2-point stoichiometric and initial rate procedures are compared for the determination of ammonia. The comparative results indicate that the precision, accuracy, and sensitivity are superior for the 2-point kinetic approach. Since the reaction is highly selective (no competing reactions), and since the time required to approach equilibrium is relatively short, many of the advantages of an initial rate approach are not realized in this situation.[9]

In Table 2.8, the 2-point stoichiometric procedure and the direct Nesslerization procedure are used to determine NH_3-N in samples of water collected from various stages of a pilot plant operation. Because of the high ammonia concentrations expected, sample size was decreased to only 2 μl, a volume which may be sampled with the automatic rotor loading station with a precision and accuracy of 2 to 4%.[10] The increased dilution factor decreased the effect of potential chemical interferents

Table 2.7. Comparison of 2-point stoichiometric (ΔA) and initial rate approaches for the enzymatic determination of ammonia

	ΔA	Initial rate
Within-run[a] precision of measurement	0.5-2.5% (1.3%)	0.5-4% (2.5%)
Run-to-run[a] reproducibility of calibration curve	0.6-1.4% (1.1%)	2%
Relative standard error[b] of calibration curve	0.3-1.2% (0.7%)	1.5-3% (2.5%)
Day-to-day[a,c] reproducibility of calibration curve	1.1%	-
Sensitivity[d]	0.03 ppm (1.4 ng)	0.16 ppm (7.3 ng)

[a]Estimated by coefficient of variation. Data given as range of results obtained (average given in parentheses).

[b]Estimated from linear least-squares regression analysis. Data given as range of results obtained (average given in parentheses).

[c]Estimated from average slope of calibration curve over a 3-day interval, using a single batch of reagent, 0 to 3 days old.

[d]Estimated by two times the average standard deviation of the measurement of 2 ppm standard ammonia solution divided by slope of the calibration curve.

Table 2.8. Comparison of enzymatic 2-point stoichiometric method with direct Nessler method for the determination of ammonia in pilot plant process streams

	NH_3-N found (ppm)	
Sample number	Direct Nesslerization	2-Point stoichiometric
1[a]	-	2.6
2[b]	228	246
3[c]	248	248
4[d]	32	21.4
5[e]	359	273

Qualitative description of samples:

[a]First byproduct scrub liquor from coal hydrocarbonization pilot plant; clear.

[b]Process feed, spiked with high levels of phenol, nitrate, ammonium ion, phosphate, thiocyanate, and ferrous ion; slight color.

[c]Process product; slight turbidity.

[d]Second scrub liquor from coal hydrocarbonization pilot plant; solution is colored.

[e]Later scrub liquor, containing high levels of phenol, ferrous ion, thiocyanate, etc.; highly colored solution.

in the Nesslerization procedure. In general, agreement between the two methods was quite good. The result of the Nesslerization procedure for sample 5 was expected to be high because of both the presence of known interferents and the high initial absorbance of the sample. (In contrast, the 2-point kinetic procedure enabled compensation for this high sample absorbance by a determination of the sample blank.)

Conclusions. The utility of the enzymatic analysis for moderate concentrations of ammonia has been demonstrated. The advantages of the method include those observed by Verdouw:[7] the risk of hydrolysis of labile nitrogen compounds is minimal under the relatively mild reaction conditions of the assay, and the assay is specific for NH_3-N. With the present system, the volume requirements for sample and reagents make the assay quite inexpensive for each test. The 2-point stoichiometric assay is an absolute method; therefore, up to 16 samples may be analyzed in a single run, requiring 10 min or less. Results may be obtained directly in concentration units.

In addition, the enzymatic procedure for ammonia may be used in a single-sample:multiple-chemistry mode. Bostick et al.[11] have proposed a "nutrient rotor" concept whereby a number of constituents, including soluble silica, orthophosphate, and ammonia could be determined simultaneously in a multicuvet rotor under a single set of observation conditions. A procedure has been developed for the simultaneous determination of silica and phosphate based on the rate of formation of their respective 12-heteropoly molybdate complexes (which have an absorption maximum near 340 nm). Data were collected over a time interval comparable to that currently used in our 2-point stoichiometric procedure; from these data, a slope (initial rate) is computed for the determination of silica, and the

intercept of the data represents a direct measure of the phosphate concentration of the sample.[11] We have thus been able to employ the 2-point stoichiometric procedure to obtain estimates of ammonia, silicon, and phosphate content of a sample in a single experimental run. The analytical capabilities of the CFA, together with the concept of a portable analyzer,[12] may yield a powerful tool for on-site environmental analysis.

Enzymatic determination of nitrate. Based on the observation that elevated nitrate in the diet and a large number of nitrate-reducing bacteria in the upper digestive tract are a primary cause of infantile methemoglobinemia, the current drinking water limit specified by the U.S. Public Health Service and the Environmental Protection Agency is now 10 ppm of nitrate-nitrogen.[13,14] However, the chemical determination of low levels of nitrate ion, an important inorganic nutrient and the predominant inorganic nitrogen form in surface waters,[15] presents a challenge to the analyst.

The determination of nitrate is usually pursued using one of four methods: (1) nitration of a phenolic-type compound, (2) nitrate oxidation of an organic compound, (3) instrumental methods, or (4) reduction of nitrate to ammonia or nitrite. Nitration methods include the use of chromotropic acid,[16] phenol-disulfonic acid,[17,18] and xylenol isomers. Nitrate oxidation methods include the use of brucine.[17,19] However, both nitration and oxidation methods involve the use of reagents containing concentrated sulfuric acid and may require heating for color development; thus, the reagents require extreme care in handling and are subject to error if the sample contains organic matter which may char. In addition,

most of these methods are vulnerable to severe interference by chloride and nitrite.[17]

Instrumental methods include polarography (often prone to exhibit anomalous behavior and a large variety of interferences[20]), ultraviolet spectroscopy (disposed to interference by organic material and turbidity[17]), and ion-selective electrodes.[21] The use of ion-electrodes is simple and rapid, but most electrodes developed to date are subject to interference from nitrite, chloride, and bicarbonate.

Although the chemical methods for the determination of nitrate ion are not especially sensitive or selective, excellent methods exist for the determination of ammonia and nitrite ion. The reduction of nitrate ion has, therefore, attracted considerable attention. Devarda's alloy[22,23] has been used to reduce nitrate to ammonia; Raney nickel,[20] zinc metal,[17,24,25] and cadmium metal[17,20,26] have been used to reduce nitrate only to the stage of nitrite formation. Of these approaches, the cadmium reductor appears to be the most reliable and is the technique employed for the analysis of nitrate in surveillance and compliance monitoring studies by the Environmental Protection Agency.[27] All heterogeneous catalysts used in nitrate reduction are subject to surface deactivation. In addition, the presence of various complexing agents can determine both the completeness of the reaction and the oxidation state of the reaction product.[20]

Biological reduction of nitrate is quite common,[13,28] and several attempts have been made to utilize microorganisms or enzyme fractions as a reagent for the determination of nitrate. Garner et al.[29] used a microorganism isolated from the rumen of a sheep to reduce nitrate to nitrite, then analyzed the nitrite formed via the diazotization-coupling reaction

with sulfanilamide and N(1-naphthyl)-ethyldiamine. In a similar manner, Hill et al.[30] utilized the bacterium Pseudomonas oleovorans.

The majority of recent applications of enzyme fractions in the reduction of nitrate to nitrite have involved the nitrite reductase from Escherichia coli.[31-34] When this organism is grown under anaerobic conditions, nitrate is primarily used as an electron acceptor (in the place of oxygen), and the enzyme isolated under these conditions is referred to as "respiratory" nitrate reductase (EC 1.9.6.1), in contradistinction to the "assimilatory" nitrate reductase (EC 1.6.6.1) predominant in other organisms in which nitrate is used in the synthesis of nitrogen-containing cell constituents.[28] The commercially available respiratory enzyme[31] uses dithionite as an electron donor and the radical cation of methyl viologen as a cofactor. Both of these reagents are unstable and oxygen sensitive; indeed, the enzyme itself may become inactivated by air or traces of oxygen.[31] However, the enzyme is relatively stable in the absence of oxygen and has been successfully immobilized to produce an enzymatic reactor in an automated system for the determination of nitrate.[33] Hussein and Guilbault[34] have combined the respiratory nitrate reductase together with nitrite reductase (EC 1.6.6.4) from E. coli to reduce nitrate and nitrite to ammonia, which they have detected by the use of an ion-selective electrode.

We have investigated the utility of the assimilatory nitrate reductase of Neurospora crassa[28,35-37] as a reagent for the determination of nitrate ion in water. The enzyme isolated from Chlorella pyrenoidosa has also been proposed, although not utilized, as a specific reagent for the determination of small amounts of nitrate.[38]

Reagent preparation. Nitrate reductase enzyme preparations were provided by Dr. Su-Shu Pan of the Department of Biology, Johns Hopkins University, Baltimore, Maryland. Two batches of enzyme preparation were examined. The first batch (W_1-27-3) was purified through three steps[39] and was indicated to contain an enzymatic activity of approximately 36,000 units/ml and a protein content of 53 mg/ml. One unit is defined as the amount of enzyme necessary to produce 1 nmole of nitrite after a 10-min incubation with a 0.1 M nitrate sample in pH 7.2 phosphate buffer.[36] The second preparation (L_1-1-4) was similar but was indicated to contain an enzymatic activity of approximately 870,000 units/ml and a protein content of approximately 35 mg/ml. Additionally, the second preparation contained FAD (10^{-4} M) and phenylmethyl-sulfonylfluoride (a potent protease inhibitor) to further stabilize the enzyme.

"Preparation buffer" was prepared as described previously[36] and contained 0.1 M phosphate buffer (pH 7.3), 10^{-4} M 2-mercaptoethanol, and 5×10^{-4} M EDTA. NADPH-FAD reagent 1, used in the monitoring of enzymatic activity at 340 nm, was prepared by the addition of 3.5 ml of "preparation buffer" and 60 µl of 1 mg/ml FAD to a 5-mg vial of NADPH. A second NADPH-FAD reagent, for the determination of nitrite nitrogen, was prepared by the addition of 7.4 ml of preparation buffer and 600 µl of 1 mg/ml FAD to a 2-mg vial of NADPH.

Analytical method. One method for enzymatic measurement of nitrate is based on monitoring NADPH consumption at 340 nm. The first step in the procedure involved manually pipetting 45 µl of sample into the sample chamber of a standard multicuvet rotor. Cuvet 1, the reference, contains water only. The sample is spun out into the cuvet by acceleration to

4000 rpm on the analyzer, and then allowing the rotor to coast to rest. The rotor is then loaded by use of the automated sample-reagent loader:[10] 5 µl of enzyme preparation (plus 25 µl of diluent) are loaded into the sample chamber, and 30 µl of NADPH-FAD reagent 1 (and 35 µl of diluent) are loaded into the reagent chambers. The solutions are brought to 30°C on the CFA and then transferred. The progress of the reaction is monitored for about 500 sec after a delay interval of 10 sec.

A second method for the enzymatic determination of nitrate is based on measurement of its reduction product, nitrite, and is similar to that described previously.[36] Sample (100 µl), NADPH-FAD reagent 2 (400 µl), and enzyme preparation (20 µl) are mixed and incubated at room temperature for 30 min. Concentrations of NADPH and FAD in the incubation mixture are approximately 2.1×10^{-4} M and 0.7×10^{-4} M, respectively. The reaction is terminated by the addition of 900 µl of water and 500 µl of sulfanilic acid reagent (1 w/v % in 20% concentrated hydrochloric acid). Color development is initiated by the addition of 0.5 ml of N(1-naphthyl)-ethylenediamine reagent (0.12 w/v %). The color is permitted to develop for 10 to 20 min, then the absorbance of an aliquot of the reaction mixture is measured at 540 nm in the CFA.

Results and discussion. Nitrate reductase (reduced-NADP:nitrate oxidoreductase), EC 1.6.6.1, catalyzes the reduction of nitrate to nitrite:

$$\text{NADPH} + NO_3^- \xleftrightarrow[\text{reductase}]{\text{nitrate}} \text{NADP} + NO_2^- + H_2O \ . \qquad (1)$$

The enzyme isolated from N. crassa is a molybdo-enzyme and requires FAD as a cofactor.[35-37] We were interested in the possibility of using this enzyme for the analytical determination of nitrate by monitoring the

decrease in absorbance at 340 nm due to the oxidation of NADPH. Thus the assay would be amenable to the concept of a "nutrient rotor," whereby a number of related inorganic species, including soluble silica and orthophosphate,[11] and ammonia[40] could be analyzed simultaneously from a single water sample within one multicuvet rotor. All assays could be conducted under a single set of observation conditions (including monitoring wavelength, 340 nm).

Figure 2.18 is a plot of absorbance (340 nm) vs time for the enzymatic reduction of nitrate ion. There is a clear differentiation among the various concentrations of analyte; however, there is also a substantial "endogenous" consumption of NADPH in the blank reaction. The nature of this blank reaction will be discussed in detail later; however, it does present difficulties in the determination of nitrate ion by monitoring NADPH oxidation. Since a decrease in absorbance is being monitored, the blank cannot be used to establish "100% transmission" in a reference cuvet and thus be automatically subtracted from the analytical measurements. Also, since the initial concentration of NADPH must be finite, the consumption of NADPH in the absence of analyte must limit the sensitivity of the assay.

The first constraint on the use of an enzyme as an analytical reagent is probably the stability of the enzyme. One justification for the use of the respiratory enzyme from _E. coli_, with all the attendant difficulties in its use, instead of an assimilatory enzyme (such as that isolated from _N. crassa_) has been the assumed instability of the latter.[30,33-35] Table 2.9 illustrates the stability of two different preparations of _Neurospora_ nitrate reductase upon storage at 2 to 4°C. It has been

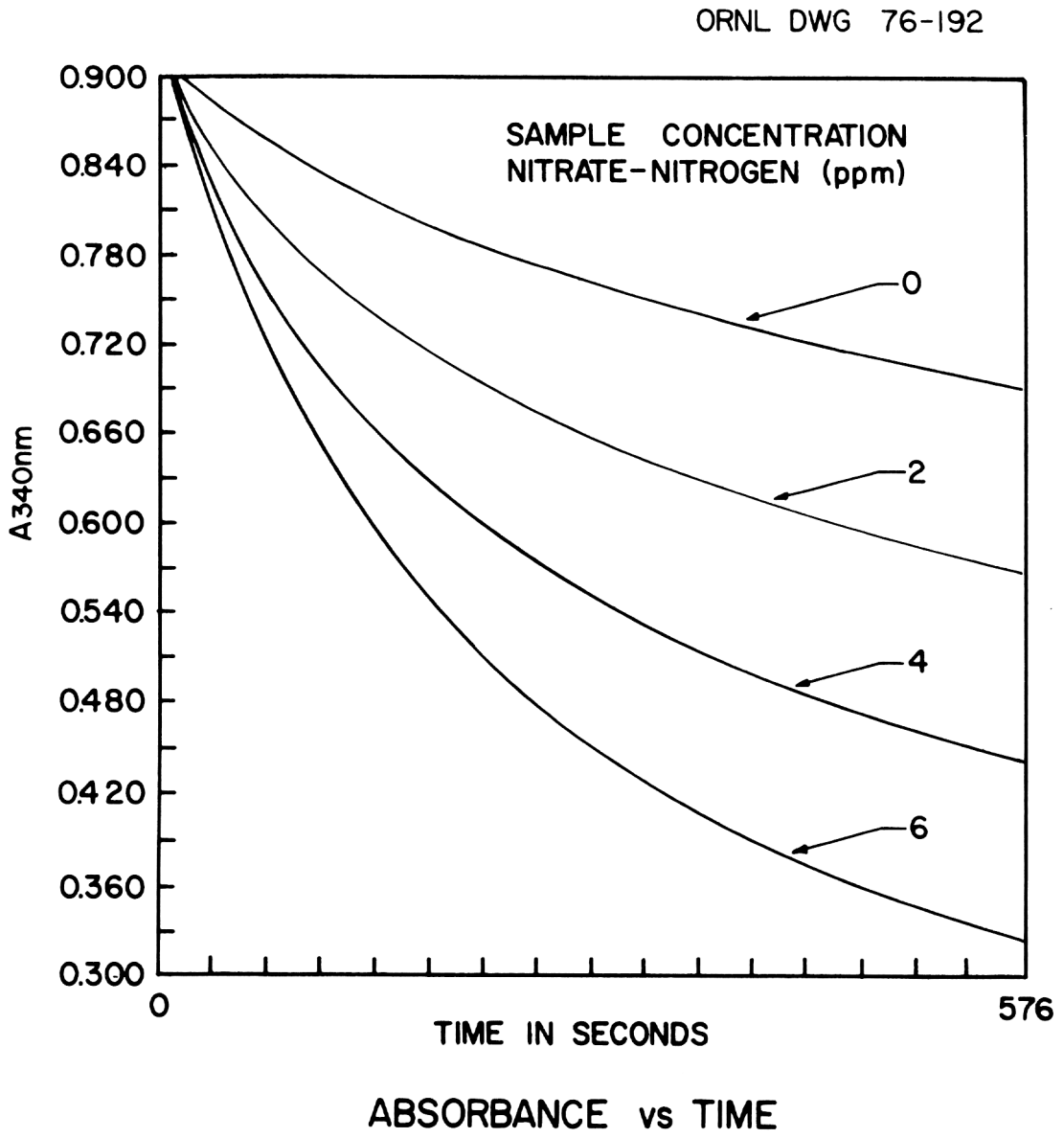

Fig. 2.18. Reaction progress curves for the enzymatic reduction of nitrate with N. crassa nitrate reductase. The decrease in NADPH in the absence of nitrate has been attributed to a "NADPH-dehydrogenase" activity in the enzyme.

Table 2.9. Stability of *N. crassa* nitrate reductase enzyme preparations to storage at 2 to 4°C

Time (hr)[c]	Initial velocity[a]		Relative initial velocity[b]
	Ø millimolar[d]	0.0459 millimolar[d]	0.0459 millimolar[d]
		Enzyme preparation W_1-27-3	
0.8	0.443	0.917	2.07
2.0	0.472	0.971	2.06
26.5	0.506	1.01	1.99
		Enzyme preparation L_1-1-4	
1.0	0.364	1.16	3.19
3.8	0.384	1.19	3.10
28.0	0.344	1.21	3.52

[a]Initial velocity, millimole/min.

[b]Velocity relative to blank reaction (i.e., to Ø millimolar NO_3^-).

[c]Hours of storage at 2 to 4°C after thawing of frozen enzyme.

[d]Reaction concentration of NO_3^-, millimolar (0.0459 millimolar reaction concentration corresponds to a sample concentration of 2.0 ppm NO_3^--N).

observed that the enzyme remains quite active for at least 3 days upon such storage, and is stable for prolonged periods of time when frozen, especially when in the presence of a protease-inhibitor such as phenylmethylsulfonylfluoride. The enzyme is not particularly stable, however, to repetitive freezing and thawing.[39] Improved isolation procedures have resulted in enzyme preparations of high activity and stability.

Figure 2.19 illustrates initial reaction velocity (calculated from the change in absorbance at 340 nm) as a function of analyte concentration. The analyte concentration for which the present assay is most sensitive (approximately 1 to 10 ppm nitrate-nitrogen sample concentration) extends beyond that for which an initial-rate analysis approach would be valid. Figure 2.20 is a Lineweaver-Burk plot for the reaction as monitored at 340 nm both with and without subtraction of the blank reaction. For the data in which the blank is subtracted, the apparent Michaelis constant, K_m, is estimated at 0.14 millimolar.[41] If one assumes that an initial rate approach is valid for substrate concentrations where the ratio of Michaelis constant to initial concentration of substrate ($K_m/[S]_o$) is ≥ 10,[42] then, for our conditions, the sample concentration of nitrate-nitrogen should not exceed approximately 1.6 ppm. Thus one would probably need to employ the additional sensitivity of a fluorometric measurement of NADPH consumption[43] in order to utilize an initial-rate approach for the determination of nitrate with this enzyme.

In Fig. 2.21, the change in absorbance at 340 nm is used to determine if the consumption of NADPH (corrected for the background consumption) is stoichiometric with respect to the reduction of nitrate. It can be clearly seen that the reaction at 8 min is stoichiometric for sample

ORNL DWG 76-185

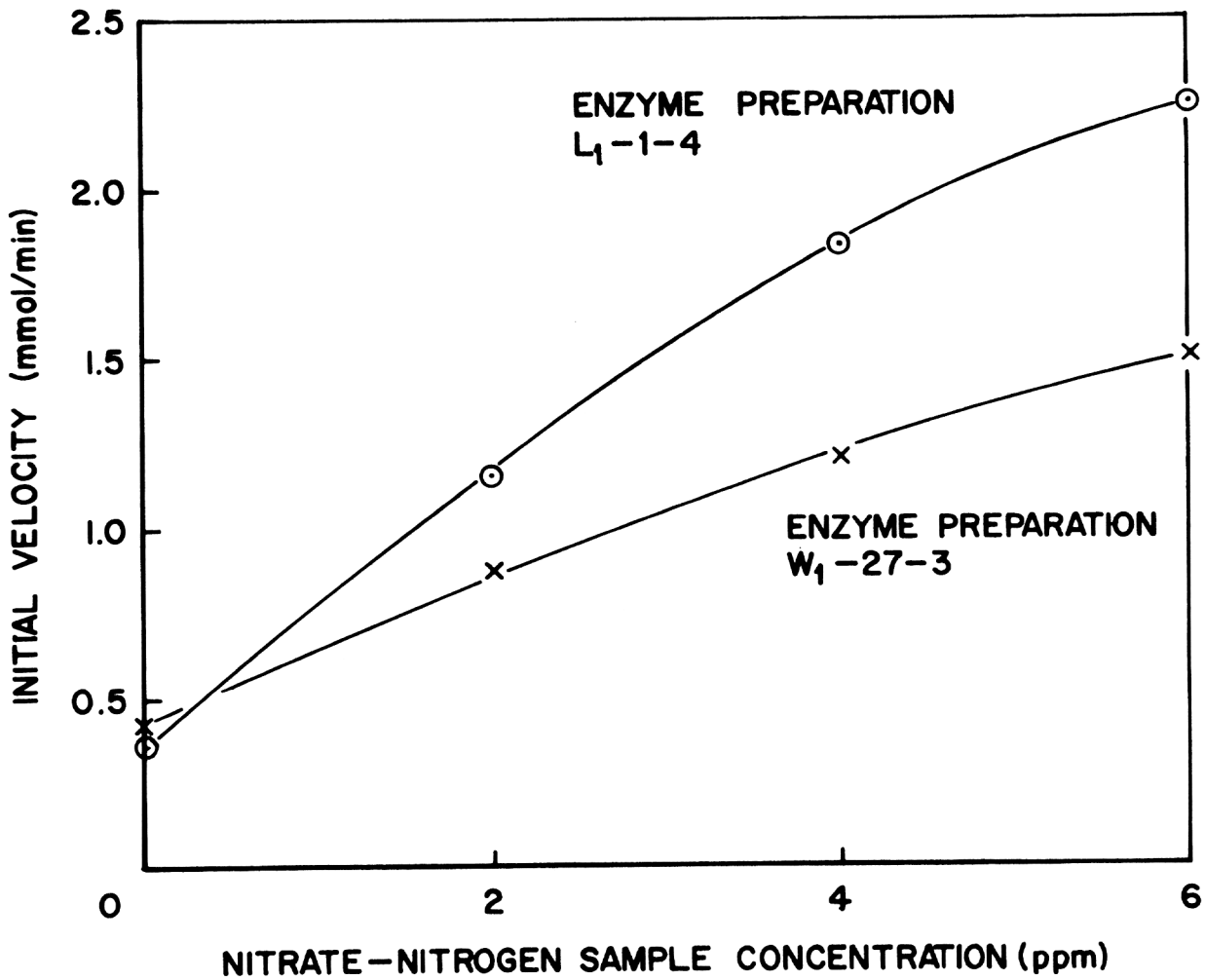

Fig. 2.19. Initial reaction velocity vs substrate concentration for two different preparations of nitrate reductase.

ORNL DWG 76-190

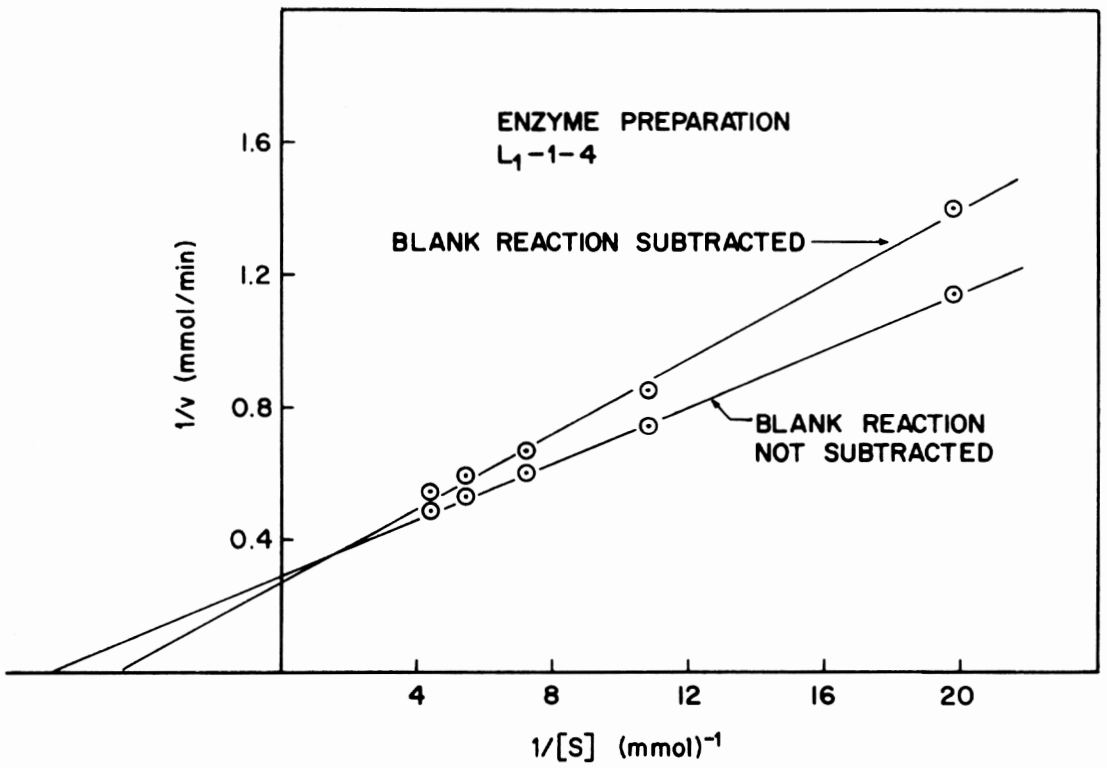

Fig. 2.20. Double-reciprocal (Lineweaver-Burk) plots for a preparation of nitrate reductase, both with and without subtraction of the blank reaction. Estimated kinetic parameters are K_m = 0.115 mM, V_{max} = 3.04 millimole/min (blank not subtracted), and K_m = 0.140 mM, V_{max} = 2.96 millimole/min (blank contribution subtracted). The enzyme preparation had been thawed and stored 1 day at 2 to 4°C prior to this experiment.

ORNL DWG-76-19IRI

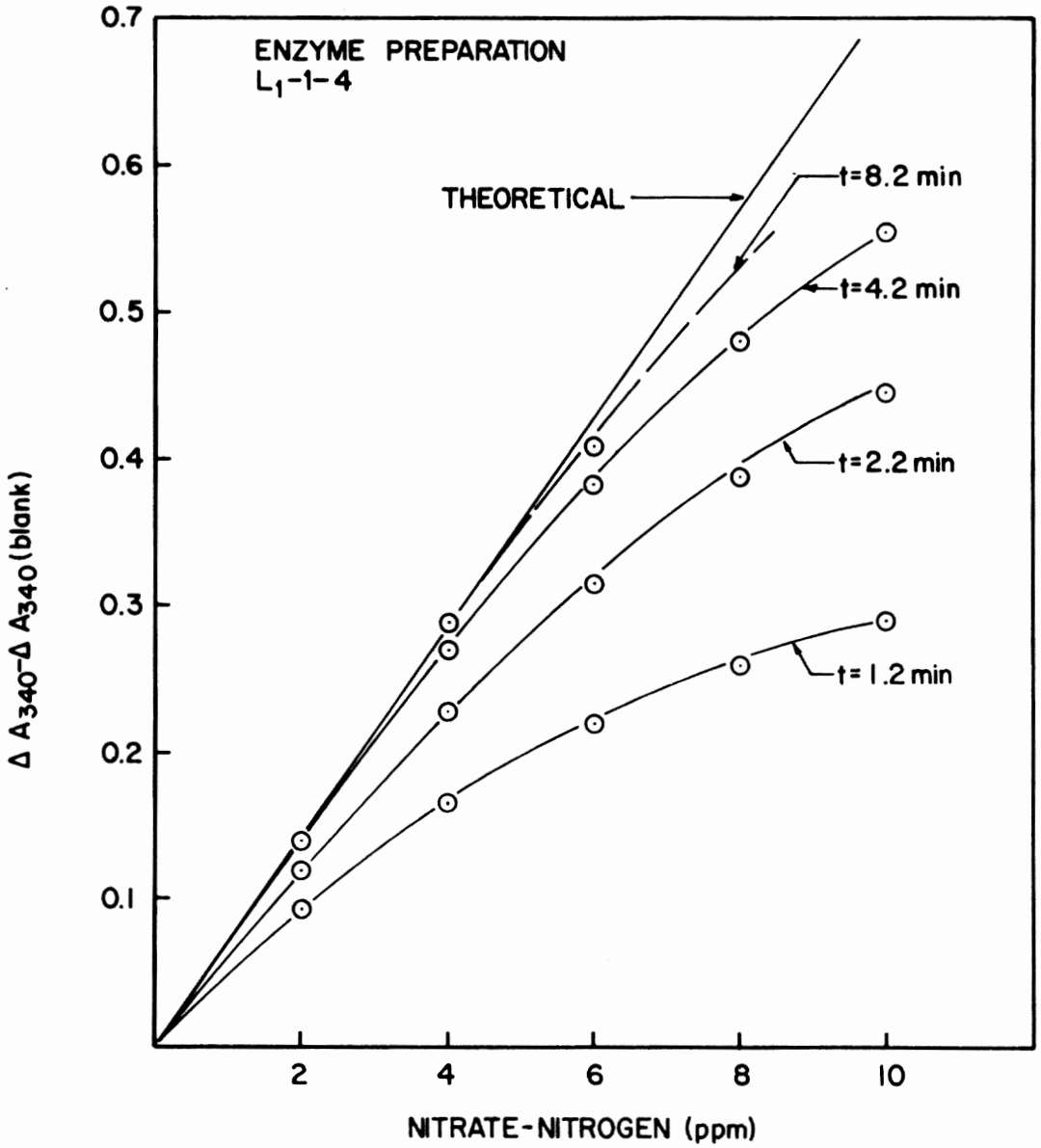

Fig. 2.21. Stoichiometry of enzyme reaction as monitored at 340 nm, with change in absorbance of blank reaction subtracted. The theoretical line is calculated on the basis of a stoichiometric consumption of NADPH (ε = 6220 liters mole cm^{-1}) with respect to nitrate ion present.

concentrations of ≤6 ppm nitrate-nitrogen. However, the substantial background reaction limits the availability of NADPH for the stoichiometric determination of much higher substrate concentrations.

We sought to elucidate this background reaction. Where it has been observed previously, it was attributed to endogenous NADPH consumption due to impure preparations of nitrate reductase.[36] If NADPH-specific enzymes and their substrates were present in the enzyme preparations, preincubation of the preparation in the presence of excess (1 mg/ml) NADPH should result in the elimination of the endogenous reaction. When this experiment was attempted (Fig. 2.22), a decrease in the relative rate of the endogenous reaction did occur (the rate of the analytical reaction was also decreased slightly); however, the endogenous reaction was not eliminated and continued until all the NADPH present had been consumed. If the enzyme preparation was contaminated by traces of nitrate, then "desalting" the preparation on Bio-Gel P-2 (exclusion limit, mol. wt 1600) would eliminate nitrate and any other low-molecular-weight substrates. This experiment was performed (FAD and NADPH were added to the diluted enzyme in the eluate); however, the effect was similar to preincubation with NADPH alone (Fig. 2.22).

In the absence of evidence that a specific substrate was responsible for the endogenous reaction, we considered the possibility that a NADPH dehydrogenase [reduced-NADP:(acceptor) oxidoreductase] may be present in the enzyme preparation.[44] The most probable electron acceptor in the system would be the added cofactor, FAD. Several inhibitors were investigated for the possible selective inhibition of the endogenous reaction: CN^- (5×10^{-5} M), Zn^{2+} (10^{-3} M), adenosine 2'-monophosphoric acid (10^{-3} M), and NADP (10^{-3} M). Cyanide and zinc were capable of an

ORNL DWG 76-186R1

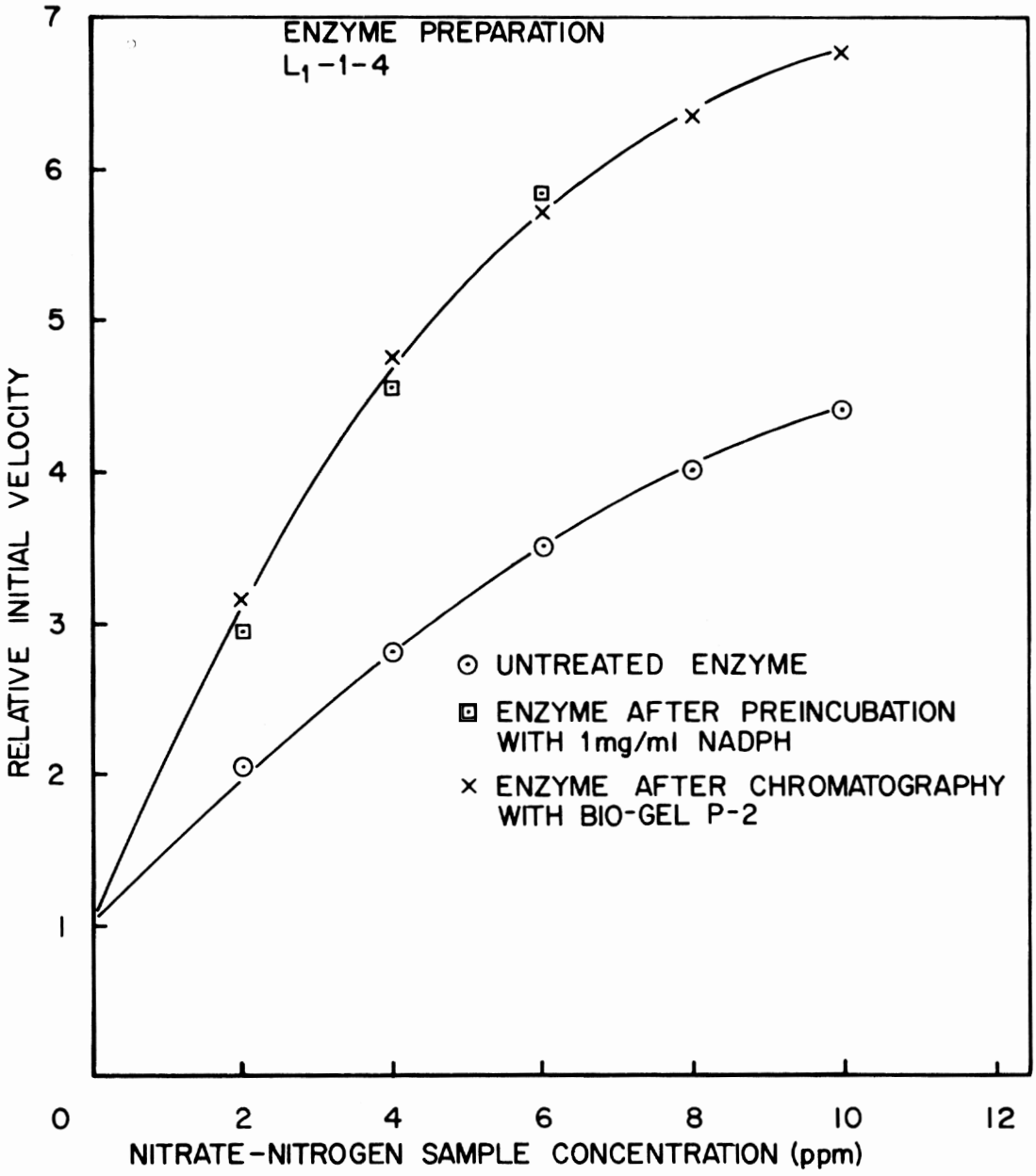

Fig. 2.22. Effect of pretreatment of enzyme preparation on the rate of the analytical reaction relative to the rate of the blank reaction. Preincubation of the enzyme with NADPH, desalting with Bio-Gel P-2, and preincubation with NADPH decreased the rate of the blank reaction but could not eliminate it.

inhibitory effect on the analytical reaction to some extent, but had much less effect on the endogenous reaction. Adenosine 2'-monophosphoric acid and NADP had little effect on either reaction.

The endogenous reaction was found to proceed rapidly in the presence of NADPH and FAD or FMN (flavin mononucleotide) and enzyme, even for very highly purified preparations of enzyme. However, the enzyme was unable to oxidize NADPH in the absence of nitrate, FAD, and FMN. This infers that the "NADPH-dehydrogenase" activity is part of the enzyme complex and involves FAD or FMN as an electron acceptor. The following mechanism has been proposed for the "endogenous" reaction:[45]

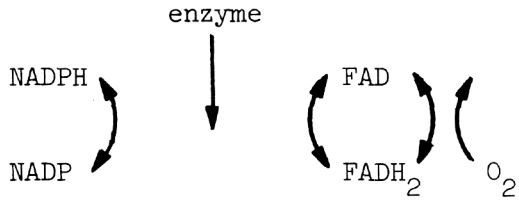

(2)

The net effect is oxidation of NADPH in the presence of FAD and the absence of nitrate. The FAD is regenerated by air-oxidation and is available as a cofactor in the analytical reaction. If the proposed mechanism is correct, the relative contribution of the blank may be diminished if the reaction is conducted anaerobically.

Since determination of nitrate by the amount of NADPH consumed is somewhat complicated by the blank reaction, we have investigated the possibility of the chemical determination of the nitrite formed via diazotization-coupling with sulfanilic acid and N(1-naphthyl)-ethylenediamine. The procedure used is similar to that used by Garrett and Nason[36] for determining enzymatic activity except that conditions are modified in order to permit the enzymatic reaction to proceed to completion with sample

concentrations of 0 to 10 ppm nitrate-nitrogen prior to the diazotization reaction. The recovery of nitrite ion carried through the enzymatic reaction is estimated at 93 to 95% (the recovery of nitrite ion via the respiratory enzyme is reported to be 85 to 90%).[31] With the assimilatory enzyme preparations tested, conversion of nitrate-nitrogen to nitrite-nitrogen is 102 to 104% of the recovery of nitrite-nitrogen. The absorbance at 540 nm is linear with respect to initial concentration of nitrate-nitrogen over the sample concentration range 0 to 10 ppm ($r = 0.9997$, relative standard error 1.0%) (see Fig. 2.23). The final absorbance of a 5-ppm nitrate-nitrogen sample carried through this procedure is precise to 1 to 2%, and the sensitivity (estimated as two times the standard deviation of the determination of a 5-ppm NO_3^--N standard divided by the slope of the linear least-squares calibration curve) is 0.1 to 0.2 ppm nitrate-nitrogen. Since the primary interferent in most chemical determinations of nitrate is chloride ion, we analyzed a 5.0-ppm NO_3^--N standard in 0.7 M NaCl (approximating the ionic strength of sea water) and "found" 4.93 ppm, for an error of -1.4%.

Conclusions. An endogenous NADPH-consuming blank reaction, attributed to a "NADPH-dehydrogenase" activity of the enzyme in the presence of FAD, complicates the determination of nitrate-nitrogen by the *N. crassa* nitrate reductase, based on the amount of NADPH oxidized. If nitrate is to be analyzed in this manner, the enzyme from another source [e.g., *Chlorella vulgaris* (Berlin strain)][46] may be preferred. The latter enzyme does not require added FAD as a cofactor, can utilize NADH as well as the less-stable NADPH, and the enzyme itself is reported to be very stable.[41] The analytical utility of this enzyme will be investigated in the future.

ORNL DWG 76-187

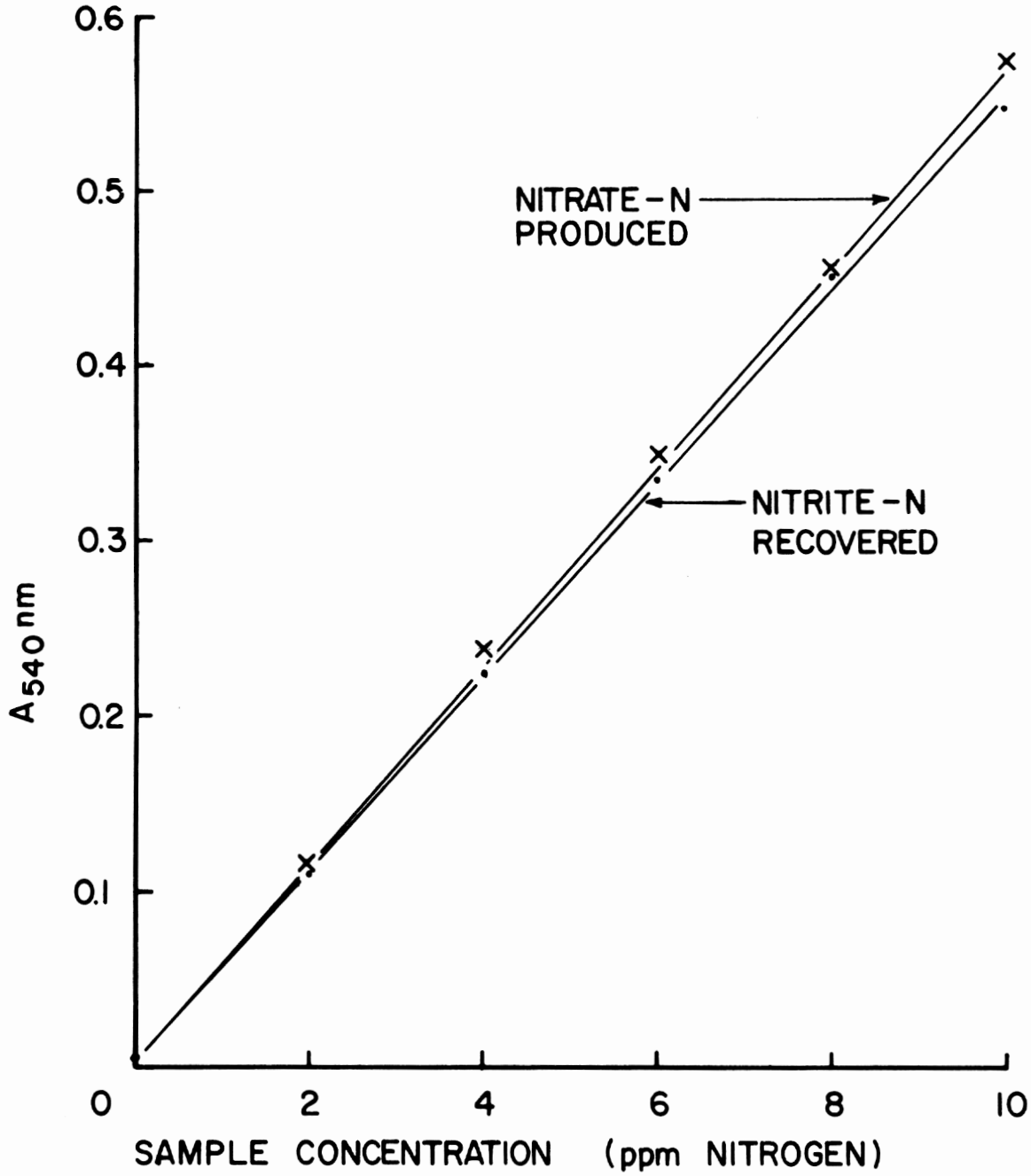

Fig. 2.23. Recovery of nitrite-nitrogen added and conversion of nitrate-nitrogen to nitrite-nitrogen, as determined by absorbance at 540 nm after diazotization-coupling reaction.

The combination of the enzymatic reduction of nitrate with the colorimetric determination of nitrite formed has the advantage of selectivity, sensitivity, and the stoichiometric conversion of nitrate to nitrite. When nitrate is present in high concentration, it may be desirable to recycle the NADPH in situ rather than have large initial concentrations of NADPH (which may interfere in the color-development of the nitrite reaction).[37] For example, hexokinase and ATP could be added to the enzyme preparation, and an excess of glucose added with the sample:

$$\begin{array}{ccc} \text{NADP} + \text{glucose} & \xleftrightarrow{\text{hexokinase}} & \text{NADPH} + \text{glucose-6-phosphate} \\ + & & + \\ \text{ATP} & & \text{ADP} \end{array} \qquad (3)$$

Thus NADPH could be maintained at a constant, low concentration.

The respiratory enzyme has been successfully immobilized in an enzymatic reactor, with the nitrite formed subsequently determined automatically in a flow system.[32] A similar procedure may be possible for the present enzyme in a much-simplified system.

2.3.2 Development of CFA rotors preloaded with reagent

One of the ultimate objectives of the CFA program is to develop rotors that contain preloaded quantities of reagent in each cuvet. With this type of rotor, the reagents would be dissolved and reconstituted at the time of analysis by the dynamic introduction of water or buffer. For the past 3 years, we have been developing such rotors, and feasibility studies have demonstrated that reagents can be lyophilized and reconstituted within the cuvets of the rotor.[47]

Following the feasibility studies, we initiated collaborative programs with two reagent manufacturers since we felt that such an arrangement would

couple the ORNL Centrifugal Fast Analyzer technology with the in-house reagent technology of the commercial firms. Consequently, subcontracts were awarded to the Worthington Biochemical Corporation and to Smith Kline Instruments (SKI). Each firm has utilized a different approach in loading the reagents into the cuvets of the rotor. For example, Worthington has utilized the technique of freeze drying (lyophilization) in which aliquots of the liquid reagent are loaded into the cuvets, and the liquid is then removed by lyophilization. Smith Kline, on the other hand, will prepare the reagents in tablet form, and one tablet will be loaded into and sealed within each individual cuvet.

Lyophilized reagents. Worthington supplied us with a total of 40 loaded rotors, 10 for each of four chemical assays (i.e., glucose, SGOT, alkaline phosphatase, and LDH-L). The rotors to be loaded were shipped from ORNL to Worthington in partially assembled fashion (i.e., the rotor body plus the bottom window as one component and the top cover window as the second component). Worthington then prepared the reagents in liquid form and loaded them into the rotors by pipetting an aliquot of the appropriate reagent (containing the necessary quantities of reactants) into cuvets 2 through 17. The reagents were subsequently lyophilized in situ, and a top cover window was placed onto each rotor and fastened with a rubber band. After each individual rotor had been inserted into a plastic bag containing a small bag of desiccant. the entire batch of rotors was shipped to ORNL. On arrival, they were assembled by bonding a cover window to the rotor body--bottom window component and then placed into individual bags which were stored in desiccators at 0°C. At desired intervals, the rotors were removed from the desiccators and evaluated by comparing the values obtained

with the lyophilized reagents with those for freshly prepared Worthington reagents (Statzyme kits).

Evaluation of these rotors[4] has demonstrated that reagents can be lyophilized in the cuvets of a rotor in situ by the reagent manufacturer and that, subsequently, they can be easily reconstituted and used for analysis. Some difficulties were encountered with regard to the quantities of reagent used for the various assays, but they can probably be eliminated by increasing the concentration of each reagent prior to lyophilization. The instability of the LDH-L reagent also poses a problem; however, it is hoped that these difficulties can be minimized by lyophilizing the reactants for this reagent in separate chambers of the rotor or by utilizing a different buffer.

Reagents in tablet form. An alternative to in-situ lyophilization of the reagents is the use of reagent tablets. These tablets would be sealed into designated cuvets and reconstituted prior to analysis. Ease and flexibility in loading are the attractive features of this approach. In addition to the general chemical problems expected to be encountered, potential physical problem areas with this approach would include: (1) dissolution time, (2) manufacture and quality control of the small tablets (10 mg), and (3) low percentage of reactants per tablet. Smith Kline chose to supply the reagents in tablet form because they routinely manufacture and market the Eskalab line of reagent tablets and thus have had considerable experience with reagent tablet technology. Due to the potential problems associated with their manufacture, SKI first supplied us with four different placebo tablet formulations. This allowed us to study some of the problem areas that are associated with the small tablets,

such as dissolution time and tablet reproducibility. The evaluation[4] indicated that effervescent formulations will dissolve in 2 min or less, while the noneffervescent ones may require up to 15 min for complete dissolution. Reagent stability is a problem with the effervescent formulation since tablets of this type lost from 20 to 80% of their optical activity when stored in the rotors for two days or more. An improved technique in the assembly and storage of the rotors that contain tablets has decreased the loss of optical activity, especially in the case of the noneffervescent formulation and, therefore, will probably be the preferred choice for future reagent tablets. This type of formulation requires a longer time for dissolution, but the reagent appears to be more stable.

(Glucose tablets.) Following the evaluation of the placebo formulations, 10-mg tablets containing reagents for the hexokinase glucose assay were received from SKI. They supplied the following specifications and performance data for lot No. 30-3-109:

Description: These tablets were formulated to yield 130 µl of reagent which meets the same performance specifications as our Glucose-Pipes "Spin Chem" product.

	Specification	Measured
(1)	pH 7.5 ± 0.1	7.54 ± 0.034, n = 9
(2)	O.D. <0.200 (340 nm, 1 cm cell)	0.1664 ± 0.014, n = 18 (1 tab/520 µl = O.D. x 4)
(3)	Weight 10.0 mg ± 0.5 mg	10.0 mg ± 0.505, n = 20
(4)	Dissolution time <1 min	24 sec, n = 20
(5)	Activity:	
	With 250 mg/dl glucose std.: 100% ± 5% theoretical recovery	252.5 ± 4.3, n = 9, at 3 min 254.5 ± 4.0, n = 9, at 6 min
	With 400 mg/dl glucose std.: 100% ± 5% theoretical recovery	386.2 ± 5.6, n = 9, at 3 min 392.3 ± 5.3, n = 9, at 6 min

In an early evaluation, four rotors were loaded with glucose tablets and then used to assay aqueous solutions of glucose. In this experiment, the tablets were reconstituted by first loading 70 μl of distilled water into each reagent chamber using the sample-reagent loader. The rotor was then placed into the analyzer, and the aliquots of water were transferred into respective cuvets by accelerating the rotor to 700 rpm and then allowing it to coast back to approximately 50 rpm.* After 10 min at this low speed, the rotor was accelerated to 4000 rpm and dynamically braked. Two such cycles were performed, followed by a final acceleration to 4000 rpm and a coasting to stop. The rotor was then returned to the loading station, and 2 μl of sample plus 50 μl of diluent were loaded into their respective sample chambers. The loaded rotor was then returned to the analyzer and the samples assayed for their glucose content. In general, precise results were obtained at all four glucose concentrations. In regard to accuracy, the results from all samples were from 6 to 9% higher than expected. However, since the samples had been prepared several weeks previously, evaporation could be responsible for the higher results. In addition to the glucose measurements, the reagent blank for nine of the tablets was also measured. The resulting mean value of 0.1169 was within that specification for the tablets (i.e., <0.200) and the tablet-to-tablet precision of ±9.71% is comparable to that observed for the placebo tablets.[4]

Following the initial evaluation, a 10-week stability study was initiated in order to assess the chemical stability of the tablets once they were sealed within the cuvets of the rotor. In this study, ten

---

*Note: We have observed that if the liquid is transferred at a higher rotor speed, the particles produced by the dissolving tablets will pack tightly at the outer edge of the cuvets. It is then difficult to get this material into solution.

rotors were filled with the glucose tablets, each placed in a plastic bag and stored in a vacuum desiccator at 0°C. At weekly intervals, a rotor was removed, the tablets reconstituted as described previously, and used to measure the glucose concentration of five aqueous glucose standards (note: for each rotor, three replicate aliquots were assayed at each concentration, with one cuvet receiving no sample and thus serving as a reagent blank). For comparative purposes, the same samples were assayed using freshly prepared CalBiochem and SKI glucose reagents. The CalBiochem reagent was reconstituted by dissolving the contents of a kit in 2 ml of water. The sample reagent loader was then used to load the following volumes: 20 µl of reagent and 50 µl of reagent diluent, 2 µl of sample and 50 µl of sample diluent. With the freshly prepared SKI glucose reagent, a vial of the SKI glucose tablets was removed from the freezer, and the 20 tablets contained in the vial were dissolved in 800 µl of distilled water. The following volumes were then loaded using the sample-reagent loader: 40 µl of reagent and 50 µl of reagent diluent, 20 µl of sample and 30 µl of sample diluent.

The data obtained from this study are summarized in Tables 2.10-2.13. In general, the data show that equivalent, accurate, and precise results were obtained from the tablet formulations as compared to the CalBiochem reagent kit. Sealing the tablets in the cuvets had no adverse effect on the reagents, as essentially identical results were obtained with both the tablets stored in the cuvets for up to 10 weeks and from tablets obtained from vials opened on the day of the assay. The analytical precision of the tablets stored in situ was slightly poorer (Table 2.12), but differences are probably too small to be meaningful. In Table 2.13, the absorbance of the reagent blank was higher and less precise than that of the tablet

Table 2.10. Within-day variation - glucose reagent tablet stability test

STANDARD #1-50 MG/DL

	CAL. BIOCHEM			S.K. IN SITU			S.K. FRESH		
EXP.#	MEAN	SD	RSD	MEAN	SD	RSD	MEAN	SD	RSD
1	50.20	0.27	0.53	50.63	0.49	0.98	48.87	0.42	0.86
2	51.93	0.32	0.62	52.78	2.73	5.17	50.98	0.68	1.34
3	52.92	1.12	2.11	52.93	0.80	1.51	49.93	1.44	2.89
4	51.32	0.65	1.26	48.26	0.41	0.84	50.36	0.21	0.41
5	51.69	0.44	0.86	49.79	0.77	1.55	48.50	1.68	3.46
6	51.10	0.20	0.39	49.49	0.60	1.22	49.68	0.87	1.75
7	52.13	0.57	1.09	51.32	0.97	1.88	50.45	0.96	1.90
8	52.06	0.17	0.32	49.55	0.37	0.74	50.95	0.10	0.19
9	52.06	0.16	0.30	48.90	0.97	1.99	50.76	1.15	2.26
10	50.24	1.18	2.34	51.14	0.05	0.09	49.55	0.32	0.65

STANDARD #2-100 MG/DL

	CAL. BIOCHEM			S.K. IN SITU			S.K. FRESH		
EXP.#	MEAN	SD	RSD	MEAN	SD	RSD	MEAN	SD	RSD
1	99.97	0.29	0.29	98.73	1.03	1.04	99.07	0.74	0.75
2	105.37	0.82	0.77	98.21	3.04	3.09	104.45	1.03	0.99
3	107.33	2.24	2.09	102.39	4.41	4.30	103.02	1.45	1.40
4	105.12	1.30	1.24	98.53	0.73	0.74	103.67	0.70	0.67
5	104.06	0.44	0.43	99.68	0.54	0.55	102.41	1.16	1.14
6	102.93	1.04	1.01	96.94	4.81	4.96	102.50	0.62	0.60
7	104.62	0.74	0.70	103.15	1.03	1.00	104.01	0.83	0.80
8	103.90	0.50	0.48	102.25	0.77	0.76	104.18	0.48	0.46
9	103.91	0.12	0.11	99.87	0.97	0.97	103.06	1.80	1.74
10	102.88	1.97	1.91	101.74	0.45	0.44	98.19	3.29	3.35

STANDARD #3-200 MG/DL

	CAL. BIOCHEM			S.K. IN SITU			S.K. FRESH		
EXP.#	MEAN	SD	RSD	MEAN	SD	RSD	MEAN	SD	RSD
1	199.47	0.85	0.43	197.77	1.16	0.59	201.33	1.10	0.55
2	207.57	1.07	0.52	204.77	0.62	0.30	206.01	3.69	1.79
3	208.22	1.44	0.69	202.02	3.29	1.63	204.65	3.14	1.54
4	203.25	0.27	0.13	199.05	2.07	1.04	202.68	2.21	1.09
5	203.76	1.42	0.70	197.29	1.47	0.74	199.88	1.94	0.97
6	205.17	0.96	0.47	196.66	4.41	2.24	202.75	0.76	0.37
7	206.07	1.51	0.73	202.82	0.91	0.45	205.25	2.55	1.25
8	205.92	1.88	0.91	199.06	2.99	1.50	204.70	1.42	0.69
9	205.15	1.22	0.59	200.17	3.07	1.54	201.38	0.60	0.30
10	200.61	1.69	0.84	198.28	0.32	0.16	197.20	3.18	1.62

STANDARD #4-300 MG/DL

	CAL. BIOCHEM			S.K. IN SITU			S.K. FRESH		
EXP.#	MEAN	SD	RSD	MEAN	SD	RSD	MEAN	SD	RSD
1	297.70	1.10	0.37	293.17	2.92	1.00	301.90	3.03	1.01
2	308.63	2.50	0.81	307.82	6.85	2.23	306.91	3.38	1.10
3	314.81	3.12	0.99	304.86	4.26	1.40	309.74	5.93	1.92
4	304.76	3.10	1.02	290.01	2.57	0.89	308.64	5.25	1.70
5	302.41	0.60	0.20	294.40	1.44	0.49	302.93	2.94	0.97
6	303.67	2.58	0.85	296.12	3.14	1.06	306.86	1.61	0.52
7	308.72	4.01	1.30	297.63	7.31	2.46	308.26	3.47	1.12
8	304.37	0.79	0.26	297.96	1.26	0.42	307.44	1.71	0.56
9	304.18	2.35	0.77	297.67	4.57	1.53	309.46	1.44	0.47
10	304.12	1.62	0.53	293.74	2.00	0.68	299.67	1.67	0.56

STANDARD #5-400 MG/DL

	CAL. BIOCHEM			S.K. IN SITU			S.K. FRESH		
EXP.#	MEAN	SD	RSD	MEAN	SD	RSD	MEAN	SD	RSD
1	376.20	1.32	0.35	387.77	7.15	1.84	402.57	2.94	0.73
2	397.23	3.62	0.91	396.46	5.31	1.34	406.64	3.36	0.83
3	403.63	6.11	1.52	404.96	0.58	0.14	406.74	2.57	0.63
4	394.80	4.63	1.17	392.75	9.04	2.30	401.52	5.55	1.38
5	390.06	2.54	0.65	387.99	2.97	0.77	395.67	2.02	0.51
6	394.20	1.53	0.39	394.48	1.85	0.47	397.22	2.21	0.56
7	395.45	5.18	1.31	402.50	6.14	1.53	410.38	5.40	1.32
8	397.50	0.79	0.20	397.44	0.41	0.10	406.92	3.83	0.94
9	393.65	1.47	0.37	396.39	5.36	1.35	405.35	4.18	1.03
10	397.97	1.39	0.35	387.63	1.02	0.26	393.86	2.53	0.64*

Table 2.11. Day-to-day variation - glucose reagent tablet stability test

	CAL. BIOCHEM			S.K. IN SITU			S.K FRESH		
STD. #	MEAN	SD	RSD	MEAN	SD	RSD	MEAN	SD	RSD
1	51.57	0.98	1.90	50.48	1.76	3.48	50.00	1.13	2.27
2	104.01	2.09	2.01	100.15	2.84	2.83	102.46	2.39	2.33
3	204.52	2.93	1.43	199.79	3.24	1.62	202.58	3.26	1.61
4	305.34	4.83	1.58	297.34	6.24	2.10	306.18	4.38	1.43
5	394.07	7.50	1.90	394.84	7.11	1.80	402.69	6.15	1.53

Table 2.12. Comparison of precision data obtained with three glucose reagent preparations

Reagent	Average within-day (± RSD)	Average day-to-day (± RSD)
CalBiochem	0.78	1.76
SKI tablets[a]	1.32	2.37
Fresh	1.12	1.83

[a]In-situ preparation.

Table 2.13. Reagent blank absorbance

EXP. #	CAL. BIOCHEM.	S.K. IN SITU	S.K. FRESH
1	0.0216	0.0952	0.0747
2	0.0223	0.1510	0.0672
3	0.0285	0.1003	0.0766
4	0.0269	0.0848	0.0673
5	0.0301	0.1072	0.0711
6	0.0308	0.1330	0.0684
7	0.0299	0.1255	0.0723
8	0.0287	0.1062	0.0789
9	0.0287	0.1184	0.0725
10	0.0282	0.1247	0.0698
Mean	0.0276	0.1146	0.0719
SD[a]	0.0032	0.0197	0.0040
RSD, %[b]	11.46	17.18	5.49

[a]SD = standard deviation.

[b]RSD = relative standard deviation.

reagents prepared fresh daily from the vial. However, it should be noted that the latter variation is actually for vial-to-vial differences, while the in-situ variation is for tablet-to-tablet. A larger tablet-to-tablet as opposed to vial-to-vial variation was also noted when the placebo tablets were studied.[4]

In summary, the 10-week stability study demonstrated that the glucose reagent tablets could be sealed with the cuvets of the rotor and are stable there for at least up to ten weeks.

(SGOT tablets.) On January 8, 1976, tablets containing reagents for the SGOT assay were received from SKI. The following specifications and performance data were supplied by SKI for lot No. 30-4-40 of the SGOT tablets:

	Specification	Measured
(1)	pH 8.0 ± 0.1	8.02 ± 0.02
(2)	O.D. 1.30 ± 0.05 (340 nm, 1-cm cell)	1 tablet per 1.3 ml di H_2O = 0.146 ± 0.006, n = 25, C.V. = 4.1%
		10 tablets per 1.3 ml di H_2O = 1.348 ± 0.01, n = 11, C.V. = 1.0%
(3)	Weight 10.0 mg ± 0.5 mg	9.99 mg ± 0.2 mg, n = 15, C.V. = 2.0%
(4)	Dissolution time	34 sec
(5)	Activity:	
	No. 4448 Eskalab abnormal at 30°C. Range 54 - 70 I.U.	56 ± 2.1, n = 8
	No. 4381 Eskalab normal at 30°C Range 16 = 22 I.U.	18 ± 2.0, n = 5

Initially, three rotors were loaded with tablets and used for preliminary studies. The tablets in two of the rotors were reconstituted by dissolving

each in 130 µl of distilled water using the same procedure as described above. The absorbances at 340 nm of the resulting solutions are summarized in Table 2.14 and confirm the SKI specification.

In another experiment, the tablets in the rotor were reconstituted with 70 µl of water and used to assay serial dilutions of a Hyland control sample. For comparative purposes, a fresh vial of the SKI tablets was opened and reconstituted by dissolving the 20 tablets in 800 µl of distilled water. Forty microliters of this reagent was then used per assay. The resulting data are summarized in Table 2.15. Equivalent results were obtained from both preparations. A 10-week stability test with these tablets is currently in progress.

2.3.3 Adaptation of Coombs test

Methods of blood grouping have been tested for their compatibility with Centrifugal Fast Analyzer technology, and a protocol has been developed for use of the CFA in this important blood-banking procedure. Quite naturally, this work has led into investigations concerning the utility of the CFA in various cross-matching procedures especially concerning its use as a sensitive detector of hemagglutination.[48,49] Some of the major factors necessary for antiglobulin testing were evaluated on the CFA by using a rotor in which cell suspensions could be washed in situ and hemagglutination measured by changes in light transmission.[49] Previously, a study of the performance of the antiglobulin test, especially as applied to cross-matching procedures with the CFA and cell washing rotor, was reported.[4]

Problems resulting in inefficient removal of wash solution from the cuvets during aspiration of the wash solution had been encountered previously. It was determined that the problems were associated with the

Table 2.14. Absorbances of Smith Kline SGOT tablets

	N	Absorbance (340 nm, 0.5-cm cell)		
		Mean	SD[a]	RSD[b] (%)
Rotor 1	16	0.6847	0.0139	2.02
Rotor 2	16	0.6731	0.0247	3.67
Combined	32	0.6789	0.0206	3.03

[a]SD = standard deviation.

[b]RSD = relative standard deviation.

Table 2.15. Comparison of SGOT enzyme activities obtained using Smith Kline SGOT reagent tablets: in situ vs fresh preparation

		Activity (IU/liter, 30°C)					
		In situ			Fresh		
Standard	Dilution Ratio	Mean	SD[a]	RSD[b] (%)	Mean	SD[a]	RSD[b] (%)
Blank	--	5.21	--	--	7.79	--	--
Standard 1	1:20	11.65	1.00	8.60	14.74	0.52	3.55
Standard 2	1:10	29.25	3.16	10.81	27.23	1.45	5.34
Standard 3	1:5	50.71	1.03	2.03	48.92	2.00	4.09
Standard 4	1:2	123.19	6.48	5.26	118.44	2.40	2.03
Standard 5	Stock	241.54	5.66	2.34	236.10	2.75	1.17

[a]SD = standard deviation.

[b]RSD = relative standard deviation

rotary seal. A loose fit between the Teflon ball and rotor apparently was causing unequal distribution of vacuum between individual cuvets in the rotor, resulting in inefficient removal of the wash solution from some cuvets. A new seal, made of Rulon®, with an O-ring gasket, a locking pin under the seal, and beveled to fit a stainless steel adapter was fabricated for the present study (see Fig. 2.24).

Experimental study of the reproducibility of aspiration. A series of experiments, using 50-µl aliquots of Blue Dextran (8 mg/ml) and 80-µl aliquots of water for a total volume per cuvet of 130 µl, was performed to determine the effectiveness of liquid removal at three rotational speeds (500, 600, and 700 rpm). Liquid additions were discretely loaded (using the rotor-loading station to add accurate volumes of 130 µl of water to each sample/reagent chamber) or dynamically loaded by injecting 2.21 ml (130 µl per cuvet) into the center of the rotor while rotating at 2500 rpm. The results of these experiments indicated that discrete additions of wash solution resulted in the most complete removal of dye at all rotational speeds (compare Figs. 2.25 to 2.27). However, if four aspirations were performed under dynamic washing conditions, a reproducible amount of the original dye solution was removed; the most complete removal was at a rotational speed of 600 rpm (see Table 2.16).

Experiments were performed to study possible cell losses during the in-situ washing step. Serial dilutions of whole blood were made with normal saline (1:100, 1:200, 1:500, and 1:1000). Fifty-microliter aliquots of a single dilution were loaded into the sample chambers of the rotor, and 80-µl aliquots of saline were placed in the reagent chambers. The rotor was then placed on the rotor holder and accelerated to 4000 rpm; it was

PHOTO 0727-76

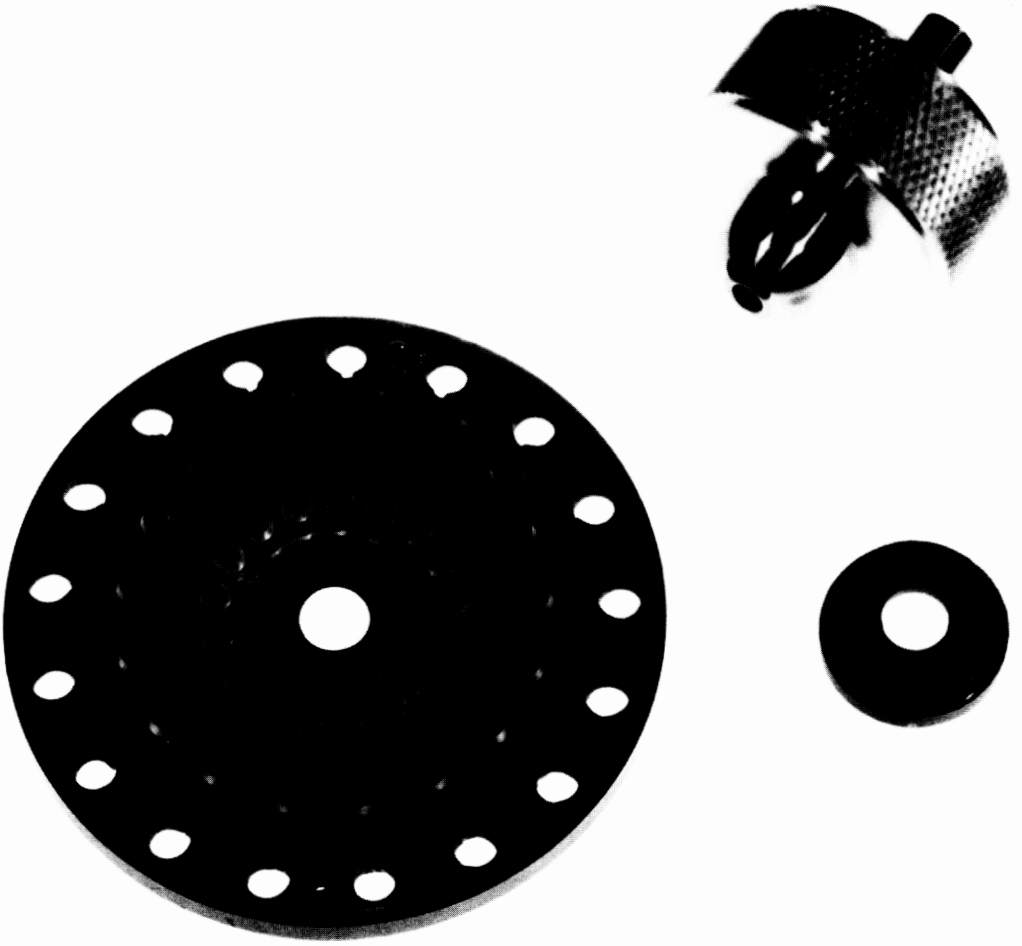

Fig. 2.24. Rotor with new Rulon® seal and adapter for in-situ washing of erythrocytes.

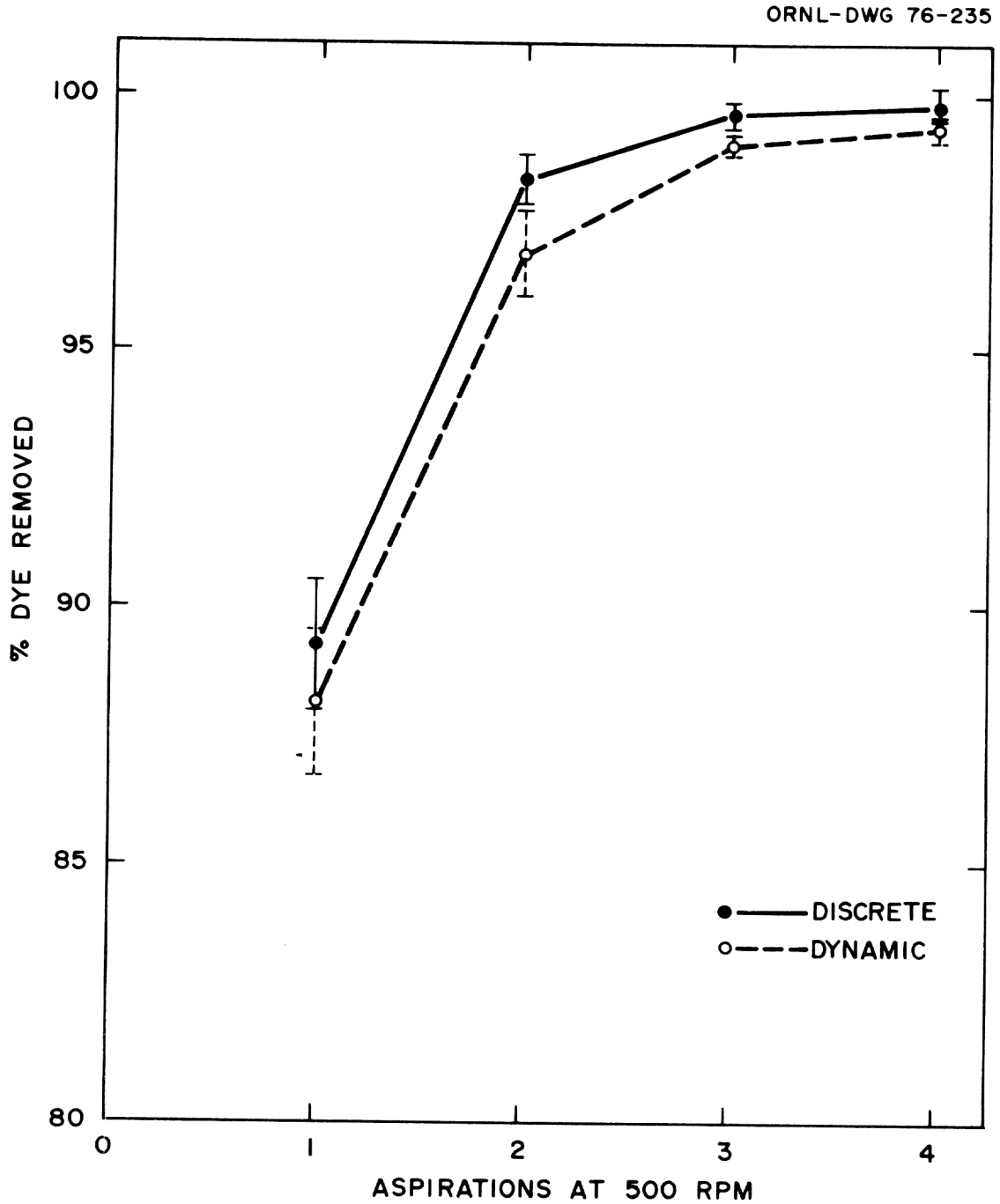

Fig. 2.25. Comparison of discrete vs dynamic additions of a washing solution to the cell-washing rotor studying removal of a dye solution with aspirations at 500 rpm.

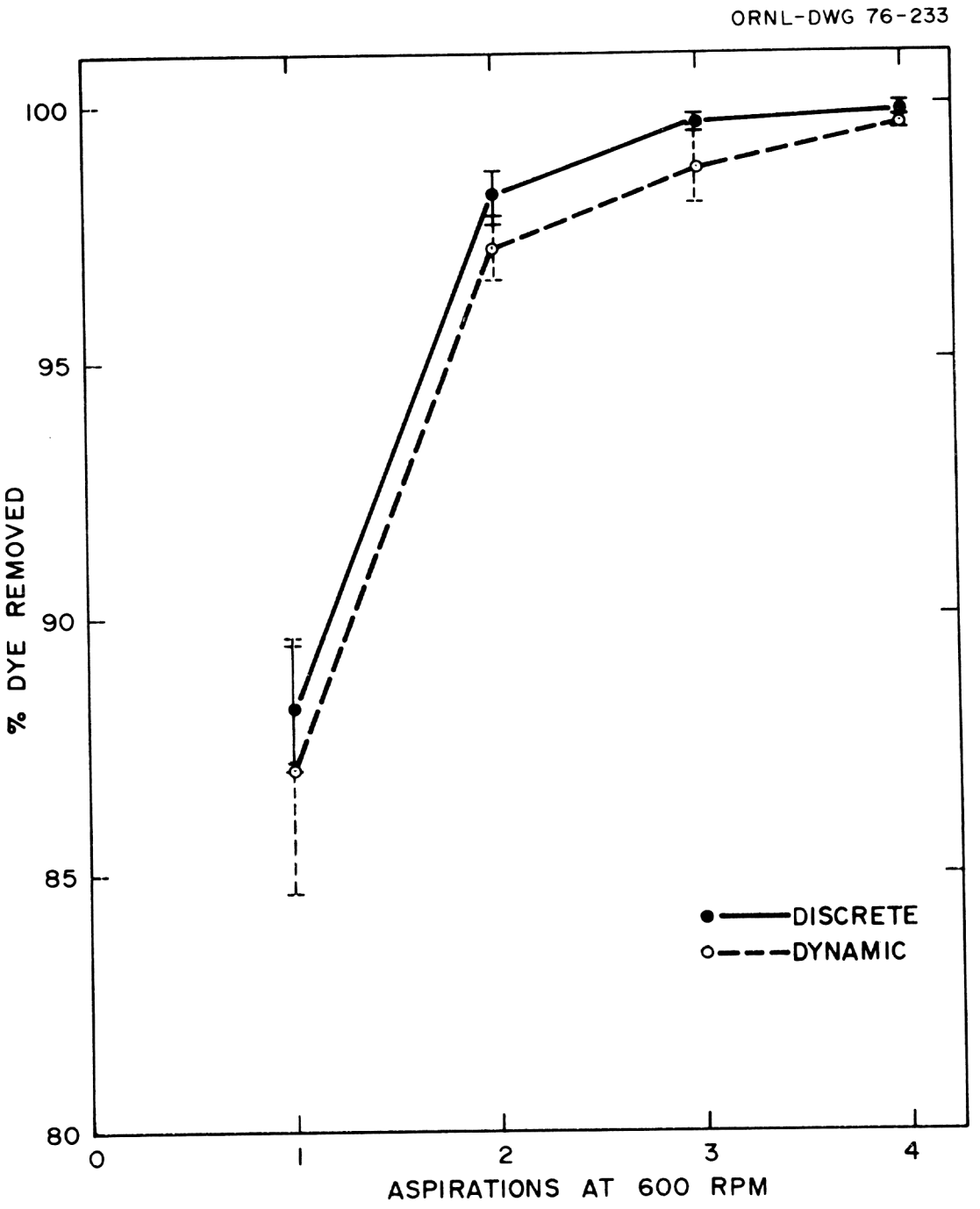

Fig. 2.26. Comparison of discrete vs dynamic additions of a washing solution to the cell-washing rotor studying removal of a dye solution with aspirations at 600 rpm.

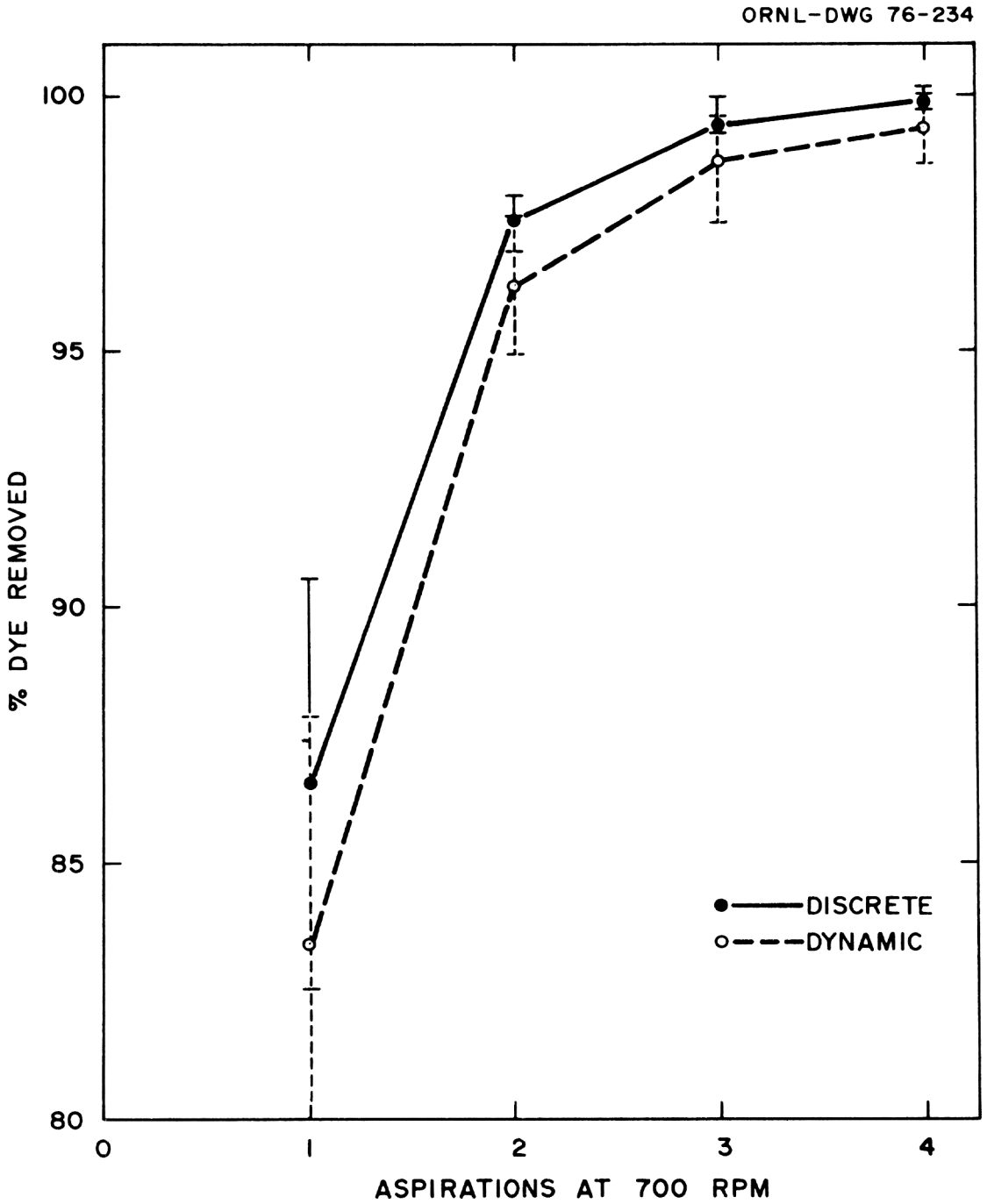

Fig. 2.27. Comparison of discrete vs dynamic additions of a washing solution to the cell-washing rotor studying removal of a dye solution with aspirations at 700 rpm.

Table 2.16. Dye studies to test reproducibility of aspiration at varying rotation rates

Aspiration number	Mean absorbance 620 nm, discrete[a]	Mean absorbance 620 nm, dynamic[c]	Percent dye removed				Ratio, discrete/dynamic
			discrete[a]	SD[b]	dynamic[c]	SD[b]	
			500 rpm				
1	0.1503	0.1558	89.29	0.76	88.14	0.86	1.013
2	0.0234	0.0405	98.33	0.31	96.92	0.52	1.015
3	0.0053	0.0128	99.62	0.14	99.03	0.12	1.006
4	0.0034	0.0083	99.76	0.24	99.37	0.12	1.004
			600 rpm				
1	0.1529	0.1646	88.29	0.74	87.15	1.51	1.013
2	0.0232	0.353	98.22	0.30	97.24	0.40	1.010
3	0.0047	0.0153	99.64	0.07	98.80	0.45	1.008
4	0.0019	0.0041	99.85	0.07	99.68	0.01	1.002
			700 rpm				
1	0.1748	0.2159	86.56	2.44	83.48	2.70	1.037
2	0.0314	0.483	97.58	0.33	96.30	0.85	1.013
3	0.0074	0.0166	99.42	0.07	98.73	0.75	1.007
4	0.0018	0.0080	99.86	0.02	99.39	0.46	1.005

[a]Rotor was loaded discretely using rotor loading station.

[b]SD = standard deviation.

[c]Rotor was loaded dynamically by syringe injection.

braked six times to homogenize the blood--saline mixture. The rotor was spun at 4000 rpm for 60 sec, slowed to 500 rpm without braking, and absorbance was measured at 415 nm to obtain blank values. At this point, excess saline was aspirated, and the rotor was returned to the rotor-loading station; distilled water (130 µl) was added to lyse the remaining cells and release the hemoglobin. The rotor was again placed on the rotor holder, accelerated to 4000 rpm, and braked six times to ensure mixing. Following the final braking, the rotor speed was adjusted to 500 rpm and the absorbance determined at 415 nm. The rotor and its contents were then spun at 4000 rpm for 60 sec, slowed to 500 rpm without braking, and the absorbance again determined at 415 nm. This sequence of operations was performed for each sample dilution. Results shown in Fig. 2.28 indicate proportional release of hemoglobin for dilutions of 1:1000, 1:500, and 1:200. The highest concentration (1:100 dilution) showed somewhat less hemoglobin released than expected; however, absorbances measured were in excess of 1.5 with attendant possibilities for nonlinear response using a filter at this high absorbance level.

To simulate in-situ cell washing, a series of experiments was performed using 50-µl aliquots of Coombs control cells in 5 cuvets and 50-µl aliquots of blood diluted 1:10 with saline in 10 cuvets as samples. (The remaining cuvets contained saline as controls.) Cell washing was performed after discretely loading the cell mixtures into the sample chambers and 80 µl of saline into the reagent chambers. The rotor was then placed on the analyzer, accelerated to approximately 3000 rpm, and braked and accelerated 10 times to ensure mixing. The rotor speed was adjusted to 500 rpm and absorbance determined at 530 nm; the rotor was accelerated to 4000 rpm for 60 sec,

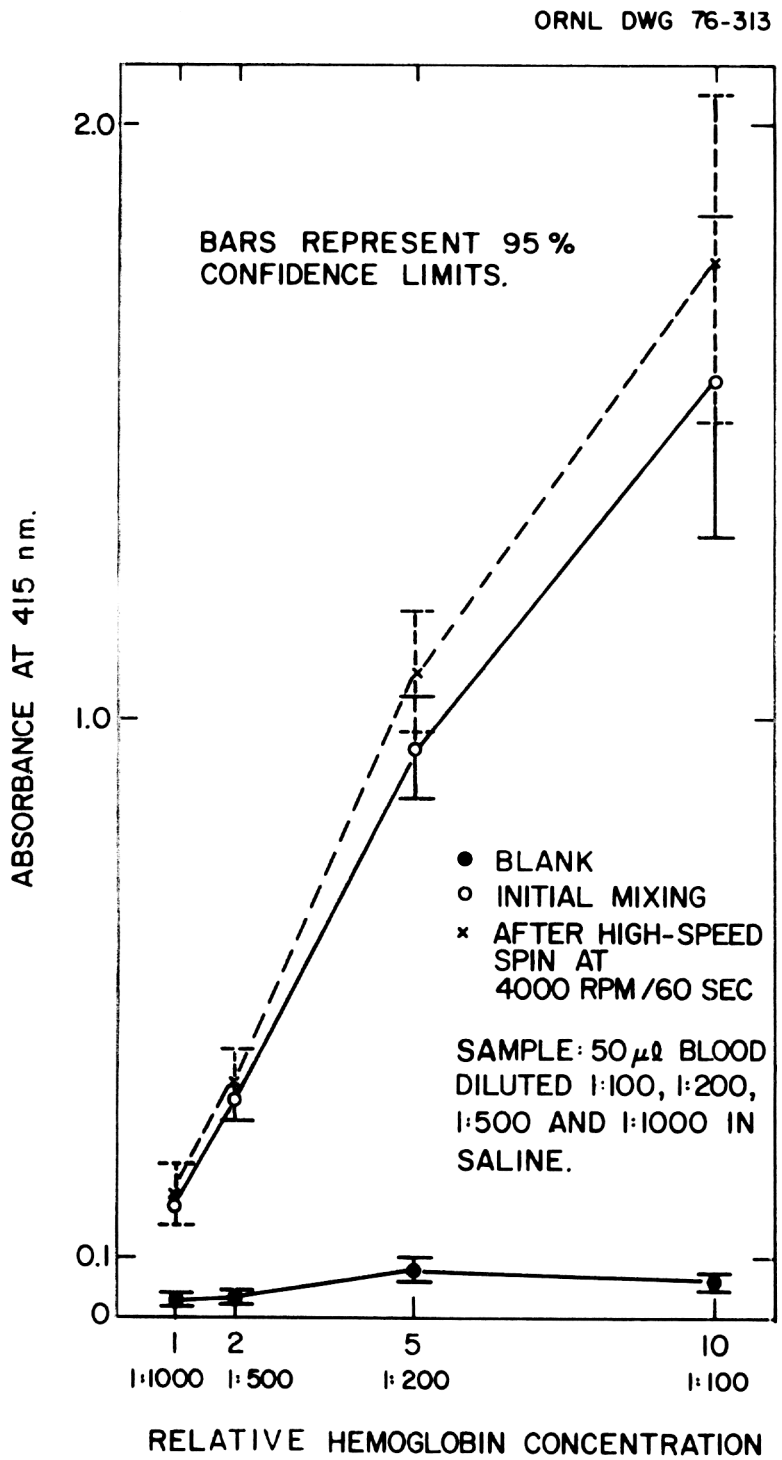

Fig. 2.28. Proportional liberation of hemoglobin is demonstrated for cells which were washed in situ on the Centrifugal Fast Analyzer. Apparent nonlinearity for the highest cell concentration may be due to the high absorbance level being measured.

slowed to 500 rpm without braking, and the absorbance again determined at 530 nm. The initial absorbance was considered test absorbance, while absorbance after the 4000-rpm spin was considered as the blank absorbance, and the resulting ΔA represented apparent change in cell mass. Each washing cycle was performed four times with wash solutions aspirated immediately after blank absorbance determinations. Cell washing and subsequent aspirations were performed at 500, 600, and 700 rpm. None of the problems previously experienced with cell washing was encountered. The results shown in Table 2.17 show that aspiration at 700 rpm is unsatisfactory; however, there is little to choose between 500 and 600 rpm. Previous data had indicated a slight advantage for aspiration at 600 rpm; thus this rotational speed has been chosen as optimum.

Coombs testing with human blood samples. Adverse reaction to blood transfusion and hemolytic disease of the newborn are two effects of antigen-antibody reactions in vivo. Sensitive monitoring for the presence of foreign antigen by means of the antiglobulin reaction (Coombs test) is vital to patient survival. A considerable variation in the degree of agglutination observed is possible.[50] Figure 2.29 illustrates a typical grading system in use at some of the area hospitals. Note that a positive reaction can range over 8 degrees of red cell agglutination, and detection of even the lowest level ($\pm$) is important to the patient's well-being.

Antiglobulin tests in the previous studies[4,49] have usually been performed on commercial Coombs control erythrocytes (human), on erythrocytes obtained from the clinical laboratory of the ORNL Health Division, or on cells from the researchers themselves. The Coombs control is prepared by sensitizing Group O red cells with IgG antibody and suspending them in

Table 2.17. Comparison of cell washing reproducibility on the Centrifugal Fast Analyzer

Wash	Control cells[a] Mean absorbance 530 nm	Control cells[a] RSD[c] (%)	Patient cells No. 1[b] Mean absorbance 530 nm	Patient cells No. 1[b] RSD[c] (%)	Patient cells No. 2[b] Mean absorbance 530 nm	Patient cells No. 2[b] RSD[c] (%)
			500 rpm			
Initial	0.8150	1.99	0.5621	5.03	0.6968	3.66
1	0.7150	5.11	0.7612	19.26	0.8123	7.61
2	0.6334	4.28	0.6227	14.39	0.7841	6.34
3	0.6340	2.52	0.6068	14.75	0.7664	6.41
4	0.6017	3.59	0.6019	12.26	0.7398	9.30
			600 rpm			
Initial	0.7808	9.58	0.6089	5.16	0.7603	7.21
1	0.6210	7.94	0.7187	14.00	0.7286	7.52
2	0.6366	7.76	0.6229	11.25	0.6971	5.39
3	0.6220	9.89	0.5913	10.01	0.6804	3.47
4	0.6075	9.53	0.5842	13.68	0.6621	3.01
			700 rpm			
Initial	0.6498	2.19	0.6202	6.90	0.7509	2.89
1	0.5131	13.82	0.5631	25.48	0.5955	8.48
2	0.5419	11.18	0.4183	15.85	0.5314	9.48
3	0.5439	11.10	0.4011	19.45	0.5031	8.81
4	0.5099	12.61	0.3876	20.77	0.4898	11.15

[a]Coombs control cell = commercial reagent sensitized Group O cells, 5 ml/dl.

[b]Patient cells obtained from ORNL Health Division, diluted 1:10 in saline.

[c]RSD = relative standard deviation.

ORNL-DWG 76-236

REACTION GRADING

The degree of red cell agglutination observed in any blood bank test procedure is significant and should be recorded. A system of grading is illustrated.

Description	Reaction*	Grade	
Button of cells remains in one clump after being dislodged from wall of test tube. Background is clear.		++++	4+s
Button breaks into two or three clumps after being dislodged. Background is clear.		++++	4+
Button breaks into four to six large clumps. Background is clear.		+++±	3+s
Button breaks into many large clumps. Background is clear.		+++	3+
Button breaks into many medium-sized clumps. Background may become slightly cloudy.		++±	2+s
Button breaks into many small clumps. Background becomes more cloudy.		++	2+
Button breaks into numerous tiny clumps. Background becomes very cloudy.		+	1+
Very fine agglutinates in a sea of free cells.		±	±
No visible agglutinates.		0	Neg.

Fig. 2.29. A commercial system for grading the degree of red cell agglutination.

5% Alsever's solution (an anticoagulant) containing inosine. Coombs testing of this suspension will always result in a highly positive antiglobulin test (4+ in Fig. 2.29), assuming the cells are viable. This is evidenced by the middle photograph in Fig. 2.30 (magnified 120X). Contrast this strongly positive agglutination with the low-level positive reactions* illustrated in the top two photographs of this figure and the positive reaction for two samples** in the lower two photographs.

It proved impossible to differentiate low-level positive reactions by use of absorbance measurements on the CFA as illustrated in Fig. 2.31. Here the patients whose red cells yielded weak positive tests (upper two photographs of Fig. 2.30) are contrasted with a known negative and the strongly positive Coombs control. On the other hand, the patients whose red cells responded strongly positive (lower two photographs of Fig. 2.30) are easily classified on the CFA (Fig. 2.32).

Based on the results of approximately 12 experiments with the low-level positive samples, it appears that an antigen-antibody reaction equivalent to about a 2+ positive (Fig. 2.29) is probably the minimum agglutination which can be reliably detected by light transmission on the CFA using the present protocol.

Previous work[49] had suggested that a strong agglutination reaction was characterized by an absorbance of less than 0.8, while a weak reaction presented with absorbances ranging from 0.8 to 1.1. A negative reaction was characterized as one presenting absorbances in excess of 1.1. These criteria

---

*Samples courtesy of D. Lay, Fort Sanders Presbyterian Hospital, Knoxville, Tennessee.

**Samples courtesy of J. Wolford, East Tennessee Baptist Hospital, Knoxville, Tennessee.

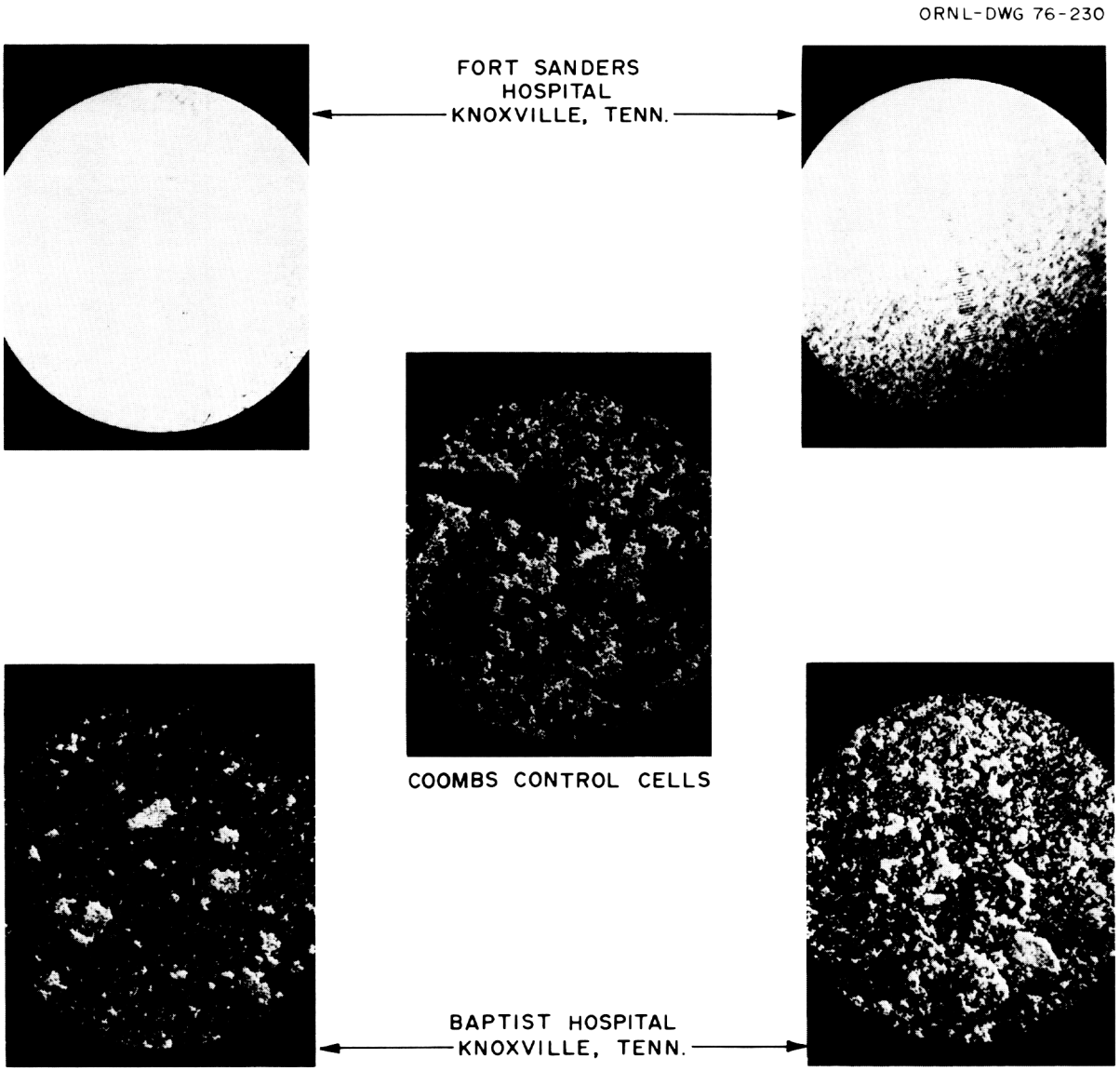

Fig. 2.30. A comparison of the degree of hemagglutination between highly positive control cells and two weakly agglutinated and two strongly agglutinated samples (upper and lower two photographs respectively).

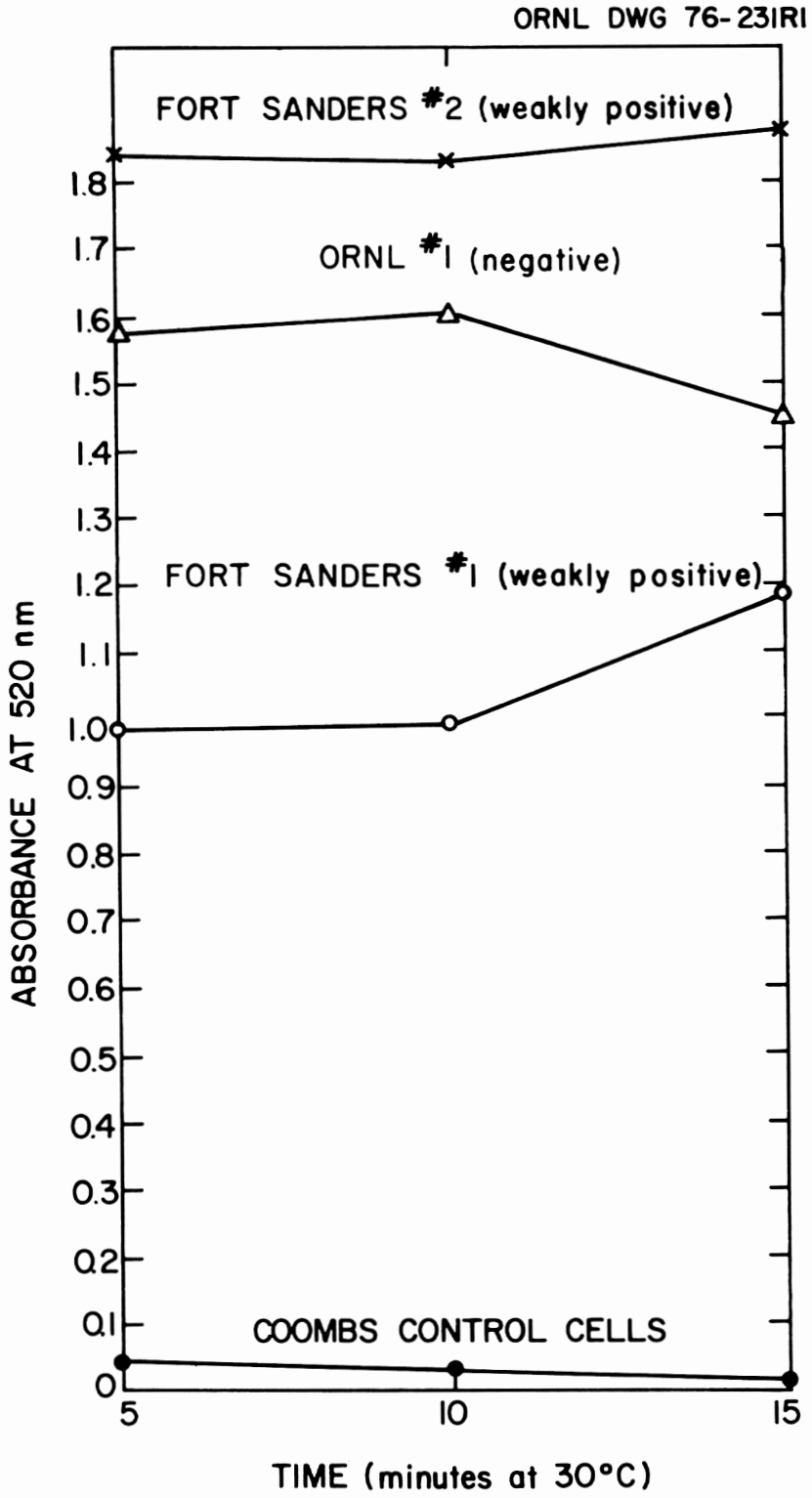

Fig. 2.31. Absorbance data on a known negative, two weakly positive, and a strongly agglutinated control demonstrating the inability to distinguish between them solely on the basis of light transmission.

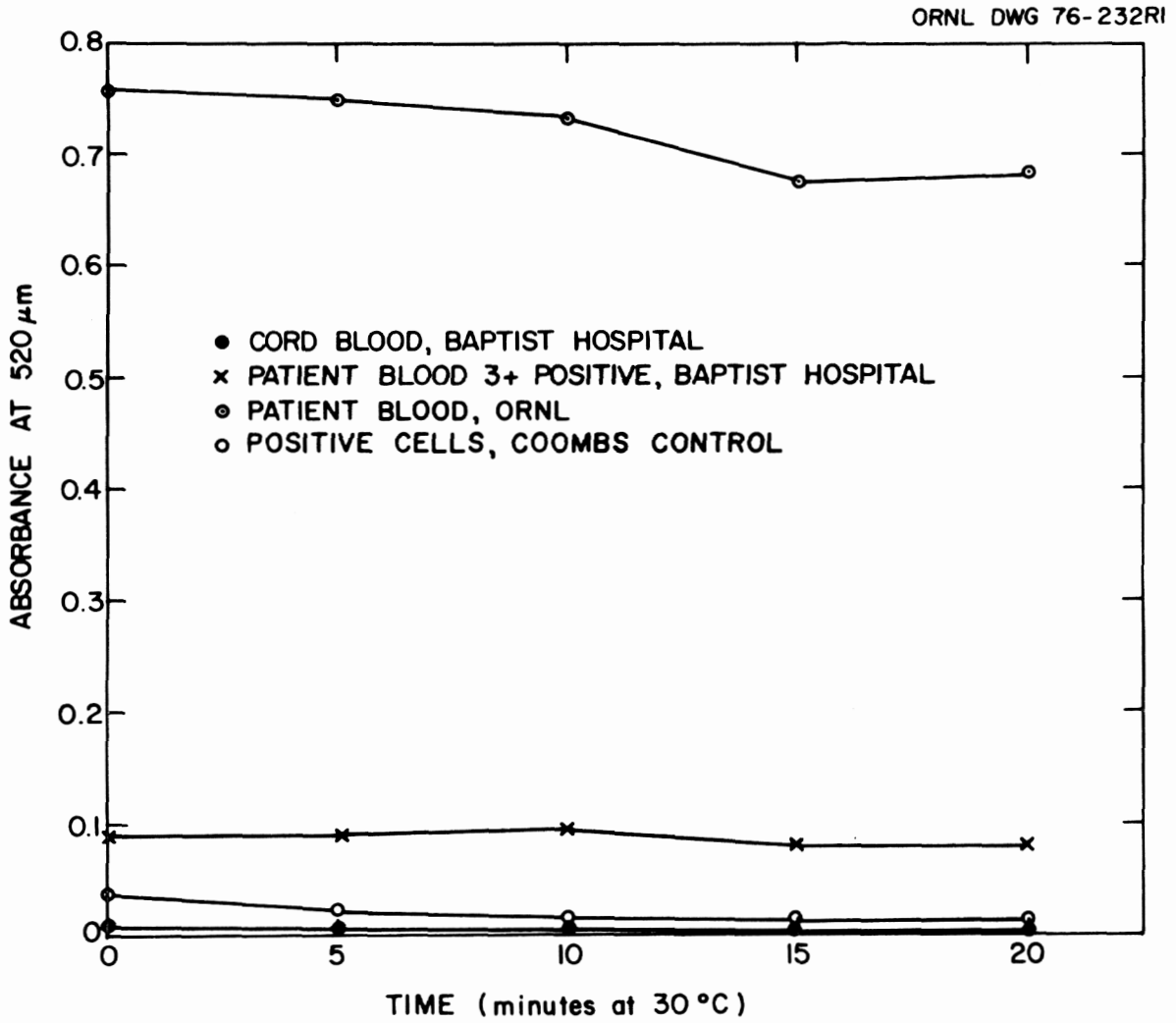

Fig. 2.32. Absorbance data on a known negative and three strongly agglutinated samples showing the ease with which light transmission measurements can differentiate positives from negatives.

are completely adequate for reactions resulting from known sensitized cells. Unfortunately, they are not adequate when applied to samples known to exhibit a positive antiglobulin reaction (although exhibiting only weak agglutination as indicated by Fig. 2.31).

Additional experimentation with weakly agglutinating samples should be performed to effectively characterize the lowest hemagglutination level which can be detected by light transmission on the CFA. To perform such studies, Coombs positive cells of any desired antigenicity will be prepared by sensitizing "D" positive cells with anti-D sera. Thus samples having varying levels of antigen and a constant total mass of cells may be examined using the protocol for the direct Coombs test on the CFA. However, instead of obtaining a single absorbance reading after resuspension of cells, the differential sedimentation of the nonsensitized and weakly sensitized cells will be monitored as a function of time. It is anticipated that the weakly sensitized cells, forming small dispersed agglutinates, will sediment more rapidly than nonsensitized cells. Although the initial absorbance of the weakly sensitized cells may indicate a false negative when only one absorbance reading is made, weak agglutination may be detected and, perhaps, even graded by the dynamic determination of sedimentation rate in a centrifugal field. In addition, light scattering should be evaluated for its utility in detecting low-level hemagglutination reactions.

Considering the importance of even a minimal positive reaction ($\pm$ in Fig. 2.29), if reliable discrimination from negative reactions cannot be made, attempts to adapt Coombs testing to the CFA should be abandoned.

2.3.4 Measurement of kinetic parameters

The measurement of kinetic parameters of enzymes such as the Michaelis-Menten constant (K_m) is extremely useful in defining differences among isoenzymes and in determining optimum conditions for kinetic assay of a particular enzyme. A number of modifications and/or refinements have been introduced into our computer software packages and these will be discussed in this section.

Computer programs for the measurement of reaction rate. The first program in the software package[41] for the determination of K_m by the Wilkinson method[51] calculates rate of reaction from measured absorbances over equal time intervals. The data are fitted to a second-order quadratic function of the form of Eq. (1):

$$A_i = a_0 + a_1 t + a_2 t^2 , \qquad (1)$$

where

A_i = measured absorbance for the ith interval,

t = time, and

a_0, a_1, and a_2 are the coefficients determined by fitting the data to the quadratic function [Eq. (1)] by the method of least-squares.

The slope $\frac{dA}{dt}$ of Eq. (1) evaluated at $t = 0$ is a measure of the initial velocity of the reaction. Those reactions which yield a linear change of absorbance with time over the full interval in which the reaction is monitored pose no problem since, under these conditions, $a_2 = 0$. However, if the reaction progress curve is curved, either due to a depletion of substrate or to a lag phase, then the a_2 coefficient will be nonzero. The natural tendency of the data to be weighted more heavily with increasing values of X (time) and y (absorbance) will result in forcing the parameters

(a_0, a_1, a_2) to fit the data more closely at that end of the curve. This, of course, may or may not result in a good fit for the data at the start of the reaction (i.e., near t = 0). Noise-induced scatter of the data tended to increase errors in the measurement of the slope using this model. We introduced a weighting factor of the reciprocal of interval number $\left(\frac{1}{x}\right)$ into the data so as to weight the front portion of the curve more heavily; however, this was also unsatisfactory, as was a weighting factor of the reciprocal of the interval number squared $\left(\frac{1}{x^2}\right)$ when data with some noise were encountered. At this point, a linear least-squares fitting of the data was reintroduced with a variable time interval. The interval over which the data were to be fitted was selected by the operator, and the program variables were made compatible with those utilized in the program for calculation of the Michaelis-Menten constant from these rate data. In addition, a calculation of the correlation coefficient was performed and printed out to give the operator some information as to the fit of the data to a linear model. The FOCAL program is shown in Fig. 2.33, and a sample output is shown in Fig. 2.34.

Table 2.18 illustrates K_m and V_{max} measured for the serum enzyme gamma-glutamyl transpeptidase at variable substrate concentration, using several methods to determine the slopes of the reaction progress curves. The differences depicted in the Michaelis-Menten constants suggest that the reaction progress curves are not strictly linear over the full observation interval. The steepest slopes of reaction progress curves were computed when the weighting factor was $1/t^2$, and the general order was the same as the K_m's listed in Table 2.18. The data suggest that kinetic parameters calculated using slope data measured by linear fitting of early data for the

ORNL DWG 76-635

```
C-GEMSAEC 2A 741163W

01.01 C-CALCULATION OF ENZYME RATE AT SELECTED INTERVALS LINKED TO X FIE
01.03 A !"STARTING POINT"T0;A !"FINAL POINT"T1;I (T0-1)1.03
01.05 I (T1-T0)1.03,1.03;I (NI-T1)1.03
01.08 S NX=T1-T0+1
01.10 F J=2,17;D 8
01.12 T !!"CUVET  TIME INTERVAL  ENZYME RATE    ACTIVITY    CORRELATION"
01.13 T  !"          SECONDS       ODU/MINUTE                COEFFICIENT"
01.20 F J=2,17;D 9
01.30 S I1=2+(XL-1)*NS*NR;S I2=I1+NS*NR-NR
01.35 F J=I1,NR,I2;D 11
01.38 A !!"DO YOU WANT TO EVALUATE KM AND VMAX?"P
01.40 IF (P-0YES)1.50,1.42,1.50
01.42 L G 13,G
01.50 A !!!"DO YOU WANT RATE FOR ANOTHER INTERVAL (YES OR NO)"AN
01.51 IF (AN-0YES)1.52,1.60,1.52
01.52 IF (AN-0NO)1.5,1.8,1.5
01.60 G 1.03
01.80 QUIT

07.10 S S1=FGET(N,0);S S2=FGET(N,1)-S1;I (-S2)7.3;T !"BLANK ERROR"!;Q
07.30 S SN=FGET(N,J)-S1;I (-SN)7.5;S AB(J)=-9.99;R
07.50 S AB(N)=.4343*FLOG(S2/(SN*FSTR(ST+J)))

08.25 F N=T0,T1;D 7
08.45 S SX=0;S X2=0;S SY=0;S Y2=0;S XY=0
08.50 F N=T0,T1;D 10
08.60 S SL(J)=60*(XY-SX*SY/NX)/(X2-SX↑2/NX);S AV(J)=SF*SL(J)
08.70 S CO(J)=(NX*XY-SX*SY)/FSQT((NX*X2-SX*SX)*(NX*Y2-SY*SY))
08.90 R

09.10 T !,%3,J,"  ",DI+(T0-1)*SI," -",DI+(T1-1)*SI,"        ",
09.20 T %8.06,SL(J),"  ",%8.05,AV(J),"    ",%8.05,CO(J)
09.90 R

10.05 S X=DI+SE*(N-1);S SX=SX+X;S X2=X2+X↑2
10.10 S SY=SY+AB(N);S XY=XY+X*AB(N);S Y2=Y2+AB(N)↑2

11.10 S I=J;S VV=0
11.20 F L=I,I+NR-1;D 11.5
11.30 S VV(J)=VV/NR
11.40 R
11.50 S VV=VV+AV(L);R
*
```

Fig. 2.33. FOCAL program for estimating slopes by linear regression analysis over operator-defined data intervals.

STARTING POINT:1
FINAL POINT:12

ORNL DWG 76-636

CUVET	TIME INTERVAL SECONDS	ENZYME RATE ODU/MINUTE	ACTIVITY	CORRELATION COEFFICIENT
2	180 - 510	0.014709	137.15800	0.99997
3	180 - 510	0.014751	137.54800	0.99995
4	180 - 510	0.013645	127.24000	0.99988
5	180 - 510	0.013627	127.07500	0.99995
6	180 - 510	0.014935	139.27100	0.99997
7	180 - 510	0.014971	139.60400	0.99991
8	180 - 510	0.013721	127.95100	0.99987
9	180 - 510	0.013867	129.31000	0.99996
10	180 - 510	0.015146	141.23900	0.99994
11	180 - 510	0.015130	141.08700	0.99993
12	180 - 510	0.013958	130.15400	0.99997
13	180 - 510	0.014034	130.86300	0.99997
14	180 - 510	0.015067	140.50000	0.99998
15	180 - 510	0.015357	143.20500	0.99996
16	180 - 510	0.013735	128.08000	0.99996
17	180 - 510	0.013658	127.35800	0.99995

Fig. 2.34. Typical output from linear regression program on PDP-8/e.

Table 2.18. Calculation of kinetic parameters for GGTP using various methods for determination of the slope of the reaction progress curve

Method of analysis	Time interval (sec)	Weighting factor	K_m	Relative standard error (%)	V_{max}	Relative standard error (%)
Least-squares, linear function[a]	10-130	none	1.323	5.9	0.0555	2.6
Least-squares, linear function[a]	10-250	none	1.135	4.3	0.0486	1.8
Least-squares, linear function[a]	10-370	none	1.101	3.8	0.0460	1.6
Least-squares, quadratic function[b]	10-370	none	1.276	6.4	0.0552	2.8
Least-squares, quadratic function[b]	10-370	$1/t$[c]	1.369	6.2	0.0595	2.8
Least-squares, quadratic function[b]	10-370	$1/t^2$[c]	1.434	7.9	0.0630	3.6

[a] $A_i = a_0 + a_1 t$.

[b] $A_i = a_0 + a_1 t + a_2 t^2$.

[c] t = Equal interval time; data taken every 15 sec after initial 10-sec delay over a total time period of 360 sec.

reaction (10 to 130 sec) agree reasonably well with slopes calculated from the first derivative $\frac{dA}{dt}$ of the quadratic function fitted to all of the data and evaluated at t = 0 (compare K_m's and V_{max}'s in Table 2.18).

As suggested previously, the use of a quadratic model for fitting of absorbance vs time data of a reaction progress curve was unsatisfactory when the data were noisy. The use of the linear model over an operator-selected interval is undesirable for CFA systems without data display scopes from which the operator could rapidly choose the optimum interval for measurement of the slope. An alternative method would entail a search of the data for a region of maximum slope subject to meeting some reasonable criterion of linearity. Such a program, previously conceived for another purpose, was modified and adapted for inclusion in the FOCAL package used to compute K_m and V_{max}. A copy of the FOCAL program is shown in Fig. 2.35 and a typical output is shown in Fig. 2.36. This program requires that one-half of the data points be included in the linear fit and that the data meet a minimum linearity criterion of a correlation coefficient ≥ 0.985. The program is relatively slow, requiring approximately 10 min to evaluate 25 points from each of 16 cuvets; however, results obtained with it have apparently overcome many of the objections and problems found for the other models. Weaknesses observed include predefinition of the number of points to be included in the final fitting and its heavy dependence on exceeding a correlation coefficient (CC) criterion. The significance of a CC is suspect on a small computer because possible losses in significant figures in certain calculations can make the final number meaningless. Further software development is aimed at overcoming these problem areas.

```
C-GEMSAEC 2A 741163W                                          ORNL DWG 76-630

01.01 C-ENZYME KINETIC PROGRAM-PART 2; MAXIMUM SLOPE SEARCH, LINEAR
01.03 D 6;S ND=FITR(NI/2);S CX=.985;G 4.06

02.06 T !!"CUVET  TIME INTERVAL  ENZYME RATE    ACTIVITY    CORRELATION"
02.07 T  !"          SECONDS      ODU/MINUTE     MMOL/MIN    COEFFICIENT"

03.01 F J=RC+1,I2; S I=1; S M=0; D 10
03.99 R

04.06 S D=FCLK(,,,,);S D=FTAK(,,NC);S D=FTAK(SC,NI,NC)
04.11 S ZZ=FCNI(2);T !"COMPUTER IS READY!"!
04.16 I (FCNI(2))4.16,4.26;Q
04.26 S D=FCLK(MD,CD,MI,CY,1)

05.11 F XL=1,VS;D 5.35;D 2;D 3
05.16 A !"IS THIS A ONE-ENZYME SYSTEM?",P
05.17 I (P-0YES)5.18,5.25,5.18
05.18 I (P-0NO)5.28,5.19,5.28
05.19 A !"EVALUATE KM'S AND VMAX'S BY NONLINEAR LEAST SQUARES?",P
05.20 I (P-0YES)3.99,5.27,3.99
05.25 L G 13,G 1.1
05.27 S XL=XL-VS;L G 15,G 3.02
05.28 T !"INVALID REPLY, ANSWER YES OR NO!";G 5.16
05.35 S I1=2+(XL-1)*NS*NR;S I2=I1+NS*NR-NR+1

06.10 T !"ENTER VARIABLES FOR ACQUIRING DATA"
06.11 A !" CUVET CONTAINING REAGENT BLANK (NOTE 1 OR 2)?",RC
06.12 A !" DELAY INTERVAL--SEC"DI;I (600-DI)6.12
06.14 A !" OBSERVATION INTERVAL-SEC"SE;I (60-SE)6.14;I (SE-1)6.14
06.16 S SI=SE;S MD=FITR(DI/60);S CD=60*(DI-60*MD);S MI=0;S CY=60*SE
06.17 S IM=FITR(968/[2*FITR(NC/2+1)]);S DT=CY/3600
06.18 T !" NUMBER OF OBSERVATIONS (NOTE ";T %3,IM," MAXIMUM)";A NI
06.24 I (NI-1)6.18;I (IM-NI)6.18
06.26 A !" NUMBER OF REVOLUTIONS AVERAGED"SC;I (100-SC)6.26

07.10 S S1=FGET(N,0);S S2=FGET(N,1)-S1;I (-S2)7.3;T !"BLANK ERROR";Q
07.30 S SN=FGET(N,J)-S1;I (-SN)7.5;S AB(J)=-9.9;R
07.50 S AB(J)=.4343*FLOG(S2/(SN*FSTR(ST+J)))
07.60 I (1-RC)7.7;R
07.70 S SB=FGET(N,RC)-S1
07.75 S AD=.4343*FLOG(S2/(SB*FSTR(ST+RC)));S AB(J)=AB(J)-AD;R

10.01 S SX=0; S SY=0; S XY=0; S X2=0; S Y2=0;S H=I+ND-1
10.06 F N=I,1,H; D 7; D 11
10.07 S M=M+1
10.10 S MM(M)=FABS(60*(XY-SX*SY/ND)/(X2-SX*SX/ND))
10.15 S CO(M)=FABS((ND*XY-SX*SY)/FSQT((ND*X2-SX*SX)*(ND*Y2-SY*SY)))
10.30 S I=I+1;I ((I+ND)-NI)10.01,10.01; D 12
10.40 R

11.05 S SY=SY+AB(J);S X=DI+(N-1)*SE;S SX=SX+X;S XY=XY+X*AB(J)
11.10 S X2=X2+X*X;S Y2=Y2+AB(J)*AB(J);R

12.01 S MAX=MM(1);S  CC=CO(1);S  IN=1
12.05 F M=2,1,(NI-1); D 13
12.08 S TO=(IN-1 )*SE+DI; S TF=TO+ND*SE
12.30 I (CC-CX)12.35,12.49,12.49
12.35 I ((NI-1)-IN)12.4,12.45
12.40 S MM(IN)=0; G 12.01
12.45 T !,%4.0,J, "     DATA DOES NOT MEET LINEARITY CRITERION"; R
12.49 S AV(J)=MAX*SF
12.50 T !,%3,J,"  ",TO," -",TF,"     ",%8.06,MAX,"      ",%8.05,AV(J),
12.51 T %10.04,CC;R

13.01 I (MAX-MM(M)) 13.1,13.1,13.2
13.10 S MAX=MM(M); S CC=CO(M); S IN=M
13.20 R
*
```

Fig. 2.35. FOCAL program for determining maximum slope of a reaction progress curve subject to constraints on the number of points to be included (50%) and the minimum acceptable correlation coefficient (0.935). Slope determined by linear regression analysis.

ORNL DWG 76-637

CUVET	TIME INTERVAL SECONDS	ENZYME RATE ODU/MINUTE	ACTIVITY MMOL/MIN	CORRELATION COEFFICIENT
2	180 - 360	0.014817	138.17000	0.9999
3	210 - 390	0.014991	139.78600	0.9999
4	240 - 420	0.013977	130.33900	0.9998
5	300 - 480	0.013777	128.47300	0.9999
6	210 - 390	0.015112	140.92000	1.0000
7	210 - 390	0.015224	141.95900	0.9998
8	240 - 420	0.014049	131.00900	0.9997
9	270 - 450	0.014039	130.91200	0.9998
10	240 - 420	0.015357	143.20100	1.0000
11	270 - 450	0.015369	143.31800	0.9999
12	210 - 390	0.014076	131.25300	0.9999
13	300 - 480	0.014116	131.63400	1.0000
14	240 - 420	0.015186	141.61000	1.0000
15	210 - 390	0.015506	144.59600	1.0000
16	240 - 420	0.013879	129.41800	0.9999
17	300 - 480	0.013832	128.98600	0.9999

*

Fig. 2.36. Typical output from maximum slope linear search program.

2.3.5 Isoenzyme measurement

The technique of analyzing an enzyme system consisting of two isoenzymes acting on the same substrate by mathematically "stripping" the individual kinetic parameters by nonlinear least-squares regression analysis was described by Tiffany, Chilcote, and Burtis.[41] This section will document the mathematical techniques and correlate program variables with their mathematical counterparts for the nonlinear regression program.

In addition, an improved computer program was recently written to make initial estimates of the Michaelis-Menten kinetic parameters for use in the nonlinear regression program.

Mathematical documentation of nonlinear regression program. The mathematical model chosen for regression analysis is based on two isoenzymes acting on the same substrate;[41] use of the Michaelis-Menten rate expression for each leads to the following expression for reaction velocity of the mixture:

$$\hat{v}_i = \frac{V_1 S_i}{K_1 + S_i} + \frac{V_2 S_i}{K_2 + S_i} , \qquad (1)$$

where

$\hat{v}_i$ = predicted reaction velocities based on estimates of V_1, V_2, K_1, K_2;

S_i = substrate concentration;

V_1 and V_2 = V_{max} for enzymes 1 and 2;

K_1 and K_2 = Michaelis-Menten constants for enzymes 1 and 2.

For regression analysis, we wish to minimize the function

$$\Phi = \sum_i (\bar{v}_i - \hat{v}_i)^2 \quad ,$$

where $\bar{v}_i$ = measured reaction velocity.

Thus, we expand Eq. (1) in a Taylor series about the rth trial value for the parameters V_1, V_2, K_1, K_2 (retaining only the linear terms):

$$\hat{v}_i \cong \left\{\frac{V_1^{(r)} S_i}{K_1^{(r)} + S_i} + \frac{V_2^{(r)} S_i}{K_2^{(r)} + S_i}\right\} + \Delta V_1^{(r)} \left\{\frac{\partial \hat{v}_i}{\partial V_1}\right\}^{(r)} + \Delta V_2^{(r)} \left\{\frac{\partial \hat{v}_i}{\partial V_2}\right\}^{(r)}$$

$$+ \Delta K_1^{(r)} \left\{\frac{\partial \hat{v}_i}{\partial K_1}\right\}^{(r)} + \Delta K_2^{(r)} \left\{\frac{\partial \hat{v}_i}{\partial K_2}\right\}^{(r)} \quad . \tag{2}$$

Thus,

$$\hat{v}_i \cong \left\{\frac{V_1^{(r)} S_i}{K_1^{(r)} + S_i} + \frac{V_2^{(r)} S_i}{K_2^{(r)} + S_i}\right\} + \Delta V_1^{(r)} \left\{\frac{S_i}{K_1^{(r)} + S_i}\right\}$$

$$+ \Delta V_2^{(r)} \left\{\frac{S_i}{K_2^{(r)} + S_i}\right\} + \Delta K_1^{(r)} \left\{- \frac{V_1^{(r)} S_i}{\left(K_1^{(r)} + S_i\right)^2}\right\}$$

$$+ \Delta K_2^{(r)} \left\{- \frac{V_2^{(r)} S_i}{\left(K_2^{(r)} + S_i\right)^2}\right\} \quad ; \tag{3}$$

and the equations to be solved are:

$$\left\{\frac{\partial\Phi}{\partial(\Delta V_1)}\right\}^{(r)} = 0 \ , \tag{4}$$

$$\left\{\frac{\partial\Phi}{\partial(\Delta V_2)}\right\}^{(r)} = 0 \ , \tag{5}$$

$$\left\{\frac{\partial\Phi}{\partial(\Delta K_1)}\right\}^{(r)} = 0 \ , \tag{6}$$

$$\left\{\frac{\partial\Phi}{\partial(\Delta K_2)}\right\}^{(r)} = 0 \ , \tag{7}$$

or

$$\sum_i \left\{\frac{\partial\hat{v}_i}{\partial V_1}\right\}^{(r)} \left\{\frac{\partial\hat{v}_i}{\partial V_1}\right\}^{(r)} \Delta V_1{}^{(r)} + \sum_i \left\{\frac{\partial\hat{v}_i}{\partial V_2}\right\}^{(r)} \left\{\frac{\partial\hat{v}_i}{\partial V_1}\right\}^{(r)} \Delta V_2{}^{(r)}$$

$$+ \sum_i \left\{\frac{\partial\hat{v}_i}{\partial K_1}\right\}^{(r)} \left\{\frac{\partial\hat{v}_i}{\partial V_1}\right\}^{(r)} \Delta K_1{}^{(r)} + \sum_i \left\{\frac{\partial\hat{v}_i}{\partial K_2}\right\}^{(r)} \left\{\frac{\partial\hat{v}_i}{\partial V_1}\right\}^{(r)} \Delta K_2$$

$$= \sum_i \left\{\bar{v}_i - \left(\frac{V_1{}^{(r)} S_i}{K_1{}^{(r)} + S_i} + \frac{V_2{}^{(r)} S_i}{K_2{}^{(r)} + S_i}\right)\right\} \left\{\frac{\partial\hat{v}_i}{\partial V_1}\right\}^{(r)} \ , \tag{4a}$$

$$\sum_i \left\{\frac{\partial\hat{v}_i}{\partial V_1}\right\}^{(r)} \left\{\frac{\partial\hat{v}_i}{\partial V_2}\right\}^{(r)} \Delta V_1{}^{(r)} + \sum_i \left\{\frac{\partial\hat{v}_i}{\partial V_2}\right\}^{(r)} \left\{\frac{\partial\hat{v}_i}{\partial V_2}\right\}^{(r)} \Delta V_2{}^{(r)}$$

$$+ \ldots\ldots\ldots\ldots\ldots\ldots\ldots + \ldots\ldots\ldots\ldots\ldots\ldots$$

$$= \sum_i \left\{\bar{v}_i - \hat{v}_i{}^{(r)}\right\} \left\{\frac{\partial\hat{v}_i}{\partial V_2}\right\}^{(r)} \ , \tag{5a}$$

$$\sum_i \left\{\frac{\partial \hat{v}_i}{\partial V_1}\right\}^{(r)} \left\{\frac{\partial \hat{v}_i}{\partial K_1}\right\}^{(r)} \Delta V_1^{(r)} + \ldots\ldots\ldots\ldots\ldots\ldots\ldots$$

$$+ \ldots\ldots\ldots\ldots\ldots\ldots\ldots\ldots + \ldots\ldots\ldots\ldots\ldots\ldots$$

$$= \sum_i \left\{\bar{v}_i - \hat{v}_i^{(r)}\right\} \left\{\frac{\partial \hat{v}_i}{\partial K_1}\right\}^{(r)} , \tag{6a}$$

$$\sum_i \left\{\frac{\partial \hat{v}_i}{\partial V_1}\right\}^{(r)} \left\{\frac{\partial \hat{v}_i}{\partial K_2}\right\}^{(r)} \Delta V_2^{(r)} + \ldots\ldots\ldots\ldots\ldots\ldots\ldots\ldots$$

$$+ \ldots\ldots\ldots\ldots\ldots\ldots\ldots + \ldots\ldots\ldots\ldots\ldots\ldots\ldots\ldots$$

$$= \sum_i \left\{\bar{v}_i - \hat{v}_i^{(r)}\right\} \left\{\frac{\partial \hat{v}_i}{\partial K_2}\right\}^{(r)} . \tag{7a}$$

Equations (4) to (7) and (4a) to (7a) written in simpler terms are:

$$\begin{aligned}
C(1,1)\Delta V_1 + C(1,2)\Delta V_2 + C(1,3)\Delta K_1 + C(1,4)\Delta K_2 &= C(1,5) , \\
C(2,1)\Delta V_1 + C(2,2)\Delta V_2 + C(2,3)\Delta K_1 + C(2,4)\Delta K_2 &= C(2,5) , \\
C(3,1)\Delta V_1 + C(3,2)\Delta V_2 + C(3,3)\Delta K_1 + C(3,4)\Delta K_2 &= C(3,5) , \\
C(4,1)\Delta V_1 + C(4,2)\Delta V_2 + C(4,3)\Delta K_1 + C(4,4)\Delta K_2 &= C(4,5) ,
\end{aligned} \tag{8}$$

where

$$C(1,1) = \sum_i \left\{\frac{\partial \hat{v}_i}{\partial V_1}\right\}^{(r)} \left\{\frac{\partial \hat{v}_i}{\partial V_1}\right\}^{(r)} , \text{ etc.} \tag{8a}$$

In the notation of the FOCAL program (see Fig. 2.37)

5.10-5.17 (FOCAL program statement number) C(NP*(J-1)+K) ≡ C(J,K), the coefficients of the matrix, Eq. (8), and the right-hand side vector [C(1,5), C(2,5), etc.] in one dimension.

5.18 CI(J) ≡ the diagonal elements of this matrix [C(1,1), C(2,2), C(3,3), C(4,4)].

The coefficients of the n x n matrix are determined in statements 6.10 and 6.20 of the FOCAL program (Fig. 2.37); here

$$\text{VJ and VK} \equiv \left(\frac{\partial \hat{v}_i}{\partial V_j}\right) \quad i = 1,n;\ j = 1,2 \quad \text{[see Eq. (8a)]},$$

and

$$\text{KJ and KK} \equiv \left(\frac{\partial \hat{v}_i}{\partial K_j}\right) \quad i = 1,n;\ j = 1,2 \quad .$$

The remaining coefficients [i.e., the right-hand side of the matrix (8)], C(1,5), C(2,5), C(3,5), and C(4,5), are determined in statements 8.30 and 8.40 (Fig. 2.37). In program statements 5.19 to 5.21, the matrix is scaled according to Eq. (27) and Eq. (28) of Marquardt's paper,[52] for example, putting Eq. (8) into matrix notation:

$$C\delta = g \ , \tag{9}$$

where

C = the matrix of coefficients,

δ = the vector of unknowns (ΔV_1, ΔV_2, ΔK_1, ΔK_2), and

g = the right-hand side vector.

ORNL DWG 76-633

```
C-GEMSAEC 2A 741163"

01.01 C-ENZYME KINETIC PROGRAM-PART 7-CONT OF INHIBITOR EVAL.

05.05 S IC=0;S KE=2;S KF=2*KE;S NP=KF+1
05.10 F J=1,KF;F K=1,NP;S C(NP*(J-1)+K)=0
05.15 F J=1,KE;F K=1,KE;F L=2,NS*NR+1;D 6
05.17 F J=1,KE;S S1=0;F L=2,NS*NR+0;D 6.1;D 8
05.18 F J=1,KF;S CI(J)=C(NP*(J-1)+J)
05.19 F J=1,KF;F K=1,KF;D 5.7
05.21 F J=1,KF;S C(NP*J)=C(NP*J)/FSQT(CI(J))
05.25 S LA=KF;F M=1,KF-1;F L=M,KF-1;F J=M,KF;D 7
05.30 S SU=0;S LL=LA+1;S H(NP)=1
05.32 F J=LL,NP;S SU=SU-C(NP*(LA-1)+J)*H(J)
05.34 S H(LA)=SU/C(NP*(LA-1)+LA)
05.36 S LA=LA-1;I (LA)5.39,5.39,5.30
05.39 F L=1,KF;S H(L)=H(L)/FSQT(CI(L))
05.40 S LS=0;F L=1,KF;S LS=LS+H(L)↑2
05.45 F L=1,KE;S VM(L)=VM(L)-H(L);S KM(L)=KM(L)-H(L+KE)
05.46 F J=1,KE;T VM(J),H(J),KM(J),H(J+KE),!
05.50 S S2=0;F L=2,NS*NR+1;D 8.1;S S2=S2+(AV(L)-EV(L))↑2
05.51 T %10.08,S1,S2,LS,!!!
05.55 I (S2-S1-.00002)5.6;T "ROUTINE IS DIVERGING",!;Q
05.60 I (12-IC)5.68;S IC=IC+1;I (LS-.03031)5.65,5.65,5.10
05.65 F J=1,KE;T "ENZYME",%2,J,"     VM=",%8.06,VM(J),"  KM=",KM(J),!
05.66 T !"STANDARD ERROR",%,FSQT(S2/(NS*NR-1)),!;Q
05.68 T "EXCESSIVE ITERATIONS",!;Q
05.70 S C(NP*(J-1)+K)=C(NP*(J-1)+K)/FSQT(CI(J)*CI(K))

06.10 S VJ=S(L)/(KM(J)+S(L));S KJ=-VM(J)*S(L)/(KM(J)+S(L))↑2
06.20 S VK=S(L)/(KM(K)+S(L));S KK=-VM(K)*S(L)/(KM(K)+S(L))↑2
06.30 S C(NP*(J-1)+K)=C(NP*(J-1)+K)+VJ*VK
06.40 S C(NP*(J-1)+KE+K)=C(NP*(J-1)+KE+K)+VJ*KK
06.50 S C(NP*(J+KE-1)+K)=C(NP*(J+KE-1)+K)+KJ*VK
06.60 S C(NP*(J+KE-1)+KE+K)=C(NP*(J+KE-1)+KE+K)+KJ*KK

07.10 S YA=C(NP*L+M)*C(NP*(M-1)+J+1)/C(NP*(M-1)+M)
07.20 S C(NP*L+J+1)=C(NP*L+J+1)-YA

08.10 S EV(L)=0;F K=1,KE;D 6.2;S EV(L)=EV(L)+VM(K)*S(L)/(KM(K)+S(L))
08.20 S S1=S1+(AV(L)-EV(L))↑2
08.30 S C(NP*J)=C(NP*J)+VJ*(AV(L)-EV(L))
08.40 S C(NP*(J+KE))=C(NP*(J+KE))+KJ*(AV(L)-EV(L))
*
```

Fig. 2.37. FOCAL program for the analysis of absorbance data at varying substrate concentrations by nonlinear regression using the two-enzyme model.

Then the scaled matrix of coefficients (C^*) is computed as shown below:

$$C^* = (c_{jj'}^*) = \frac{c_{jj'}}{\sqrt{c_{jj} * c_{j'j'}}} \; ; \tag{10}$$

and the scaled right-hand side vector (g^*) is computed as follows:

$$g^* = (g_j^*) = \left(\frac{g_j}{\sqrt{c_{jj}}}\right) . \tag{11}$$

Here the scaling factors (the square roots of the diagonal elements) cause the matrix C to be transformed into the matrix of simple correlation coefficients (C^*) among the $\frac{\partial \hat{v}_i}{\partial V_j}$ $\frac{\partial \hat{v}_i}{\partial K_j}$, i = 1,n; and j = 1,2. In the notation of the FOCAL program (see statements 5.21 and 5.70 of Fig. 2.37) the following occurs:

for C^*: C(NP*(J-1)+K) = C(NP*(J-1)+K)/$\sqrt{CI(J)*CI(K)}$;

for g^*: C(NP*J) = C(NP*J)/$\sqrt{CI(J)}$.

In the FOCAL program, the equations to be solved are (in 1 dimension and after scaling):

$$\begin{aligned}
&C(1) * H(1) + C(2) * H(2) + C(3) * H(3) + C(4) * H(4) = C(5) , \\
&C(6) * H(1) + C(7) * H(2) + C(8) * H(3) + C(9) * H(4) = C(10) , \\
&C(11) * H(1) + C(12) * H(2) + C(13) * H(3) + C(14) * H(4) = C(15) , \\
&C(16) * H(1) + C(17) * H(2) + C(18) * H(3) + C(19) * H(4) = C(20) .
\end{aligned} \tag{12}$$

Here H(LA) (see Fig. 2.37, statement 5.34) are corrections to the initial estimates of the parameters (V_1, V_2, K_1, and K_2) which are being sought, i.e., ΔV_1, ΔV_2, ΔK_1, ΔK_2.

In program statements 5.25 to 5.36, the solution to this series of linear equations [(12)] is determined; LA, M, L, and J are counting variables used in the solution. The solution is by the straightforward method of elimination, i.e., statement 5.25 converts Eq. (12) into the upper triangular matrix:

$$
\begin{aligned}
&C(1) * H(1) + C(2) * H(2) + C(3) * H(3) + C(4) * H(4) = C(5) ,\\
&\quad 0 \quad + C(7)' * H(2) + C(8)' * H(3) + C(4)' * H(4) = C(10)' ,\\
&\quad 0 \quad + \quad 0 \quad + C(13)'' * H(3) + C(14)'' * H(4) = C(15)'' ,\\
&\quad 0 \quad + \quad 0 \quad + \quad 0 \quad + C(19)''' * H(4) = C(20)''' .
\end{aligned}
\tag{13}
$$

Program statements 5.30 through 5.36 then solve for the H's; that is,

$H(4) = C(20)'''/C(19)'''$,

$H(3) = (C(15)''-C(14)''*H(4))/C(13)''$,

etc.

Program statements 5.40 and 5.45 calculate the current estimates of V_1, V_2, K_1, and K_2. Program statements 5.50 and 8.20 compute $\Phi = (\bar{v}_i - \hat{v}_i)^2$, where $AV(L) = \bar{v}_i$ (measured velocity) and $EV(L) = \hat{v}_i$ (calculated velocity); here S1 is the value of Φ from the previous iteration and S2 is the value for the current iteration. Finally, the necessary checks are performed to ensure that the program is converging and, if diverging, so indicate and stop.

Initial estimation of parameters. Since the actual model, Eq. (1), is replaced by a linear approximation, Eq. (2), in the nonlinear regression analysis program, convergence is not uniformly guaranteed. The linearized form of the Taylor series is an adequate representation of the complete series expansion (a rigorous representation of the model) only when the corrections to the rth estimates (ΔV_1, ΔV_2, ΔK_1, and ΔK_2 in Eqs. (4a)-(7a) are small. Under these conditions, higher-order terms can be justifiably

neglected. Consequently, the initial estimates to the parameters must be quite good to ensure a high probability of convergence.

An improved computer program was written to obtain the initial estimates of the four kinetic parameters needed for the nonlinear regression analysis program. The program, reproduced in Fig. 2.38, is based on linear least-squares estimation of slopes (S_o and S_∞) at the extremes of the curve shown in Fig. 2.39. Intercepts (I_o, I_∞; Fig. 2.39) are obtained by extrapolation to $\frac{1}{S} = 0$.

The FOCAL program first computes a slope for the first two points at the extreme low-substrate end of the curve. The region is expanded one point at a time until deviation from linearity is observed as measured by a decrease in the correlation coefficient. After determining S_∞ and I_∞, the program computes slope data starting at the extreme high-substrate concentration end of the curve.

Figure 2.40 represents a typical output of the parameter estimation program for duplicate measurements of gamma-glutamyl transpeptidase activity at varying L-glutamyl-p-nitroaniline concentrations. Note that for duplicate measurements, points are fitted in groups of two as indicated by the print-out indicating "No. Points Used." These estimations furnished the input to the nonlinear regression program and converged to a solution in 13 iterations (program output shown in Fig. 2.41). The Lineweaver-Burk plot for these data was nonlinear as shown in Fig. 2.42, and the continuous line shown in this figure represents the curve generated using the converged parameters. The computer output of the nonlinear regression program, illustrated in Fig. 2.41, presents the following information for each iterative cycle:

ORNL DWG 76-628

```
C-GEMSAEC 2A 741163"

01.01 C-ISOENZYME STRIPPING PROGRAM SOLVE FOR INITIAL PARAMETERS.

03.02 S A=3.99985;D 9
03.04 F K=1,JS-1;S C(K)=0;S CO(K)=0
03.10 S J=2*JR+1
03.11 S J=JS-1
03.12 S SX=0;S SY=0;S XY=0;S X2=0;S Y2=0
03.15 F K=2,J; D 4.
03.20 G 5.01

04.10 S SX=SX+1./S(K);S SY=SY+1./A"(K);S Y2=Y2+1/(A"(K)*A"(K))
04.11 S XY=XY+1./(S(K)*A"(K));S X2=X2+1./(S(K)*S(K))

05.01 S MM=(XY-SX*SY/(J-1))/(X2-SX*SX/(J-1))
05.03 S BI(J)=SY/(J-1)-SX*MM/(J-1);S C(J)=MM
05.05 S CO(J)=((J-1)*XY-SX*SY)/FSQT(((J-1)*X2-SX*SX)*((J-1)*Y2-SY*SY))
05.07 I (J-2*JR-1) 5.10,5.11,5.10
05.10 I (A-CO(J))5.11,5.11;I (CO(J+1)-CO(J))5.12,5.12,5.13
05.11 S J=J-1;S J=J+JR;D 3.12
05.12 S SI=C(J);S II=BI(J);D 10;G 5.15
05.13 S SI=C(J+1);S II=BI(J+1);D 10.
05.15 D 3.04
05.21 D 3.10;D 3.12
05.23 S J=1
05.27 F I=2,J;D 6
05.29 G 7.10

06.09 S K=JS*JR-I+3;D 4

07.10 D 5.01;D 5.03;D 5.05
07.13 I (J-2*JR-1) 7.17,7.18,7.17
07.17 I (A-CO(J))7.18,7.18;I (CO(J)-CO(J-1))7.30,7.40,7.40
07.18 S J=J+1;S J=J+JR;D 3.12;G 5.27
07.30 S SL=C(J-1);S IO=BI(J-1);G 11.05
07.40 S SL=C(J);S IO=BI(J);G 11.05

08.10 S DD=(SL+SI)/(II+IO);S BB=(SL*II+SI*IO)/(II*IO);S CC=SL*SI/(IO*II)
08.20 S AA=IO*II/(II+IO)
08.30 S SU=FSQT(BB↑2-4*CC)/2;S KM(1)=BB/2+SU;S KM(2)=BB/2-SU
08.40 S VM(2)=(DD-KM(2))/(AA*(KM(1)-KM(2)));S VM(1)=1/AA-VM(2)
08.50 T !!!!!!"                    PARAMETER ESTIMATES FOLLOW"!!
08.60 T !,"KM1=",KM(1)," KM2=",KM(2)," VM1=",VM(1)," VM2=",VM(2),!!!!!
*
09.10 T !!!"                    DATA SUMMARY"!!!
09.20 T " J      A"(J)      S(J)     1/A"(J)      1/S(J)"!!
09.30 F J=2,JS*JR+1;T !%2,J;T #%8.05,"    ",A"(J),S(J),1/A"(J),1/S(J)
09.40 T !!!"SEARCH FOR LINEARITY WITH REQUIRED CORRELATION COEF.= ",A,!!
09.50 T "***LOW SUBSTRATE CONCENTRATIONS***"!
09.60 T "NO. POINTS USED      SLOPE      CORRELATION COEFFICIENT"!

10.05 S L=JS-1
10.10 F J=2*JR,JR,J;D 10.30
10.20 G 10.40
10.30 T !%6,J;T #%8.05,"                    ",C(L),"      ",CO(L);S L=L-1
10.40 T !!!"***HIGH SUBSTRATE CONCENTRATIONS***"!
10.50 D 9.60

11.05 S L=1
11.10 F J=2*JR,JR,J;D 11.30
11.20 D 8.;G 20.05
11.30 T !%6,J;T #%8.05,"                    ",C(L),"      ",CO(L);S L=L+1

20.05 F I=1,2;S DY=KM(I);S D=FSTR(950+I,DY);S DY=VM(I);S D=FSTR(955+I,DY
20.10 L G 39,G
20.25 F I=1,2;S KM(I)=FSTR(950+I);S VM(I)=FSTR(955+I)
20.26 L G 16,G 5.05
*
```

Fig. 2.38. FOCAL program for the initial estimation of kinetic parameters (V_1, K_1, V_2, K_2) of the two-enzyme model. Corrections to these estimates are determined by nonlinear regression.

ORNL-DWG 76-623

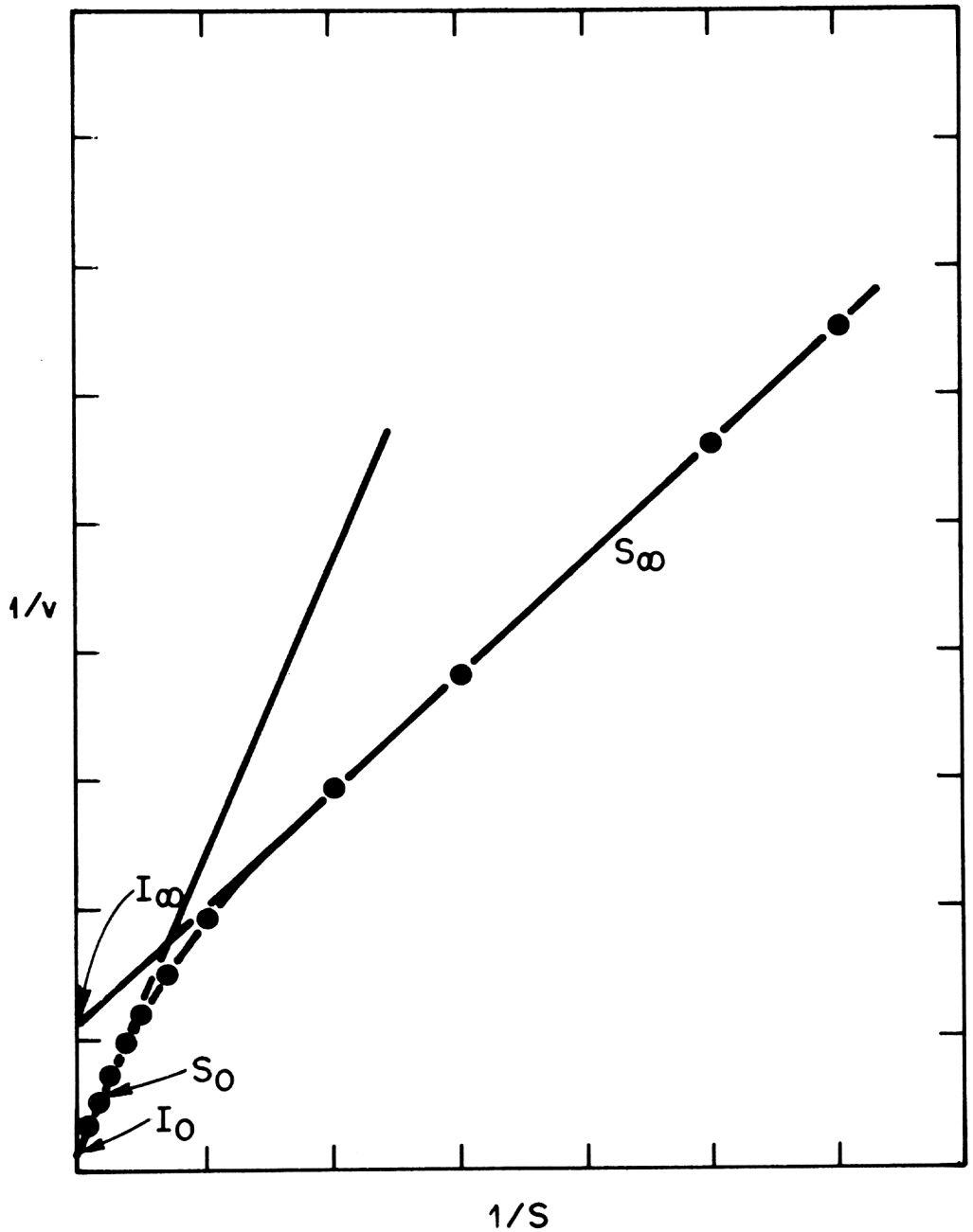

INITIAL ESTIMATION OF Km_1, Km_2, Vm_1 AND Vm_2

Fig. 2.39. Lineweaver-Burk plot for two enzymes, differing in K_m's but acting on the same substrate.

ORNL DWG 76-632

11-6-75
ANALYSIS OF CAB SERUM SAMPLE FOR POSSIBILITY OF ISOENZYMES OF GGTP
BY USE OF ENZYME STRIPPING ROUTINES, FILES 15 AND 16.

DATA SUMMARY

J	AV(J)	S(J)	1/AV(J)	1/S(J)
2	0.01087	0.29570	91.96820	3.38181
3	0.01185	0.29570	84.36920	3.38181
4	0.01629	0.51450	61.40070	1.94364
5	0.01591	0.51450	62.85000	1.94364
6	0.02165	0.73930	46.20000	1.35263
7	0.02115	0.73930	47.28380	1.35263
8	0.02462	1.03500	40.61600	0.96618
9	0.02597	1.03500	38.50610	0.96618
10	0.03011	1.47860	33.20890	0.67632
11	0.02945	1.47860	33.96020	0.67632
12	0.03528	2.07000	28.34480	0.48309
13	0.03627	2.07000	27.56840	0.48309
14	0.03766	2.51360	26.55570	0.39784
15	0.04025	2.51360	24.84260	0.39784
16	0.04144	2.95710	24.13150	0.33817
17	0.04026	2.95710	24.83790	0.33817

SEARCH FOR LINEARITY WITH REQUIRED CORRELATION COEF.= 0.99985

LOW SUBSTRATE CONCENTRATIONS

NO. POINTS USED	SLOPE	CORRELATION COEFFICIENT
4	18.10880	0.97865
6	19.98560	0.98749

HIGH SUBSTRATE CONCENTRATIONS

NO. POINTS USED	SLOPE	CORRELATION COEFFICIENT
4	20.35690	0.67979
6	24.13060	0.92515

PARAMETER ESTIMATES FOLLOW

KM1= 1.48578 KM2= 0.94316 VM1= 0.06157 VM2= 0.04719

Fig. 2.40. Typical output of the parameter-estimation program for duplicate measurements of serum gamma-glutamyl transpeptidase at varying L-glutamyl-p-nitroaniline concentrations.

ORNL DWG 76-631

```
- 0.01557   0.07714   3.31626-   1.83047
  0.08468-  0.03749   0.48865    0.45451
 0.01153040  0.01067340  3.56456000


 0.05459700- 0.07016550  4.57754000- 1.26128000
 0.01601730  0.06865960  0.48091100  0.00774002
 0.01067340  0.00033947  1.60052000


 0.04999720  0.00459984  1.95773000  2.61980000
 0.01612270- 0.00010537  0.43954020  0.04137150
 0.00033947  0.00015691  6.86510000


 0.04329620  0.00670095  3.24832000- 1.29029000
 0.02728790- 0.01116533  0.62697830- 0.18743930
 0.00015691  0.00007273  1.70015000


 0.05881490- 0.01551870  2.30944000  0.93857900
 0.01040800  0.01688020  0.40794400  0.21903500
 0.00007273  0.00001649  0.92943200


 0.05118240  0.00763252  3.04286000- 0.73341900
 0.01984090- 0.00943291  0.57116530- 0.16322200
 0.00001649  0.00001392  0.56469100


 0.05622210- 0.00503968  2.86157000  0.18128700
 0.01423630  0.00560454  0.41912100  0.15204400
 0.00001392  0.00000910  0.05603910


 0.05425670  0.00196544  3.08926000- 0.22768700
 0.01699020- 0.00275388  0.47608700- 0.05696580
 0.00000910  0.00000883  0.05509760


 0.05457220- 0.00031551  3.03326000  0.05600320
 0.01638870  0.00060152  0.45939700  0.01668970
 0.00000883  0.00000882  0.00341536


 0.05445940  0.00011274  3.06025000- 0.02699720
 0.01661570- 0.00022698  0.46418300- 0.00478585
 0.00000882  0.00000882  0.00075182


 0.05449910- 0.00003975  3.05054000  0.00970975
 0.01653340  0.00008229  0.46241400  0.00176920
 0.00000882  0.00000882  0.00009742


 0.05448480  0.00001436  3.05420003- 0.00365584
 0.01656360- 0.00003026  0.46335630- 0.00064304
 0.00000882  0.00000882  0.00001378


 0.05449040- 0.00000566  3.05277000  0.00142620
 0.01655170  0.00001188  0.46280300  0.00025311
 0.00000882  0.00000882  0.00000210


ENZYME  1    VM=  0.054491  KM=  3.052770
ENZYME  2    VM=  0.016552  KM=  0.462803

STANDARD ERROR 0.766595E-003
*
```

Fig. 2.41. Thirteen iterations performed by the nonlinear regression program. Converged parameters were determined for serum gamma-glutamyl transpeptidase using initial estimates from the parameter estimation program. Each iteration presents, respectively, V_{max_1}, ΔV_1, K_{m_1}, ΔK_1, V_{max_2}, ΔV_2, K_{m_2}, ΔK_2, ϕ_1, ϕ_2, and LS, the magnitude of the error vector.

ORNL DWG 76-627 R1

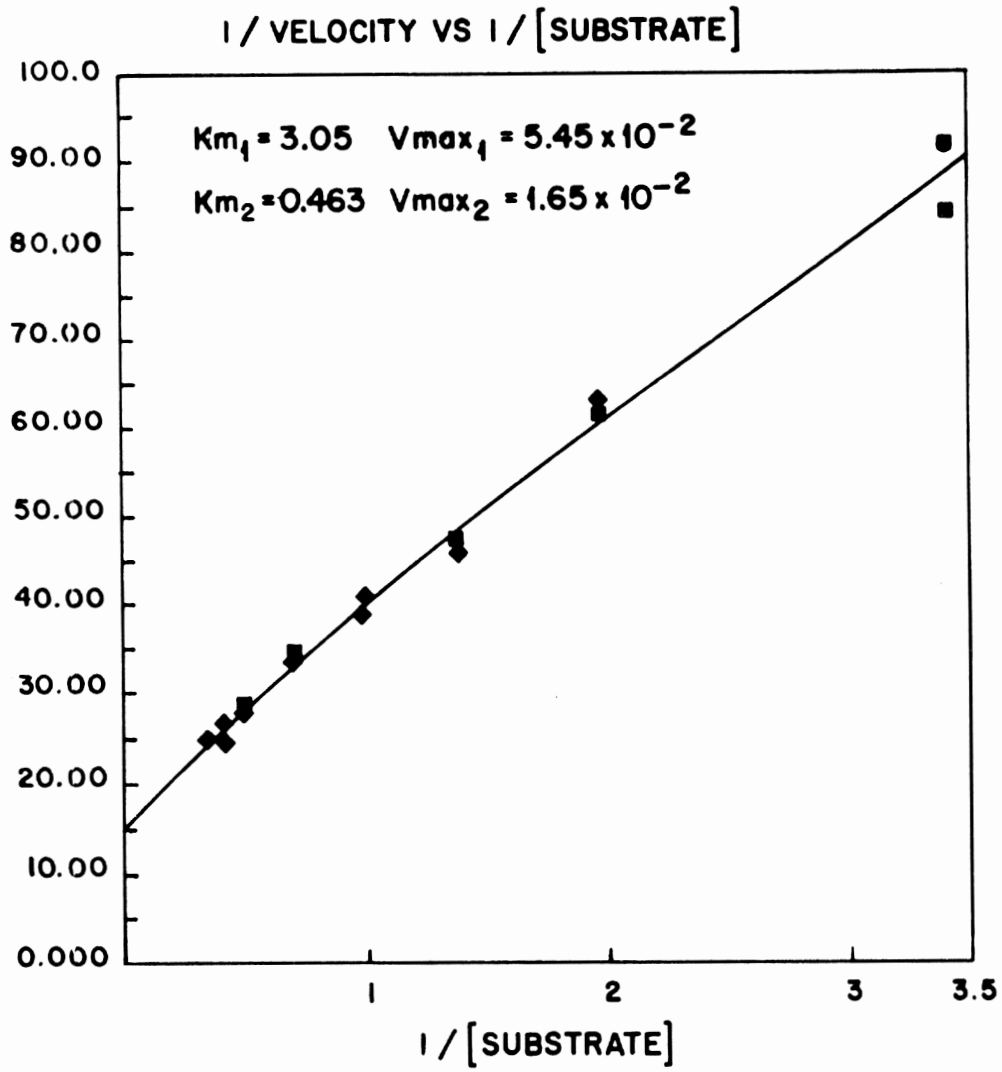

Fig. 2.42. Lineweaver-Burk plot for serum gamma-glutamyl transpeptidase velocity data at varying substrate concentrations. Continuous line is the two-enzyme function plotted using the converged parameters, while the data points represent measured reaction velocities. These data are presented for illustrative purposes only and should not be viewed as indicating the presence of two isoenzymes of GGTP without other confirmatory work.

V_{max_1}	ΔV_{max_1}	K_{m_1}	ΔK_{m_1}
V_{max_2}	ΔV_{max_2}	K_{m_2}	ΔK_{m_2}
ϕ_1	ϕ_2	LS	

where

V, K = current estimates of the kinetic parameters;

ΔV, ΔK = corrections to the parameters from the previous iteration;

$\phi_1 = \sum_i (\bar{v}_i - \hat{v}_i)^2$, previous iteration;

$\phi_2 = \sum_i (\bar{v}_i - \hat{v}_i)^2$, current iteration;

$\bar{v}_i$ = observed reaction velocity;

$\hat{v}_i$ = calculated velocity using current parameter estimates;

$LS = \sum_{i=1,2} (\Delta v_i^2 + \Delta K_i^2)$, that is, the magnitude of the error vector.

2.3.6 Biochemical markers of cancer - kinetic analysis for serum gamma-glutamyl transpeptidase

Previous studies[4] had demonstrated the utility of a commercial reagent kit* for the kinetic assay of serum gamma-glutamyl transpeptidase (GGTP) on the Centrifugal Fast Analyzer (CFA). However, the substrate (L-glutanyl-*p*-nitroaniline) had several problems associated with its use: (1) limited solubility that required heating at 37°C to solubilize the reagent, and (2) complete utilization of the reconstituted reagent was necessary within 1 to 2 hr to minimize reagent self-hydrolysis. A new substrate, L-glutamyl-2-amino-5-nitrobenzoate, now available in the form of a reagent kit,** was

---

*Worthington Statzyme.

**Available from Bio-Dynamics/bmc, Indianapolis, Indiana 46250.

designed to overcome the solubility problems with L-glutamyl-p-nitroaniline.

A sample of this new reagent kit was obtained* and tested using sera and control samples previously measured using L-glutamyl-p-nitroaniline. The composition of the new reagent kit differs somewhat from that containing the less-soluble substrate since glutamine has been deleted. Rock and Slickers[53] and Gerhardt, Persijn, and Rosalki[54] have reported finding no effect of added glutamine on the measured activity of GGTP, essentially refuting the work of Bondar and Moss[55] whose work apparently resulted in the inclusion of glutamine in the Worthington reagent kit for GGTP. Literature accompanying the new reagent kit indicated that kinetic assays for GGTP with the new substrate would duplicate those using L-glutamyl-p-nitroaniline with added glutamine, therefore eliminating the need for redetermining normal ranges. As shown in Table 2.19, our results using the new substrate were essentially identical to the previously obtained data confirming this point. The four cancer sera shown in this table have been frozen at -70°C for approximately 5 months since the first analysis. The results suggest stability of the enzyme over this period of time and indicate that two freeze-thaw cycles have not appreciably affected activity, although some loss in activity may have occurred for low-activity samples (see No. 2 in Table 2.19).

The new substrate was quite soluble and appeared to be stable over several days when kept at refrigerator temperatures. Results obtained with it were more precise than those obtained with L-glutamyl-p-nitroaniline (compare C.V.'s for Statzyme control sera in Table 2.19).

---

*Courtesy of Dr. H. Rehkaemper, Bio-Dynamics/bmc, Indianapolis, Indiana.

Table 2.19. Comparison of serum gamma-glutamyl transpeptidase activities using the substrates L-glutamyl-p-nitroaniline and L-glutamyl-2-amino-5-nitrobenzoate

Sample	GGTP activity (IU/liter)			
	Glu NA[a]	CV (%)	Glu ANB[b]	CV (%)
Statzyme control sera	9.27[c]	12.5	9.11	3.6
Serum 1	112.5	ND[d]	109.2	0.5
Serum 2	18.2	ND	11.2	10.1
Serum 3	66.1	ND	65.7	0.3
Serum 4	256.8	ND	252.0	0.9

[a]Activity measured about 5 months ago using L-glutamyl-p-nitroaniline.

[b]Activity measured using L-glutamyl-2-amino-5-nitrobenzoate.

[c]Freshly prepared control sera.

[d]Not determined.

Heterogeneity of serum GGTP. In a number of instances, the heterogeneity of an enzyme system has been used clinically to confirm specific organ or tissue damage within the body or as a diagnostic aid. Notable examples include use of the MB isoenzyme of creatinine kinase as a sensitive and specific test of myocardial infarction;[56] dramatic changes demonstrated in the pattern of five isoenzymes of serum lactate dehydrogenase indicate various disease states, including myelogenous leukemia and hepatitis.[57] Several workers have demonstrated the heterogeneity of serum GGTP since the first description of this finding by Kokot and Kuska.[58]

Azzopardi and Jayle[59] separated five zones of GGTP activity from normal human sera by acrylamide gel electrophoresis. Sephadex gel filtration enabled the separation of at least three components, indicating that GGTP isoenzymes of serum may reflect differences not only in charge, but also in molecular weight.[59-62] Miyazaki and Okumura[63] reported three zones of activity for serum GGTP by agar gel electrophoresis and indicated that the middle zone (GT-II) was enhanced in all malignant lesions involving the hepatobiliary and/or pancreatic areas. Hetland, Andersson, and Gerner reported that the predominance of serum GGTP activity was always found in fractions corresponding to either α_1-, α_2-, or β-globulins when electrophoretic separations were performed on agarose gel.[64] These authors noted the predominance of α_2- and/or the β-fraction in most cases associated with malignancy involving the liver and/or pancreas.

Electrophoresis is generally used to visualize variability of serum isoenzymes; however, it is highly operator-dependent and laborious. Our initial approach to investigating possible differences in serum GGTP between patients with cancer and clinically normal subjects was to measure

the Michaelis-Menten kinetic parameter, K_m, for variable substrate concentrations. Table 2.20 lists K_m's for several normal male and female subjects and for cancer patients with total GGTP activities ranging from slightly above the upper limit (95% confidence) of our normal data to greater than 2000 IU/liter. The data, shown in Table 2.20, were measured only as a function of substrate concentration at a pH of 8.1. All dilutions of substrate were performed on the automated rotor-loading system, and the K_m's show reasonably good precision even for the low-activity normal sera. Calculations were performed by the Wilkinson method[51] coupled with an iterative procedure to refine the parameters.[41] Maximum reaction velocities (V_{max} values) were also computed; however, since they are a function of enzyme concentration and K_m's are a qualitative property of the enzyme itself, the velocities were not included in the tabular data.

Note that K_m's determined for GGTP in normal sera displayed a wider range of values (0.55 to 2.02 millimoles) than those for cancer patients (0.84 to 1.16 millimoles). The greater variability observed for normal subjects may represent variability in individual tissue isoenzyme contributions to the total serum activity, whereas the uniformity in K_m found for cancer patients may represent the overriding contribution of the afflicted tissue (usually the liver) enzyme to the total activity. Additional experiments on patients with localized malignancies such as pancreatic and kidney tumors that had not yet metastasized to the liver would be useful. However, in general, the differences among the various K_m's appear to be no greater than a factor of 4. The only literature data on K_m's of serum GGTP are those of Jacyszyn and Laursen who measured the kinetic parameters for electrophoretically separated serum fractions.[62] Their measurements suggested

Table 2.20. Determination of the Michaelis-Menten parameter for serum GGTP at variable substrate concentrations

Serum Sample	Sex	Description	Total GGTP Activity (IU/liter)	K_m (millimoles)	Relative Error (%)
CB	Male	Normal	32.8	1.10	3.8
JM	Male	Normal	11.0	0.69	9.0
1425	Female	Normal	8.4	2.02	10.2
1819	Female	Normal	10.9	0.55	11.7
1665	Unknown	Colon cancer[a]	37.6	0.98	6.6
1573	Unknown	Colon cancer[a]	35.5	1.10	6.6
1841	Unknown	Colon cancer[a]	68.5	0.93	5.7
2245	Unknown	Cancer	84.3	1.16	5.1
2124	Unknown	Cancer	111.4	1.13	1.4
2250	Unknown	Colon cancer[a]	212.0	0.99	3.8
501	Unknown	Colon cancer[a]	2023[b]	0.84	11.3

[a]With liver involvement.

[b]Sample diluted 1:10 with normal saline.

differences of approximately a factor of 2 (K_m's ranged from 0.7 to 1.2 for serum and from 1.15 to 1.5 for urine fractions of GGTP).

Differences found in K_m's of GGTP seem to indicate little difference in the affinity for substrate among the various serum samples (see Table 2.20). However, studies of the thermal stability of this enzyme system may enable conditions to be found which will differentiate among the isoenzymes. For example, Hamada[65] found that the M_4 isoenzyme of lactate dehydrogenase from neoplastic tissues was significantly more resistant to heat inactivation than the same isoenzyme from noncancerous tissue. A variant isoenzyme of alkaline phosphatase (AP) which is less stable to heat than the Nagao[66] and Regan[67] isoenzymes of placental AP was reported to have been isolated from several patients with hepatocellular carcinoma.[68] Relatively rapid screening of serum samples for residual enzyme activity after heat inactivation in external block heaters can be performed with the unique capabilities of the miniature CFA.

Heat stability studies were performed on sera from a number of cancer patients with subsequent measurement of GGTP. Temperatures studied ranged from 55° to 70°C with exposures ranging from 5 to 40 min. Figure 2.43 illustrates typical results obtained at 55°, 60°, and 65°C. Very little effect on GGTP activity was noted for sera subjected to a temperature of 55°C for 40 min; however, exposure to 65°C for 10 min destroyed all activity. A temperature of 60°C resulted in a linear decrease of the log of percent residual activity with time. This is an Arrhenius-type plot typical of heat inactivation of enzymes. Six sera from cancer patients were studied at 60°C. The results (Table 2.21 and Fig. 2.44) suggest great similarity in the semilogarithmic curves for four of the samples (compare

ORNL DWG 76-298

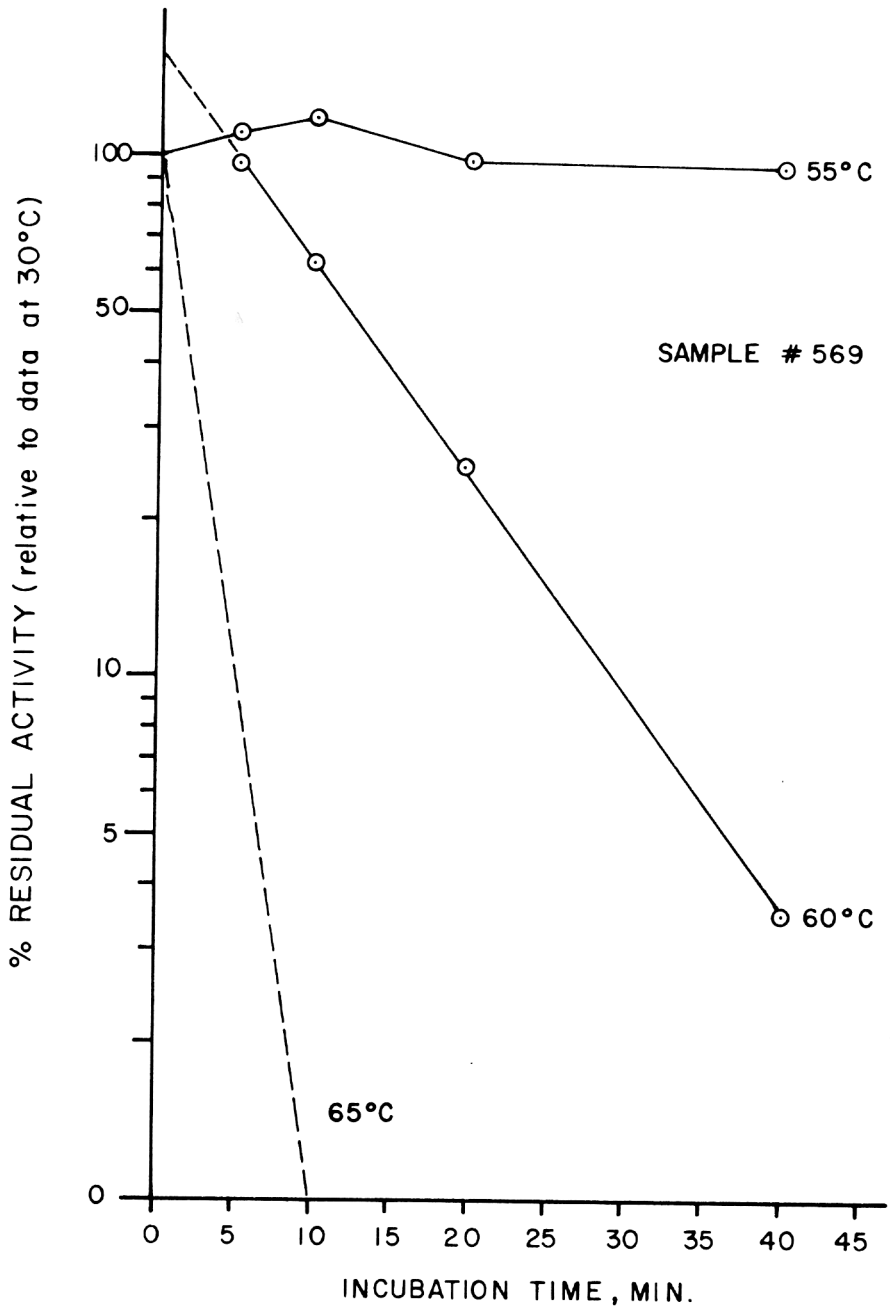

Fig. 2.43. The effect of heat inactivation on serum gamma-glutamyl transpeptidase activities in serum.

Table 2.21. Heat inactivation of gamma-glutamyl transpeptidase activity in cancer-patient sera

Sample number	Initial[a] activity	Loss in activity at 60°C[b] (%/min)	Extrapolated initial activity[c] (%)	Correlation coefficient
146	48	12.0	143	-0.9963
197	235.5	12.7	126	-0.9999
461	239.5	13.4	126	-0.9997
569	247.6	17.9	160	-0.9996
2673	272.2	14.6	121	-0.9992
568	319	15.9	129	-0.9999

[a]I.U. at 30°C.

[b]Calculated relative to results at 30°C.

[c]Calculated from linear least-squares analysis; listed as percent of initial activity.

x = time (min) incubation at 60°C.

y = log (fractional activity remaining, relative to results at 30°C).

Slope x 4.34 = percent loss in activity per minute at 60°C.

Antilog (y-intercept) = extrapolated initial percent activity.

ORNL DWG 76-297

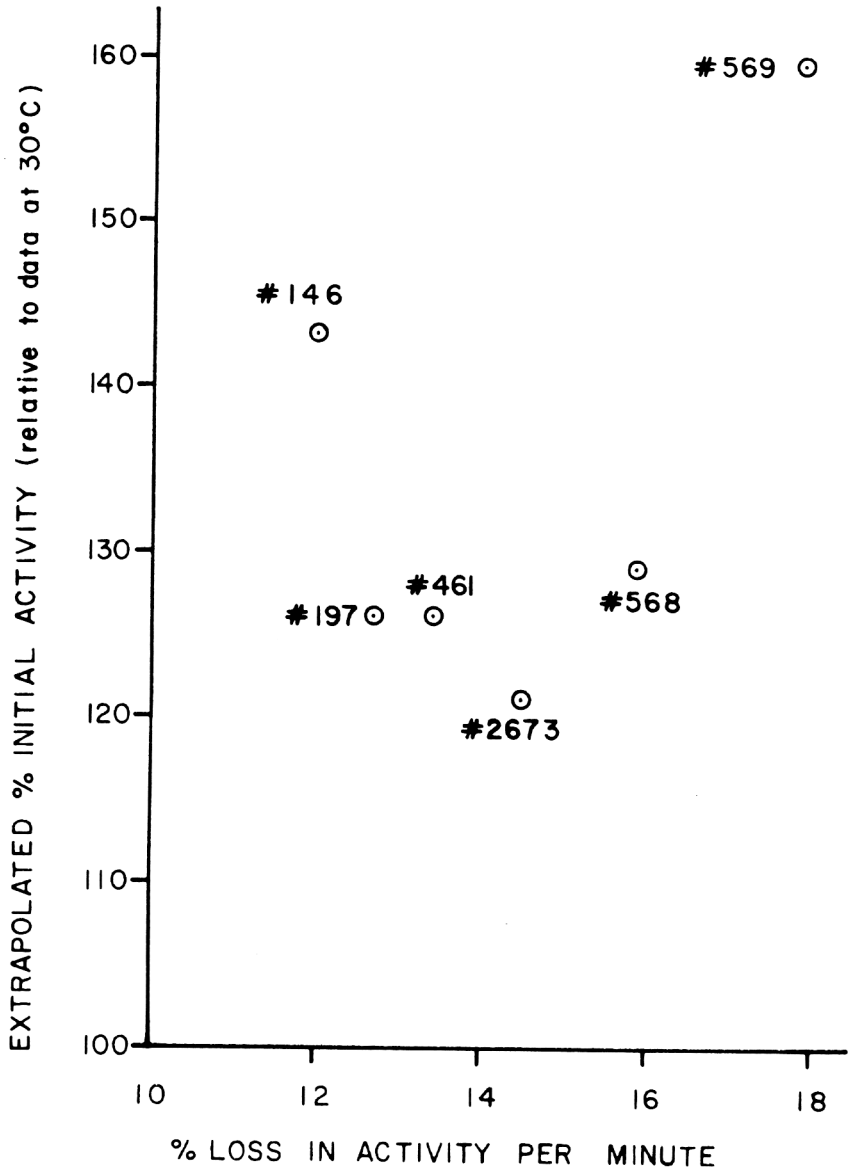

Fig. 2.44. The effect of heat inactivation at 60°C on the activities of gamma-glutamyl transpeptidase in several sera from cancer patients.

slopes and extrapolated intercepts for sample Nos. 197, 461, 2673, and 568 in Table 2.21). Sample No. 569, on the other hand, differed rather dramatically (see Fig. 2.44) in displaying a faster rate of loss in activity and a different intercept. The larger intercept noted for sample No. 146 is discounted to some extent because of the uncertainties in activity measurements at this low-activity level. The initial increase in activity noted for these studies may be due to the destruction of an inhibitor of GGTP present in the serum.

Variations in the rate of heat inactivation have been documented for different isoenzymes of malate dehydrogenase in maize.[69] Rates of inactivation differed for both the soluble and mitochondrial forms of MDH isoenzymes. Any means of differentiating isoenzymes offers the possibility of identifying the source tissue or organ from which an elevated amount of isoenzyme originated and, therefore, identifies the injured organ or tissue by a noninvasive technique. This, of course, has sparked our interest in the use of heat inactivation coupled with rapid kinetic assay on the CFA as an additional means of evaluating this enzyme as to its potential utility as a biochemical marker of malignancy.

2.4 References for Section 2

1. C. A. Burtis, J. M. Begovich, and J. S. Watson, "Factors Influencing Evaporation from Sample Cups, and Assessment of Their Effect on Analytical Error," Clin. Chem. 21, 1907 (1975).

2. C. A. Burtis, W. D. Bostick, and W. F. Johnson, "Development of a Multipurpose Optical System for Use with a Centrifugal Fast Analyzer," Clin. Chem. 21, 1225 (1975).

3. T. O. Tiffany et al., "Enzymatic Kinetic Rate and End-Point Analyses of Substrate, by Use of a GeMSAEC Fast Analyzer," Clin. Chem. 18, 829 (1972).

4. C. A. Burtis, J. E. Mrochek, and C. D. Scott, Biochemical Technology Program Progress Report for the Period July 1-December 31, 1975, ORNL/TM-5167 (January 1976).

5. C. A. Burtis, W. F. Johnson, and J. B. Overton, "Automated Loading of Discrete, Microliter Volumes of Liquids into a Miniature Fast Analyzer," Anal. Chem. 46, 786 (1974).

6. H. Verdouw, "Enzymatic NH_3-N Determination: A Specific Method for the Determination of Ammonia in Water and Sediments," Water Res. 7, 1129 (1973).

7. K. Kodama, Methods of Quantitative Inorganic Analysis, pp. 462-63, Interscience, New York, 1963.

8. R. G. Bond and C. P. Staub (eds.), Handbook of Environmental Control. Vol. III: Water Supply and Treatment, CRC Press, Cleveland, Ohio, 1973.

9. H. V. Malmstadt, C. J. Delaney, and E. A. Cordos, "Reaction-Rate Methods of Chemical Analysis," Anal. Chem. 2, 559 (1972).

10. C. A. Burtis et al., "Development of an Analytical System Based Around a Miniature Fast Analyzer," Clin. Chem. 19, 895 (1973).

11. W. D. Bostick, C. A. Burtis, and C. D. Scott, "Simultaneous Determination of Silica and Phosphate in Water From a Single Experiment Using a Miniature Centrifugal Fast Analyzer," Anal. Lett. 9, 65 (1976).

12. C. D. Scott et al., "A Small, Portable Centrifugal Fast Analyzer System," Clin. Chem. 20, 1003 (1974).

13. B. Schuknecht et al., "Nitrates in Wisconsin Ground Water," Environ. Lett. 9, 91 (1975).

14. International Water Supply Association (London), "Nitrates in Water Supplies," International Committee on Water Quality and Treatment, Aqua 1, 5 (1974).

15. P. L. Brezonik, "Nitrogen: Sources and Transformations in Natural Waters," Chapter I in Nutrients in Natural Waters, ed. by H. E. Allen and J. R. Kramer, Wiley-Interscience, New York, 1972.

16. P. W. West and T. P. Ramachandran, "Spectrophotometric Determination of Nitrate Using Chromotropic Acid," Anal. Chim. Acta 35, 317 (1966).

17. APHA, AWWA, and WPCF, Standard Methods for the Examination of Water and Wastewater, 13th ed., APHA, 1971.

18. J. B. Mullin and J. P. Riley, "The Spectrophotometric Determination of Nitrate in Natural Waters, with Particular Reference to Sea Water," Anal. Chim. Acta 12, 464 (1955).

19. D. Jenkins and L. L. Medsker, "Brucine Method for the Determination of Nitrate in Ocean, Estuarine, and Fresh Waters," Anal. Chem. 36, 610 (1964).

20. D. W. Hatcher, "Studies of Nitrate Reduction. I. Complexation Mechanism of Nitrate Reduction. II. Analytical Applications of Nitrate Reduction," Ph.D. Thesis, Purdue University, 1967.

21. A. Hulanicki, R. Lewandowski, and M. Maj, "Determination of Nitrate in Water with a New Construction of Ion-Selective Electrode," Anal. Chim. Acta 69, 409 (1974).

22. L. R. McKenzie and P. N. W. Young, "Determination of Ammonia-, Nitrate- and Organic Nitrogen in Water and Waste Water with an Ammonia Gas-Sensing Electrode," Analyst 100, 620 (1975).

23. W. H. Strowd, "The Determination of Nitrites and Nitrates in Plant Tissue," Soil Science 10, 333 (1920).

24. D. L. Heans, "Determination of Nitrate in Soil and Water by an Adaptation of an Orange 1 Method," Analyst 100, 316 (1975).

25. T. J. Chow and M. S. Johnstone, "Determination of Nitrate in Sea Water," Anal. Chim. Acta 27, 441 (1962).

26. A. W. Morris and J. P. Riley, "The Determination of Nitrate in Sea Water," Anal. Chim. Acta 29, 272 (1963).

27. "Methods for Chemical Analysis of Water and Wastes," U.S. Environmental Protection Agency, Office of Technological Transfer, Washington, D.C., 1974.

28. A. Nason, "Nitrate Reductases," Chapter 25 in The Enzymes, Vol. VII, ed. by P. D. Boyer, H. Lardy, and K. Myrback, Academic Press, New York, 1963.

29. G. B. Garner et al., "Microbiological Determination of Nitrate," Anal. Chem. 28, 1589 (1956).

30. R. M. Hill et al., "Improved Microbiological Method for Nitrate Determination," J. Agr. Food Chem. 7, 261 (1959).

31. "Nitrate Reductase (E. coli), Cytochrome:Nitrate Oxidoreductase," Worthington Biochemical Corporation, Freehold, NJ.

32. R. H. Hageman et al., "Use of Dissimilatory Nitrate Reductase from Escherichia coli and Formate as a Reductive System for Nitrate Assays," J. Agr. Food Chem. 19, 229 (1971).

33. D. R. Senn, "I. The Effect of the Reaction $B+C \underset{k_{-2}}{\overset{k_2}{\rightleftharpoons}} A+D$ on the Determination of the Kinetic Parameters of the ECE Mechanism.

II. The Trace Determination of Nitrate in Environmental Samples Employing an Enzyme Catalyzed Reaction," Ph.D. Thesis, University of Georgia, 1975.

34. W. R. Hussein and G. G. Guilbault, "I. Nitrate and Ammonium Ion-Selective Electrodes as Sensors. II. Assay of Nitrate Ion and Nitrate and Nitrite Reductases in Stationary Solutions and Under Flow-Stream Conditions," Anal. Chim. Acta 76, 183 (1975).

35. A. Nason and H. J. Evans, "Triphosphopyridine Nucleotide-Nitrate Reductase in Neurospora," J. Biol. Chem. 202, 655 (1953).

36. R. H. Garrett and A. Nason, "Involvement of a β-Type Cytochrome in the Assimilatory Nitrate Reductase of Neurospora crassa," Proc. Nat. Acad. Sci. USA 58, 1603 (1967).

37. R. H. Garrett and A. Nason, "Further Purification and Properties of Neurospora Nitrate Reductase," J. Biol. Chem. 244, 2870 (1969).

38. B. Venneland and C. Jetschmann, "The Nitrate Reductase of Chlorella pyrenoidosa," Biochim. Biophys. Acta 229, 554 (1970).

39. S. Pan, Johns Hopkins University, Baltimore, Maryland, personal communication, 1975.

40. W. D. Bostick, R. C. Lovelace, and C. A. Burtis, "Enzymatic Determination of Ammonia with a Miniature Centrifugal Fast Analyzer," Water Res. (submitted for consideration).

41. T. O. Tiffany, D. D. Chilcote, and C. A. Burtis, "Evaluation of Kinetic Enzyme Parameters by Use of a Small Computer Interfaced 'Fast Analyzer' - An Addition to Automated Clinical Enzymology," Clin. Chem. 19, 908 (1973).

42. J. D. Ingle, Jr., and S. R. Crouch, "Theoretical and Experimental Factors Influencing the Accuracy of Analytical Rate Measurements," Anal. Chem. 43, 697 (1971).

43. M. Roth, "Fluorimetric Assay of Enzymes," pp. 189-285 in Methods of Biochemical Analysis, vol. XVII, ed. by D. Glick, Interscience, New York, 1969.

44. T. E. Barman, p. 211 in Enzyme Handbook, vol. I, Springer-Verlag, New York, 1969.

45. A. Nason, Johns Hopkins University, Baltimore, Maryland, personal communication, 1975.

46. L. P. Solomonson and B. Vennesland, "Properties of a Nitrate Reductase of Chlorella," Biochim. Biophys. Acta 267, 544 (1972).

47. C. A. Burtis, J. E. Mrochek, and C. D. Scott, Biochemical Technology Program Progress Report for the Period January 1-June 30, 1975, ORNL/TM-5006 (August 1975).

48. P. Blume and H. F. Polesky, "An Instrumental Method for the Detection of Erythrocyte Agglutination," J. Lab. & Clin. Med. 74, 691 (1965).

49. T. O. Tiffany et al., "Blood Grouping with a Miniature Centrifugal Fast Analyzer," Clin. Chem. 20, 1043 (1974).

50. Technical Methods and Procedures of the American Association of Blood Banks, Sixth Edition, J. B. Lippincott Company, Philadelphia, 1974.

51. C. N. Wilkinson, "Statistical Estimations in Enzyme Kinetics," Biochem. J. 80, 324 (1961).

52. D. W. Marquardt. J. Soc. Indust. Appl. Math. 11(2), 431 (1963).

53. R. C. Rock and K. A. Slickers, "Glutamate and γ-Glutamyl Transpeptidase Activity," Clin. Chem. 21, 166 (1975).

54. W. Gerhardt, P. Persijn, and S. B. Rosalki, "Lack of Significant Effect of L(+)-Glutamate on Serum γ-Glutamyltransferase Activity Determined in the Presence of Glycylglycine," Clin. Chem. 21, 1515 (1975).

55. R. J. L. Bondar and G. A. Moss, "Enhancing Effect of Glutamate on Apparent Serum γ-Glutamyltranspeptidase Activity," Clin. Chem. 20, 317 (1974).

56. G. S. Wagner et al., "The Importance of Identification of the Myocardial-Specific Isoenzyme of Creatinine Phosphokinase (MB Form) in the Diagnosis of Acute Myocardial Infarction," Circulation 47, 263 (1973).

57. E. S. Vesell and A. G. Bearn, "Localization of Lactic Dehydrogenase Activity in Serum Fractions," Proc. Soc. Exp. Biol. Med. 94, 96 (1957).

58. F. Kokot and J. Kuska, "The Significance of the γ-Glutamyl Transpeptidase Isoenzyme in Clinical Diagnosis," Clin. Chim. Acta 11, 118 (1965).

59. O. Azzopardi and M. F. Jayle, "Formes Moléculaires Multiples de la Gamma-Glutamyltranspeptidase," Clin. Chim. Acta 43, 163 (1973).

60. S. B. Rosalki, "Gamma-Glutamyl Transpeptidase," Advan. Clin. Chem. 17, 53 (1975).

61. M. Orlowski, A. Szczeklik, and B. Kolaczkowska, "Heterogeneity of Human γ-Glutamyl Transpeptidase Studied by Sephadex Gel Filtration," Arch. Immunol. Therap. Exptl. (Engl. Transl.) 13, 564 (1965).

62. K. Jacyszyn and T. Laursen, "A Method for the Determination of the Heterogeneity of γ-Glutamyl Transpeptidase," Clin. Chim. Acta 19, 345 (1968).

63. S. Miyazaki and M. Okumura, "Change of Serum γ-Glutamyl Transpeptidase Level and Isoenzyme Pattern in Hepatobiliary Pancreatic Disease," Clin. Chim. Acta 40, 193 (1972).

64. Ö. Hetland, T. R. Andersson, and T. Gerner, "The Heterogeneity of the Serum Activity of γ-Glutamyl Transpeptidase in Hepatobiliary Diseases as Studied by Agarose Gel Electrophoresis," Clin. Chim. Acta 62, 425 (1975).

65. M. Hamada, "Relationship Between the Change in the Tertiary Structure of Human Tumor Lactate Dehydrogenase and Carcinogenosis," p. 143 in Isozymes, Vol. II. Physiological Function, ed. by C. L. Markert, Academic, New York, 1975.

66. T. Nakayama, M. Yoshida, and M. Kitamura, "L-Leucine-Sensitive, Heat-Stable Alkaline Phosphatase Isoenzyme Detected in a Patient with Pleuritis Carcinomatosa," Clin. Chim. Acta 30, 546 (1970).

67. W. H. Fishman et al., "A Serum Alkaline Phosphatase Isoenzyme of Human Neoplastic Cell Origin," Can. Res. 28, 150 (1968).

68. K. Higashino et al., "Hepatocellular Carcinoma and a Variant Alkaline Phosphatase," Ann. Internal Med. 83, 74 (1975).

69. Ning-Sun Yang, "Biochemical Properties and Development Expression of Genetically Determined Malate Dehydrogenase Isozymes in Maize," p. 191 in Isozymes, Vol. III. Developmental Biology, ed. by C. L. Markert, Academic, New York, 1975.

3. ADVANCED ANALYTICAL SYSTEMS

J. E. Mrochek, R. K. Genung, N. E. Lee,
L. H. Thacker, and S. R. Dinsmore

Several advanced analytical systems employing high-resolution chromatographic separations are being utilized to analyze specific molecular constituents of physiologic fluids. The chief value of these systems has been their ability to provide specific and sensitive analyses for individual molecular species in a complex matrix such as serum or urine. Fast analysis, while desirable, is secondary to specificity when attempting to correlate changes in the clinical status of certain patients with alterations in one or more potential biochemical markers of a clinical dysfunction.

3.1 High-Resolution Liquid Chromatographic Systems

We have continued our study of protein-bound carbohydrates in patients with breast cancer. Measurements have been extended to include the terminal carbohydrate n-acetylneuraminic acid (also known as sialic acid). Additional studies are reported in connection with the development of the analytical procedure for this acidic carbohydrate, together with analyses of sera from both normal female subjects and those with breast cancer. Analytical data are reported for protein-bound fucose, mannose, and galactose found in the sera of breast-cancer patients whose clinical status has been defined based on observations of changes in tumor mass.

3.1.1 Chromatographic analysis for protein-bound sialic acid

The methyl pentose fucose is one of the terminal sugars of glycoproteins. The second terminating molecule found in carbohydrate side

chains of glycoproteins is sialic acid. The former compound, with its terminal methyl group, is hydrophobic in nature; the latter, with its polar carboxyl and amine groups, is hydrophilic.

Evaluation of the efficacy of measurements for both fucose and sialic acid as potential biochemical markers of cancer is desirable. However, hydrolysis and chromatographic conditions for these two compounds differ substantially. Sialic acid is destroyed under hydrolysis conditions required to liberate fucose (1 N HCl for 4 hr), whereas fucose is not released under hydrolysis conditions which liberate sialic acid nondestructively (0.1 N H_2SO_4 at 80°C for 1 hr).[1,2] This behavioral difference makes it virtually impossible to analyze both compounds in the same sample.

Elution studies of reference n-acetylneuraminic acid revealed that it could be analyzed chromatographically using ammonium acetate--acetic acid buffer at pH 4.4 as eluent with detection by the cerate-oxidimetric detector system.[3] Linearity of both the peak area and the peak height was observed for amounts of sialic acid ranging from 6.5 to 39.1 μg eluted from the anion-exchange column.[4]

Evaluation of experimental variables. Five samples of n-acetylneuraminic acid were exposed to hydrolysis conditions of 0.1 N sulfuric acid at 80°C for 1 hr. They were then cooled to room temperature and adjusted to approximately pH 4 with 1 N sodium hydroxide. Analysis by liquid chromatography gave an average recovery of 97.2% for the sialic acid with a coefficient of variation (C.V.) of 2.2%, indicating that these hydrolysis conditions would probably not affect sialic acid recovery.

The glycoprotein mucin (from bovine submaxillary glands) was analyzed for protein-bound sialic acid. The protein, in amounts ranging from 1 to 4.9 mg, was hydrolyzed according to the above procedure; the hydrolysate

was centrifuged and then chromatographically analyzed. Proportional liberation and recovery of sialic acid were demonstrated (as shown in Fig. 3.1). A mean analysis of 71.9 μg of sialic acid per milligram of mucin, with a C.V. of 5.4%, was found by least-squares analyses of nine samples.

To test the analytical procedure on human serum, a pooled serum was analyzed four times in order to establish its protein-bound sialic acid content (with a relative standard deviation of 4.0%). A known amount of sialic acid was added to the precipitated protein from this pooled serum, the normal hydrolysis procedure was employed, and the hydrolysate analyzed for sialic acid. The results for six independent hydrolyses indicated an average recovery of 92.2% (with a standard deviation of 3.4%). The statistical variation is similar to that obtained for analysis of the pooled serum and apparently confirms this as a realistic estimate of the variation to be expected for this analytical procedure.

Analysis of protein-bound sialic acid in human sera. Serum samples from clinically normal female subjects and patients with breast cancer were analyzed for protein-bound sialic acid. In general, the latter were patients who, after initially exhibiting some improvement, later showed signs of progressive malignancy. Analyses ranged from 28.5 to 78.3 mg/dl (mean = 48.8 mg/dl) for six normal subjects and from 69.- to 110.6 mg/dl (mean = 86.6 mg/dl) for eight cancer patients.

3.1.2 Variation in protein-bound carbohydrates with changes in clinical status of breast cancer

We have continued analytical studies on protein-bound fucose, mannose, and galactose by using a chromatographic method that has been described

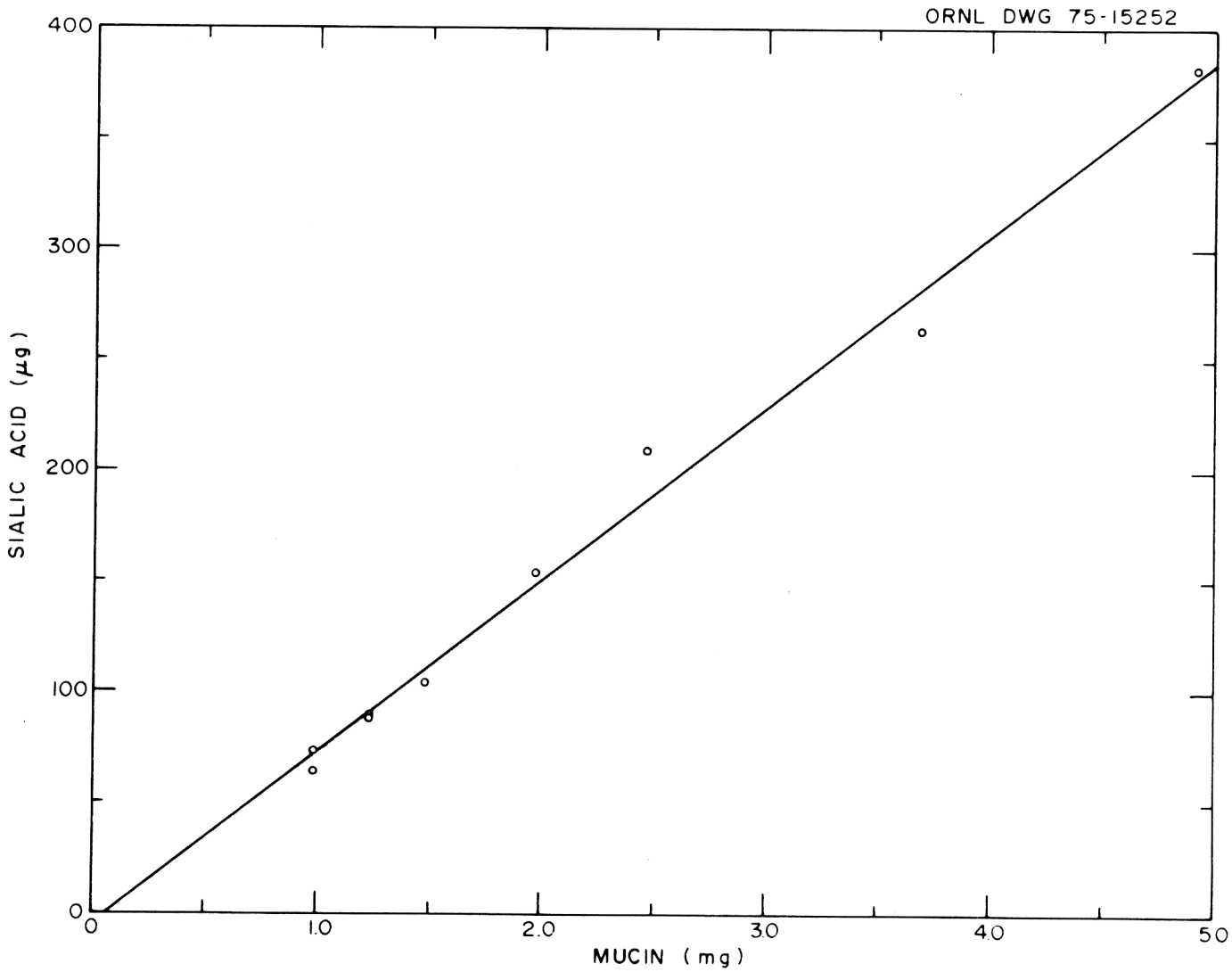

Fig. 3.1. Proportional recovery of protein-bound sialic acid from bovine submaxillary mucin after hydrolysis in 0.1 N acid at 80°C for 1 hr.

previously.[3,4] Emphasis has been on analyzing the serum from breast-cancer patients whose disease status places them in one of three different groups: (1) stable, (2) responsive, or (3) progressive. These categories are based on estimations of tumor size made by experienced clinicians. Measurements of sialic acid are in the process of being performed on these same samples; thus data shown in Figs. 3.2, 3.3, and 3.4 are not as extensive as that for fucose, mannose, and galactose. In general, results recorded in these three figures indicate that protein-bound fucose analyses seem to reliably mirror changes in patient status, whereas analyses for mannose and galactose do not seem to correlate as well. The data reported for sialic acid are too few to make a clear judgment at present. Trends in this analysis with changes in clinical status are apparent, but whether they will mirror patient status will require more extensive follow-up. Samples analyzed for sialic acid are the same as those previously used for the analyses for fucose, mannose, and galactose; thus they have been thawed and refrozen at least twice. The effect of this treatment on the samples represents an unknown factor at this time.

3.1.3 Development of a liquid chromatographic monitor for optically active substances

A new polarization monitor has been developed for detecting optically active materials in eluates from liquid chromatographs. A prototype has been fabricated and is being tested with very encouraging results.

The new instrument (Fig. 3.5) uses ultraviolet radiation (254 nm) to maximize the optical rotation caused by a given sample concentration. The 254-nm line from a low-pressure quartz-mercury lamp is isolated by an interference filter. Plane polarization of incident light is induced by a

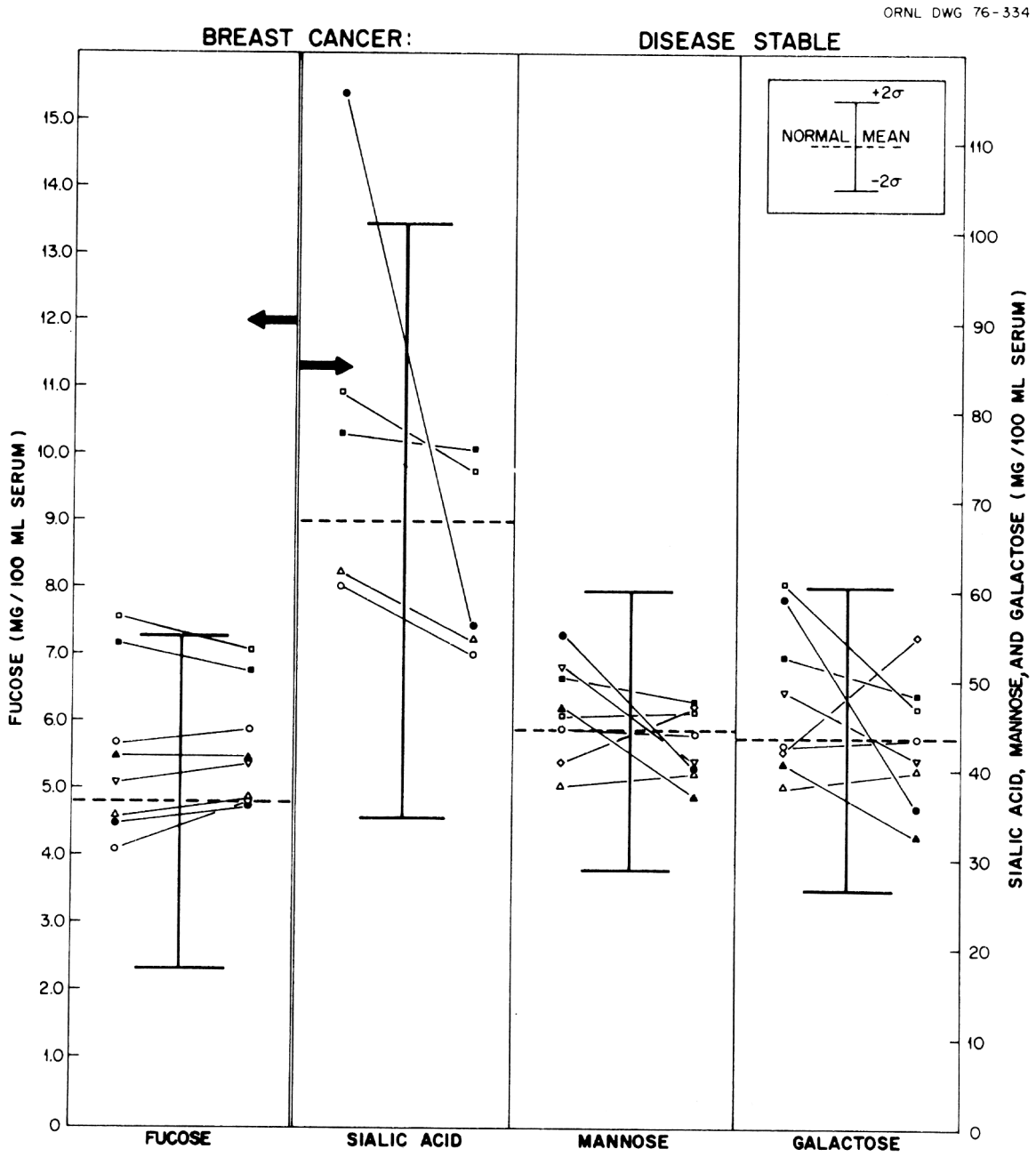

Fig. 3.2. Comparison of variations in four protein-bound carbohydrates for breast-cancer patients with clinically stable malignancies. Each individual patient has the same symbol for all analyses.

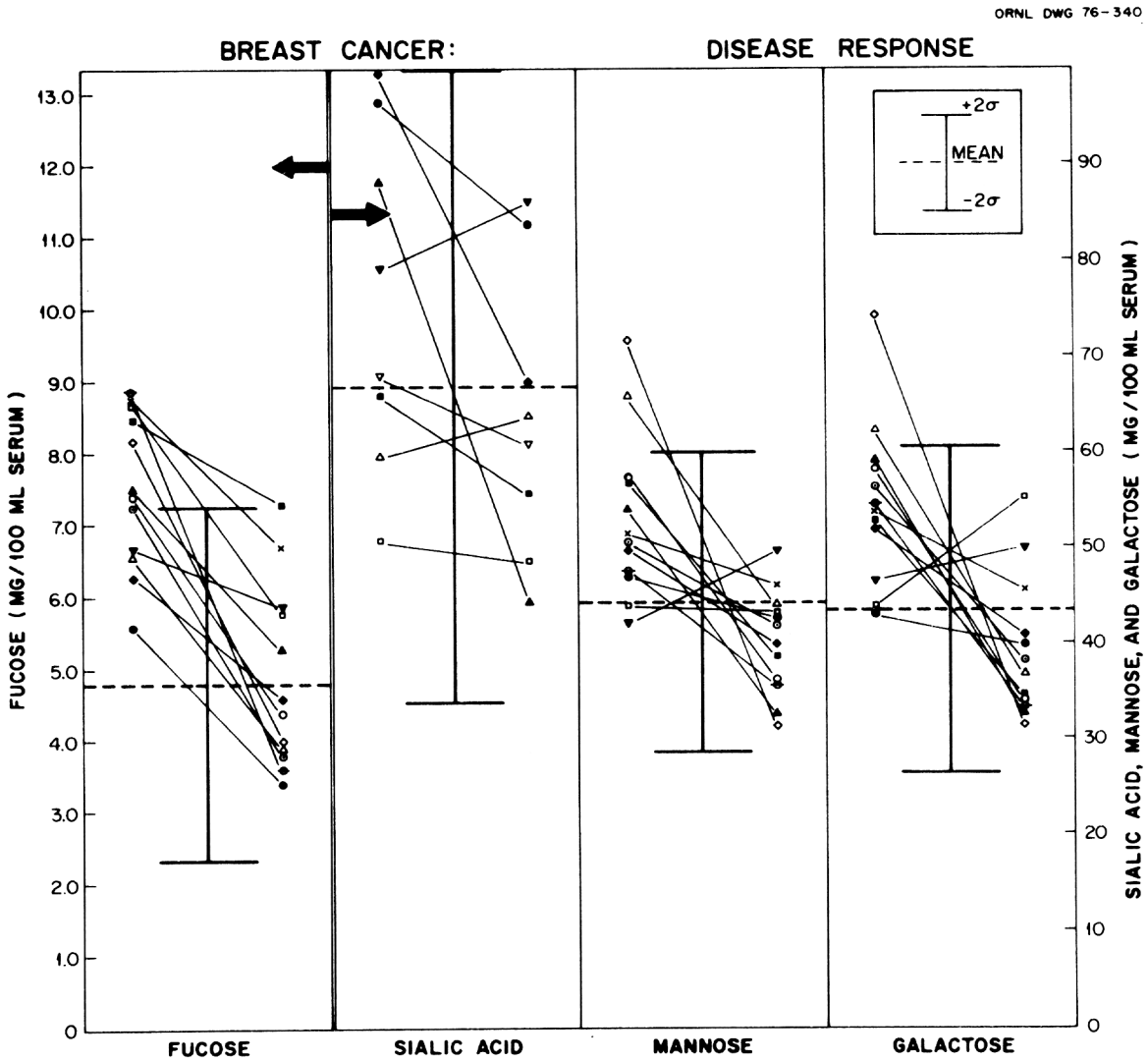

Fig. 3.3. Comparison of variations in four protein-bound carbohydrates for breast-cancer patients with clinically responsive malignancies. Each individual patient has the same symbol for all analyses.

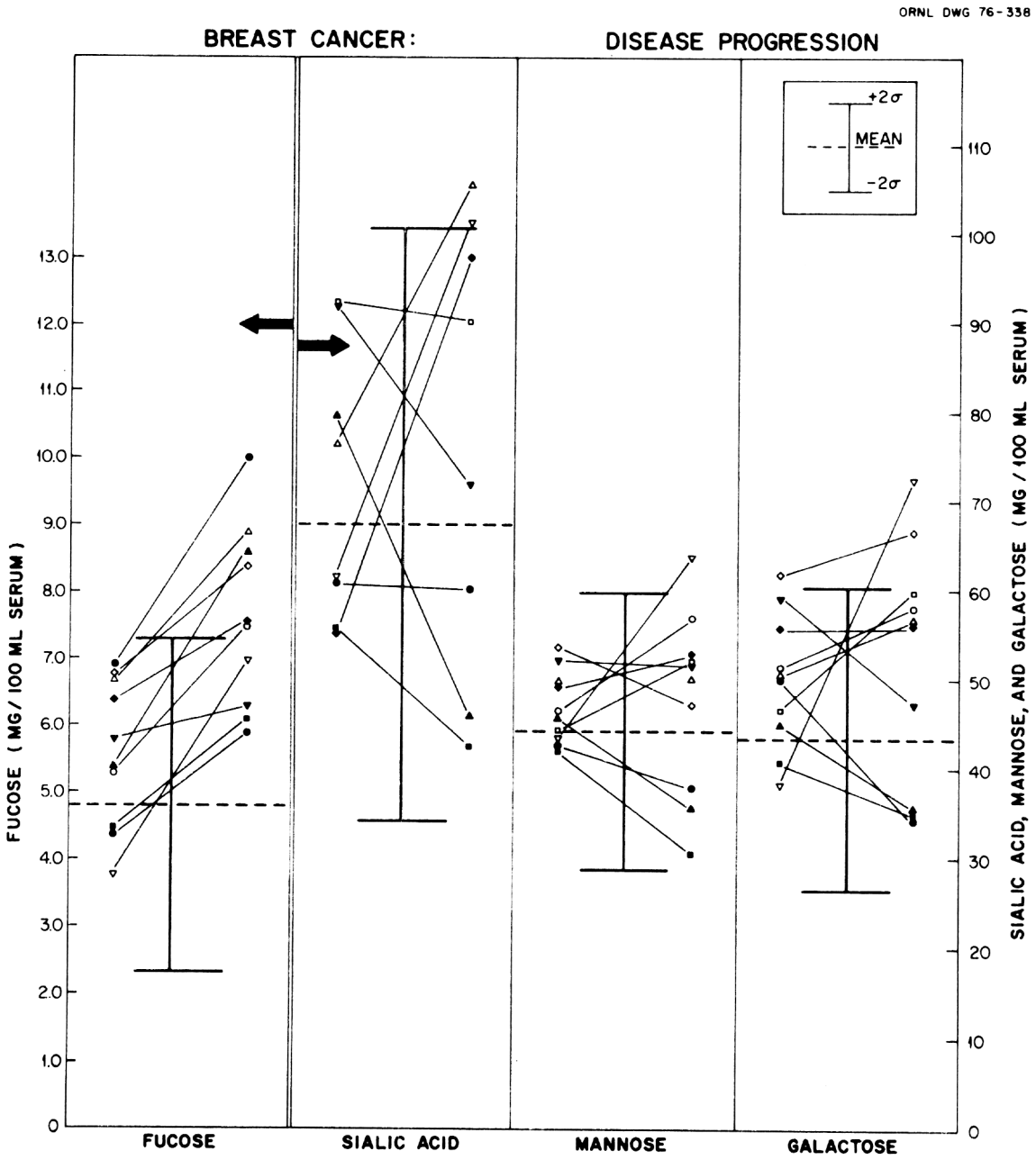

Fig. 3.4. Comparison of variations in four protein-bound carbohydrates for breast-cancer patients with clinically progressive malignancies. Each individual patient has the same symbol for all analyses.

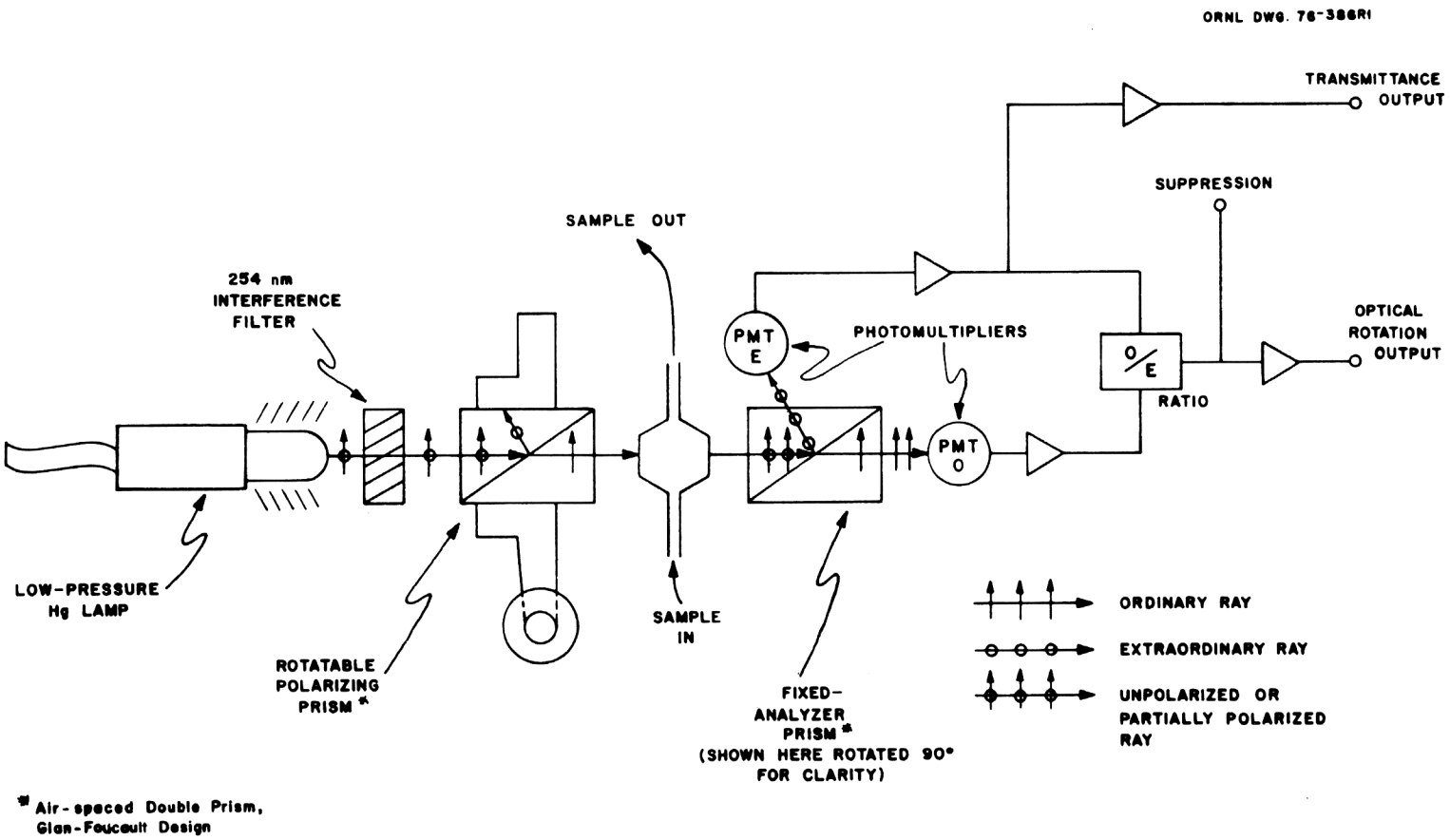

Fig. 3.5. Schematic diagram of a new flow detector monitoring changes in optical activity.

polarizing prism; a quartz flow cell with a 1-cm pathlength is mounted between the polarizing prism and a second, analyzer prism. Two photomultipliers (PMT) sense the plane-polarized ordinary (undeviated) ray and the extraordinary (deviated) ray passed by the sample material in the flow cell. The electronic circuit takes the ratio of the ordinary to the extraordinary component and effectively eliminates sensitivity of the optical rotation signal to changes in sample transmittance[5] and light source variations. Transmittance measurements may be made by direct observation of the extraordinary ray intensity; however, the transmittance signal is sensitive to optical rotation in at least some modes of operation.

Satisfactory performance has been observed in at least two modes of operation:

(1) With crossed polarizers rotated only a few degrees from the null position such that PMT-0 (Fig. 3.5) is seeing the change in a very small signal. In this case, it has not yet been found practical to use the ratio mode, and the only means of compensation is to use changes in light source intensity; however, good response is obtained for some sugars in concentrations below 0.003 M.

(2) With the prisms set at 45° to provide equal signals from the two PMT's, the ratio circuit provides a high degree of stability with independence from transmittance and light source variations.

It should be emphasized that the first prototype of this detector is relatively crude and intended only for "proof of principle" and rough sensitivity measurements. Based on the initial results, design modifications will be undertaken to improve detector sensitivity and stability.

3.2 Blood Sample Preparation System

Genetic mutation is commonly monitored by the determination of variant cellular isoenzymes using electrophoretic techniques coupled with the staining of specific proteins. Statistically meaningful results necessitate the analysis of large numbers of blood samples which, in turn, require a large commitment of technical manpower to prepare the necessary cellular hemolysates for analysis. A system automating this procedure is under development and will be designed to have the following capabilities: (1) to separate whole blood into plasma and erythrocyte fractions; (2) to wash the cells, collecting portions of the plasma and washed cells; and (3) to facilitate the preparation of a clean hemolysate for electrophoretic analysis.

3.2.1 Summary of experience with original prototype

Previous studies[4] indicated improved resolution of lactate dehydrogenase (LDH) and malate dehydrogenase (MDH) when hemolysates obtained from the blood sample preparation system were subjected to starch gel electrophoresis after additional centrifugation (20 min) had been performed at 18,000 rpm. These studies also indicated that improved lysing of red blood cells resulted when a 1% solution containing Saponin* was incorporated in the lysing procedure. This method is a three-step process consisting of (1) introduction of 16 cc of 1.0% (by weight) Saponin-water solution into the rotor containing the cells, followed by accelerating, agitating, and braking several times to facilitate mixing; (2) addition of 6 cc of 0.05 M HCl in 0.005 M KH_2PO_4 as the dark hemolysate band appears and repeating the mixing procedure; and (3) addition of 4 cc of carbon tetrachloride and again

---

*A commercial hemolysing agent.

repeating the mixing procedure, accelerating to 2600 rpm, and, finally, centrifuging for 15 to 20 min to sediment the stroma.

Recent studies were conducted with the prototype blood preparation system which utilized the lysing procedure described above, along with an improved mixing technique attained by using full air injection capability, and centrifuging at 2600 rpm. No significant differences were observed between those samples taken directly from the system and those that had undergone the additional high-speed centrifugation. Electrophoretic separation of LDH and MDH on acrylamide gel demonstrated this lack of difference (see Fig. 3.6). When starch gel electrophoresis[6] was performed to separate isoenzymes of LDH, isocitrate dehydrogenase (ICD), and phosphohexose isomerase (PHI),[7] only slight differences were observed (and, then, only for LDH, as shown in Fig. 3.7). A comparison of the accrylamide gel and starch gel electrophoretic separations of LDH (compare Figs. 3.6 and 3.7) shows slight smearing of the patterns on the starch gel; however, no smearing of the band was apparent for other isoenzyme separations in this system (see b and c of Fig. 3.7).

3.2.2 Design and fabrication of new prototype

As a result of the crazing and cracking problem reported earlier,[4] and since this and previous studies had indicated the feasibility of the rotor design, further studies were conducted to accomplish two goals: (1) to find a material of construction which could withstand exposure to either toluene, carbon tetrachloride, or whole blood, and (2) to determine a rotor design with a maximum number of sample cavities within the available constraints of the previously designed centrifugal system.

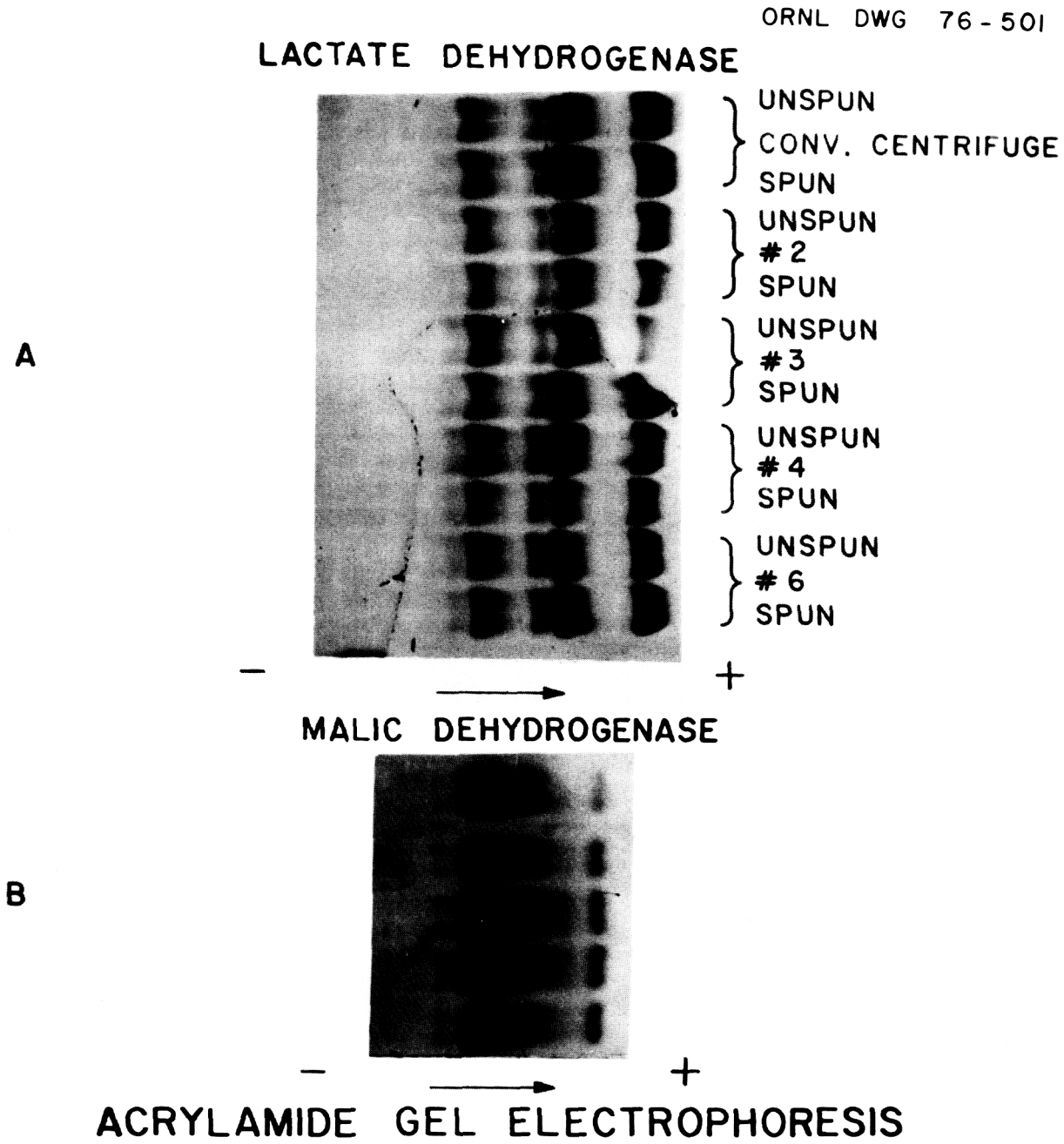

Fig. 3.6. Electrophoretic separation of isoenzymes from hemolysate samples prepared on the automated blood sample preparation system. Separations are on acrylamide gel and, for LDH, compare samples which have been subjected to an additional high-speed centrifugation (spun) with those taken directly from the automated system (unspun).

ORNL DWG 76-502

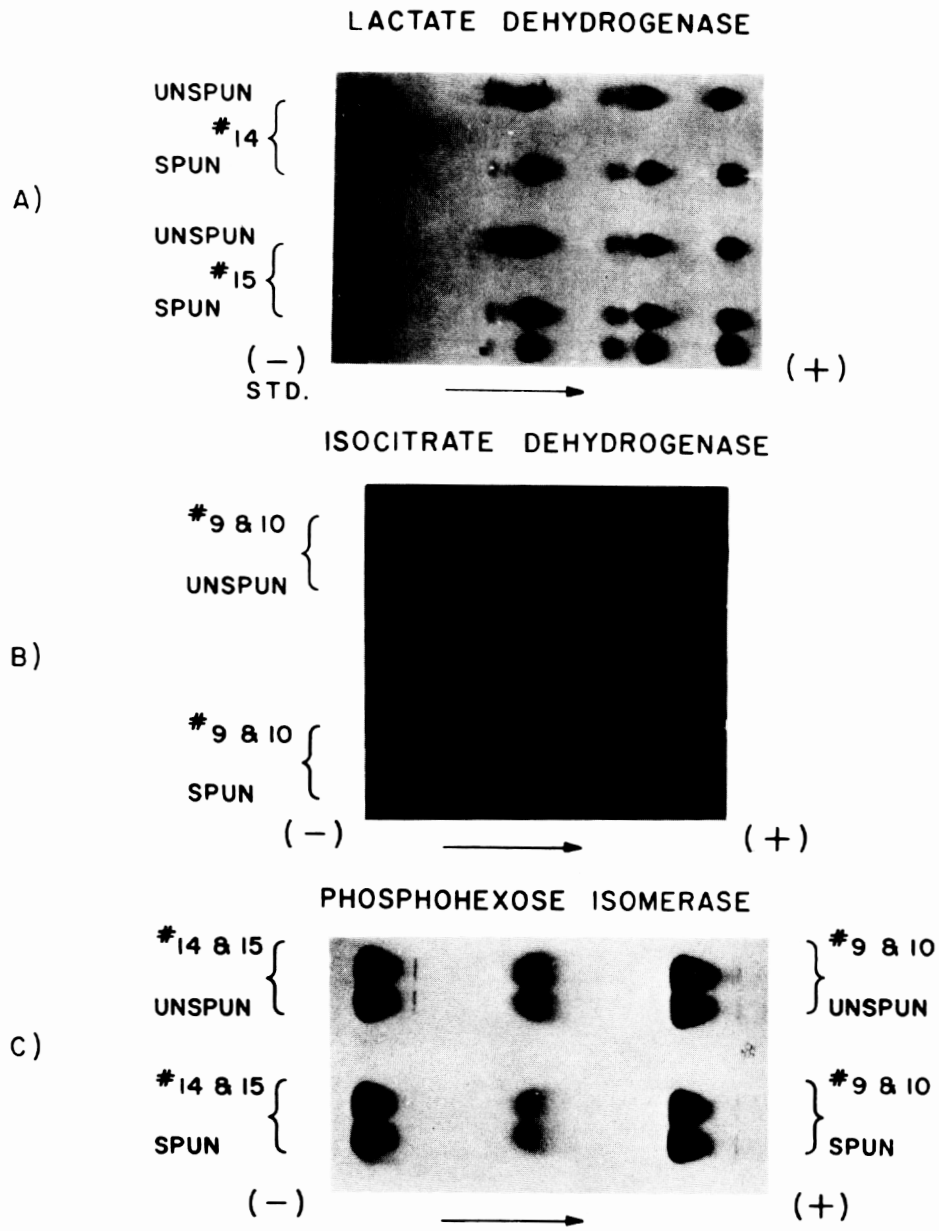

STARCH GEL ELECTROPHORESIS

Fig. 3.7. Electrophoretic separation, on starch gel, of hemolysate samples prepared on the automated blood sample preparation system. No difference in resolution between samples taken directly from the automated system (unspun) and those subjected to an additional high-speed centrifugation (spun) with the exception of LDH where a slight smearing was observed for unspun samples.

Tests were conducted in which different material formulations were exposed to contact with toluene, carbon tetrachloride, and whole blood for periods of up to 10 weeks in an effort to find a material for rotor fabrication that would withstand attack by the organic solvents used to aid sedimentation of cell debris from hemolysates.

It was determined from these studies that an epoxy formulation could be cast in the necessary dimensions, and the casting could be machined to yield the desired rotor. Shell's epoxy resin (Epon 828), catalyzed by triethylene tetramine, was cast into a cylindrical block that measured 7 in. in diameter by 1-1/4 in. in thickness for the rotor body; two 7-in.-diam by 3/16-in.-thick discs were cast for the top and bottom covers. In order to maximize the number of processing chambers that could be accommodated, a short computer program was written to perform the analytical geometric calculations necessary to determine the maximum number of chambers that could be machined into a rotor. A rotor containing 30 chambers, each with a 5-ml total volume capacity resulted (Fig. 3.8). A matching 30-chamber plasma collection ring was machined from Lucite (Fig. 3.9), since contact by organics is not experienced in this stage of sample preparation. The following two processed red-blood-cell collection rings were also fabricated: (1) a ring which could accommodate 30 cryo-vials, and (2) a ring which could accommodate 60 cryo-vials (Fig. 3.10). This system, incorporating both rotor and collection rings, has been fabricated and will be tested as soon as minor imperfections in the epoxy casting can be corrected.

A preliminary design for a rotor washer has been completed which provides for the introduction of a wash solution into the rotor together

PHOTO 0730-76

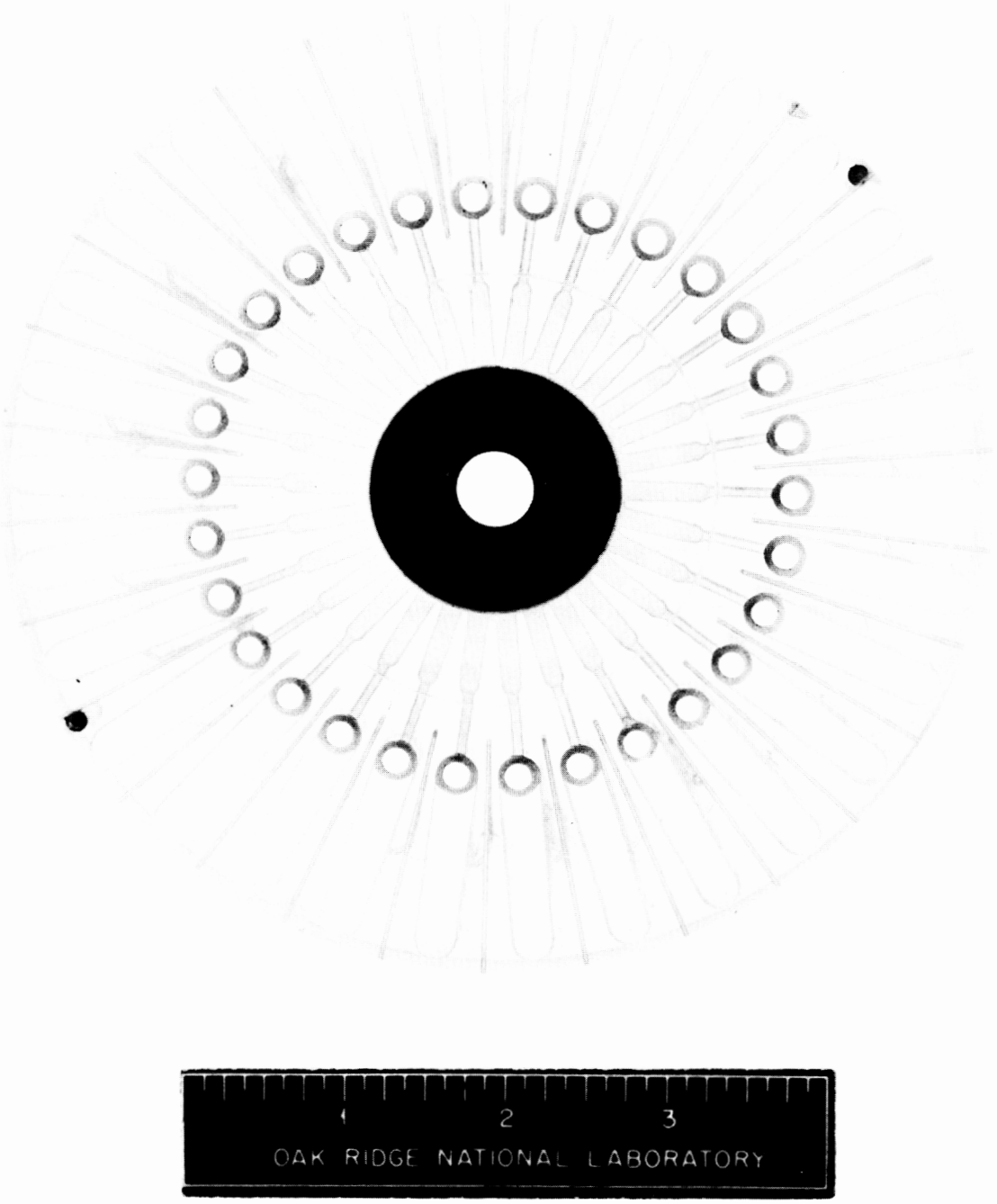

Fig. 3.8. Thirty-chamber rotor for the blood preparation system fabricated from epoxy resin.

PHOTO 0729-76

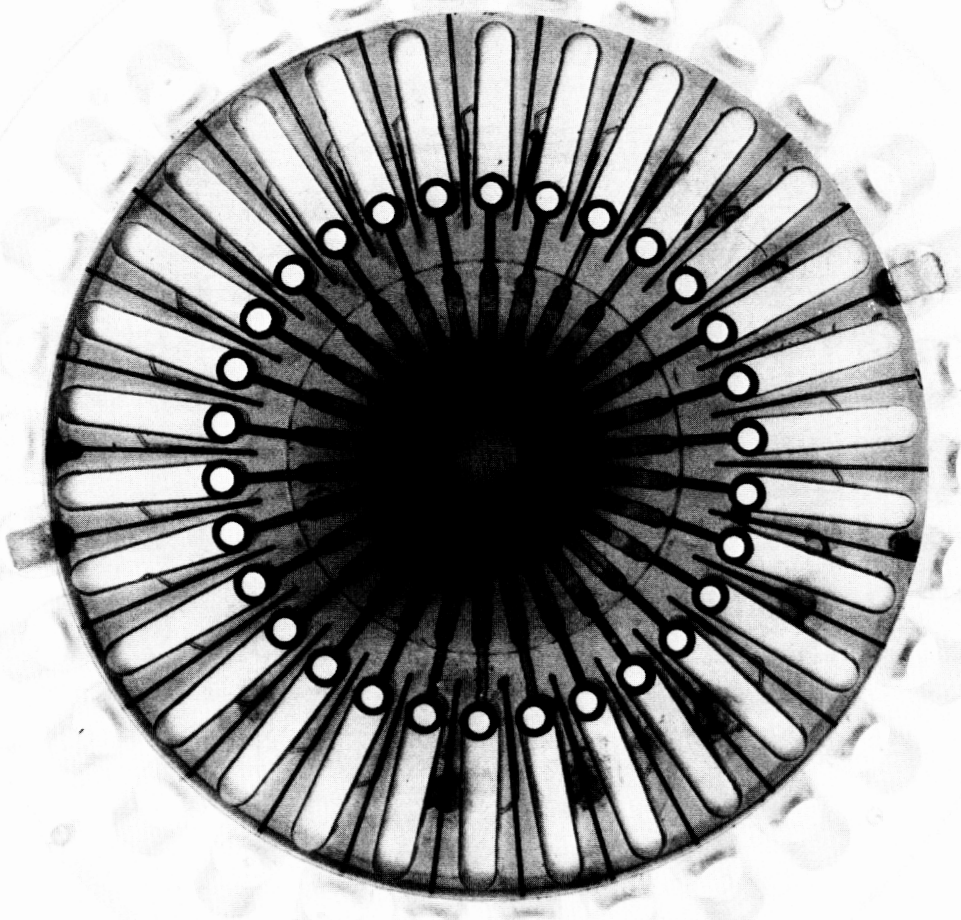

Fig. 3.9. Thirty-chamber rotor for the blood preparation system with sample collection ring attached.

PHOTO 0731-76

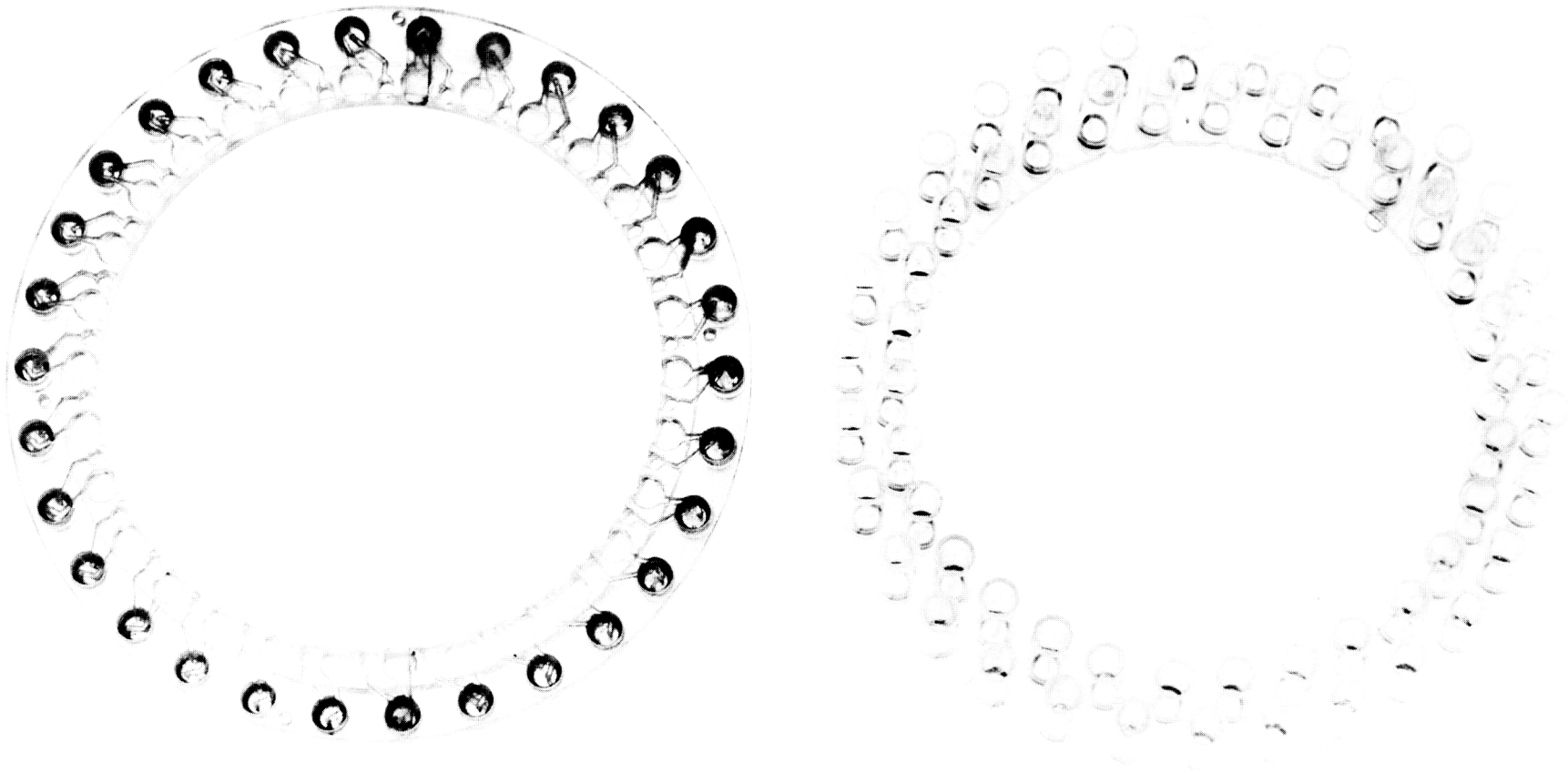

Fig. 3.10. Collection rings employing removable cryovials for low-temperature storage of washed cells and hemolysate fractions.

with rapid acceleration and braking of the rotor in order to dislodge sedimented cell debris from the processing chamber walls.

3.3 Automated Elution Electrophoresis

Development efforts for the automated elution electrophoresis system described earlier[8] have been readily divided into two phases, each of which is concerned with identification of dominant mechanistic parameters. The first phase involves the electrophoretic separation; the second phase is concerned with the maintenance of resolution during the elution process.

3.3.1 Electrophoretic mobility studies

In the first phase, investigation of the electrophoretic mobility of bovine serum albumin (BSA) in a bed of particulate packing (varying composition and size) has been performed by members of the MIT Practice School. An extensive analysis of their data for different buffer systems is in progress and will be presented in ORNL-MIT Report 230. Figures 3.11 and 3.12 include data from earlier work which demonstrate the difficulty in obtaining reproducible rate measurements. The ordinate (v_t) in these figures is defined as the volume of eluent required to move the sample zone peak from its column position to the uv-monitor. The range indicated in each case is attributable to a varying flow rate during the elution process. After each hydrostatic electrophoresis step, the eluent flow was initiated and flow measurements begun. Initial flow rates were routinely below precalibrated values, thus suggesting a compression of the packing during electrophoresis. A summary (based on a packed bed void fraction of 0.4) of the data in Figs. 3.11 and 3.12 is given in Table 3.1; volumes based on initial flow rates were used in each case. Thus the effective

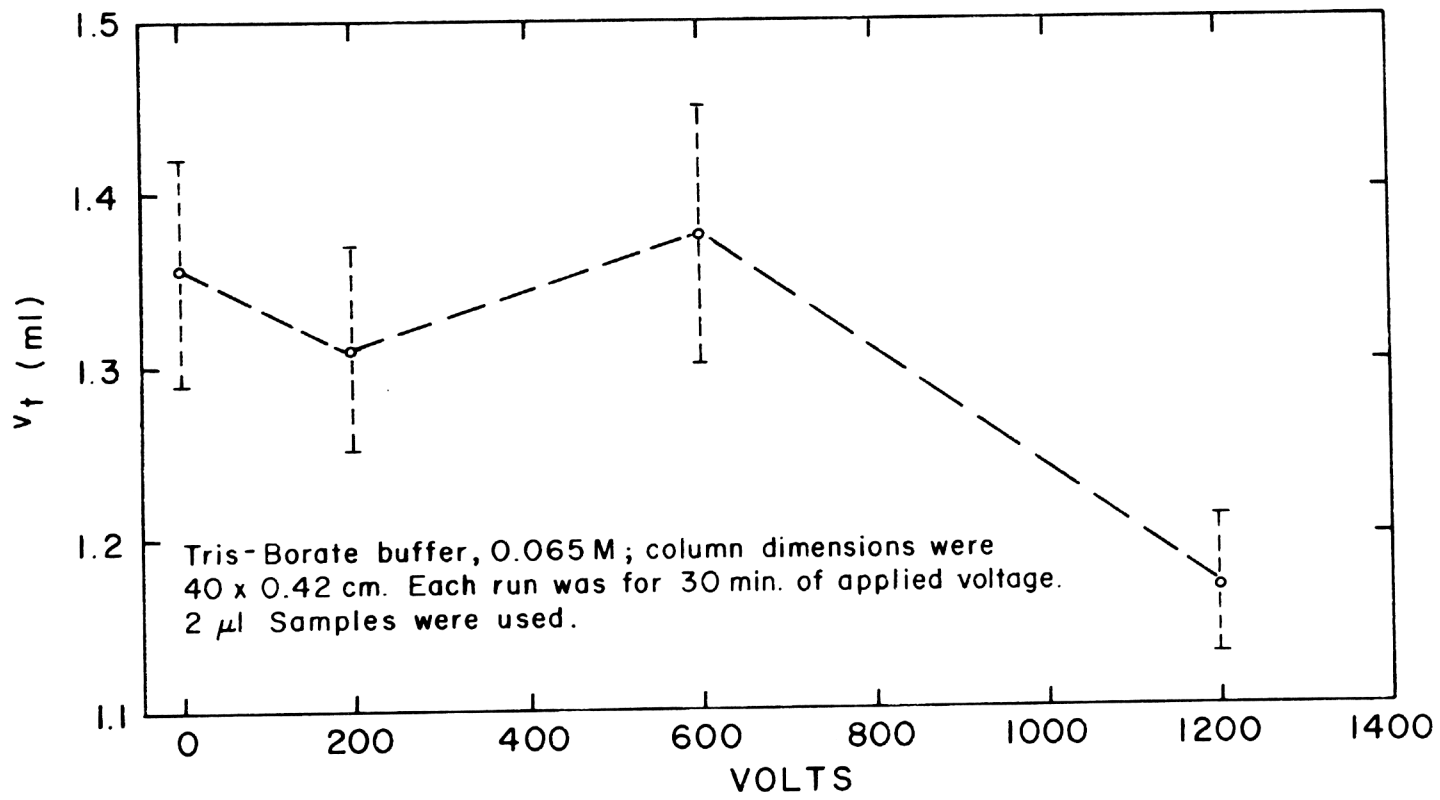

Fig. 3.11. Effect of applied DC voltage on the elution volume of bovine serum albumin (BSA) on P-2 Bio-Gel (200-400 mesh). Mobility only observed above 600 V.

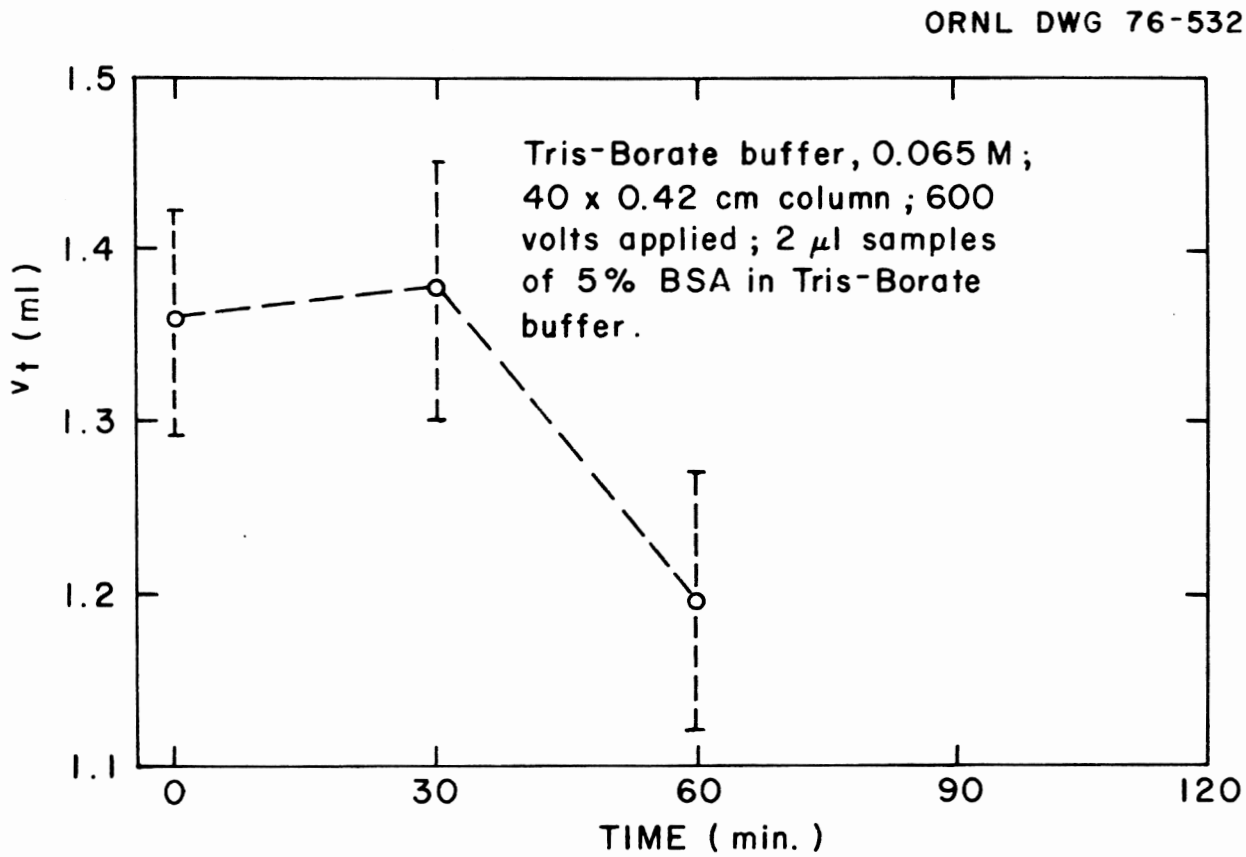

Fig. 3.12. Effect of electrophoresis time on the elution volume of bovine serum albumin (BSA) on P-2 Bio-Gel (200-400 mesh). Mobility only observed for electrophoresis times in excess of 30 min.

Table 3.1. Electrophoretic migration rates[a] for BSA in P2 Bio-Gel, 200-400 mesh

Gradient (volts/cm)	Migration rate (cm/sec) x 10^5
5	40
15	-10
30	160

[a]Tris-borate buffer, 0.065 M; data taken from Fig. 3.12.

linear distance traveled by the BSA during the time of electrophoresis was calculated by using the equation

$$L = 4(v_t^o - v_t)/(\alpha\pi D^2) ,$$

where

v_t^o = the eluent volume required without electrophoresis,

v_t = the eluent volume for a particular run,

α = void fraction,

D = column diameter.

The voltage gradient used in Table 3.1 cannot be assumed to represent the effective gradient experienced by the migrating molecules since the electrical resistance contributed by the materials chosen to hold the packing in place within the separations column has been shown to contribute significantly to the overall resistance. An example (included in Table 3.2) demonstrates that the voltage drop in the packing can be considerably less than the voltage drop between electrodes. Additionally, as shown in Fig. 3.13, a simple Ohm's law relationship does not describe

ORNL DWG 76-533

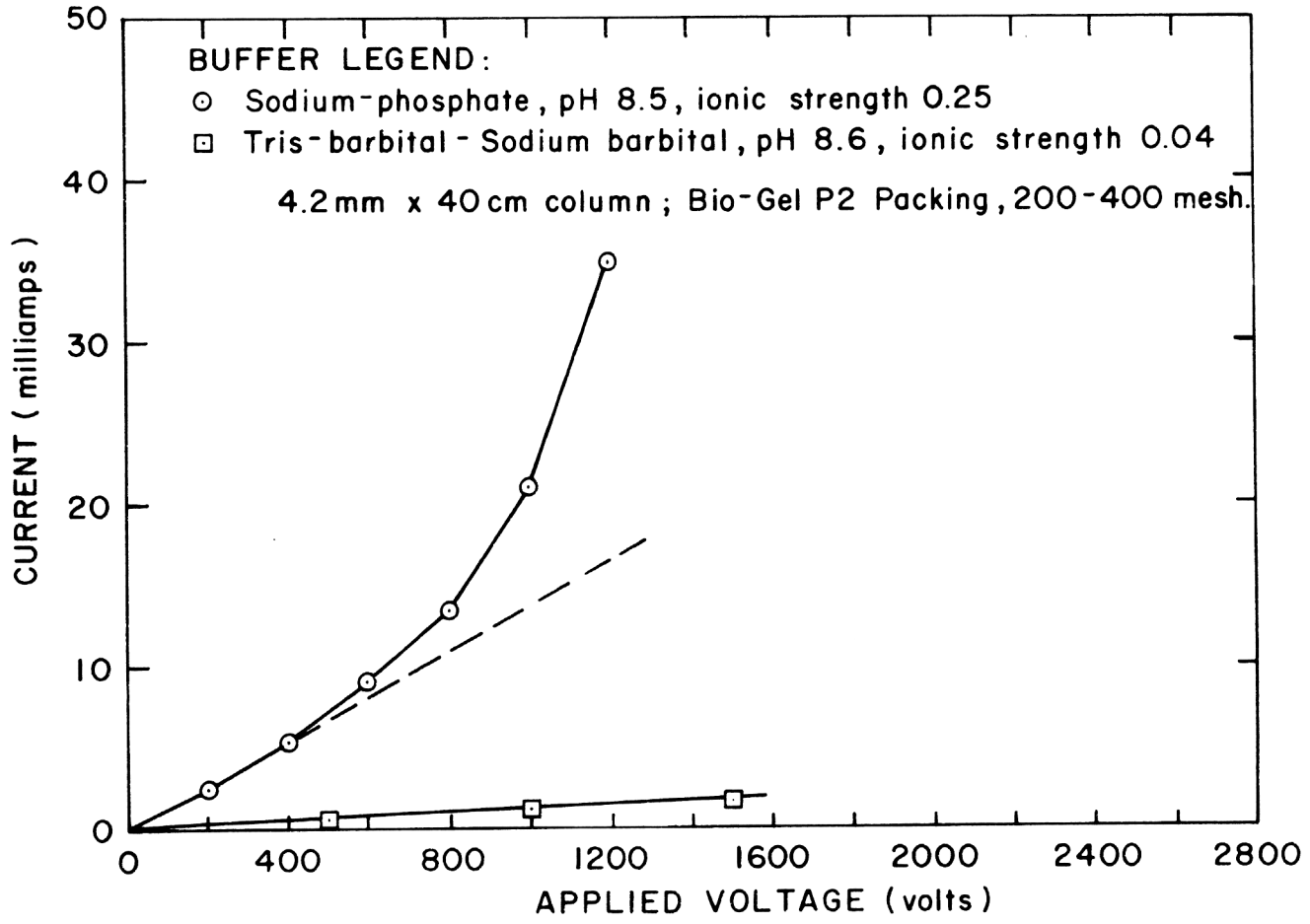

Fig. 3.13. Current-voltage relationship for low- and high-ionic-strength buffers. Nonohmic behavior for high-buffer concentration is probably due to increasing solution conductivity caused by a lack of cooling capacity.

Table 3.2. Overall static resistance measurements[a] for different elution electrophoresis column configurations

	Resistance
Buffer[a] only	69 KΩ
Buffer; glass wool supports (2)	70 KΩ
Buffer; glass frits supports (2)	110 KΩ
Buffer; glass frits supports (2); packing[a]	115 KΩ

[a]Refer to ORNL-MIT Report 230; 0.065 M Tris-borate buffer and Bio-Gel P2, 200-400 mesh, packing; 10 cm between electrodes and 7 cm between packing supports; 20°C.

the electrical behavior of the system with a relatively high-ionic-strength buffer present. The exponential increase in current with increasing voltage probably introduces convective- or electroosmotic-like motion, thus complicating analysis of the electrophoretic motion of the proteins. As seen in Fig. 3.13, a system using a low-ionic-strength buffer exhibited behavior consistent with Ohm's law. Since heat production generally accompanies high currents, the cooling capacity of the system, based on the difference between inlet and outlet cooling water temperatures, was monitored during these runs. This temperature difference (less than 1°C) remained constant during the runs. However, the inlet cooling water temperature (determined by the precooling apparatus) increased during the run. Figure 3.14 shows the relationship between this inlet temperature (a measure of the packing temperature) and current. Additional work may require an improvement in the column cooling system since the voltage-current characteristics of the system depend strongly on temperature control of the packed bed. In general, definitive work for the entire first phase is still in progress.

ORNL DWG 76-534

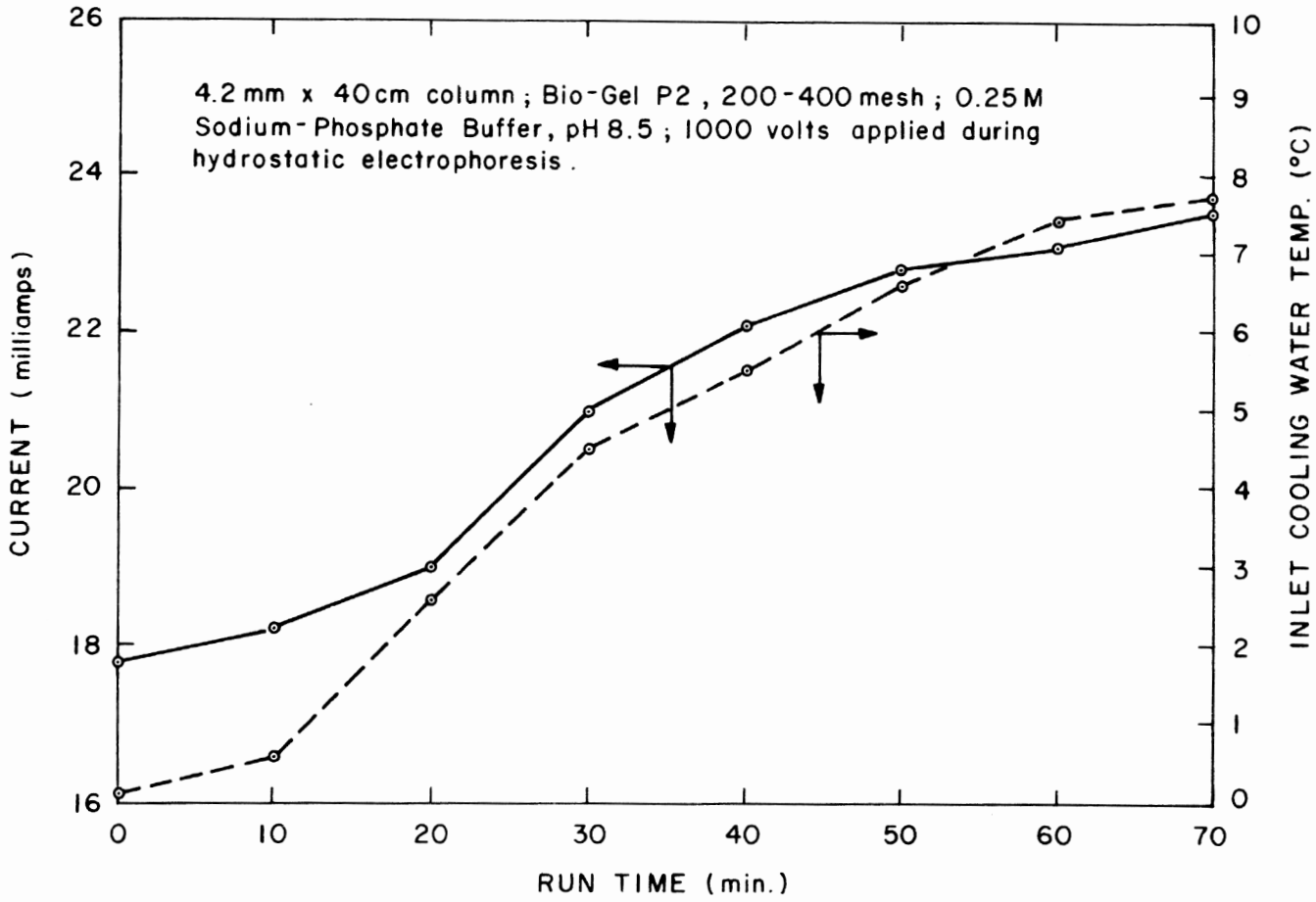

Fig. 3.14. Increase in current is proportional to the inlet cooling water temperature during an elution electrophoresis run.

3.3.2 Zone elution studies

In the second phase of this work, attention has been given to the elution of separated components with minimal loss of resolution. Ideally, the movement of separated zones during elution from the column will be modeled by plug flow; in the nonideal case, mixing effects lead to dispersion of the sample zones as discussed by Levenspiel.[9] Efforts have been made to relate this dispersion to the choice of packing, buffer ionic strength, and elution flow rates. Changes in dispersion related to the biophysical state of the components were initially assumed small when compared to changes in dispersion due to choices of elution flows and packing materials. Again, a detailed analysis of dispersion during elution is presently under way and will be published in ORNL-MIT Report 230. Some preliminary data demonstrating the strong dependency of dispersion during the elution process on packing material are shown in Fig. 3.15. Initial observations also indicate that the design and position of the eluate exit point must be altered to maintain resolution. Visualization of flow patterns in the packed bed with bromphenol blue dye showed back-mixing patterns in the column exit region as illustrated in Fig. 3.16. Theoretical analysis of the elution curves (ORNL-MIT Report 230) support the combination of the plug flow and backmixing models. These design changes are presently under consideration.

Attempts to apply the information acquired in the mechanistic studies to serum protein separations have not resulted in resolution competitive with the cellulose acetate separations routinely used in clinical situations. However, as described in this report, many improvements in the system are required before a successful application can be expected. In

ORNL DWG 76-535

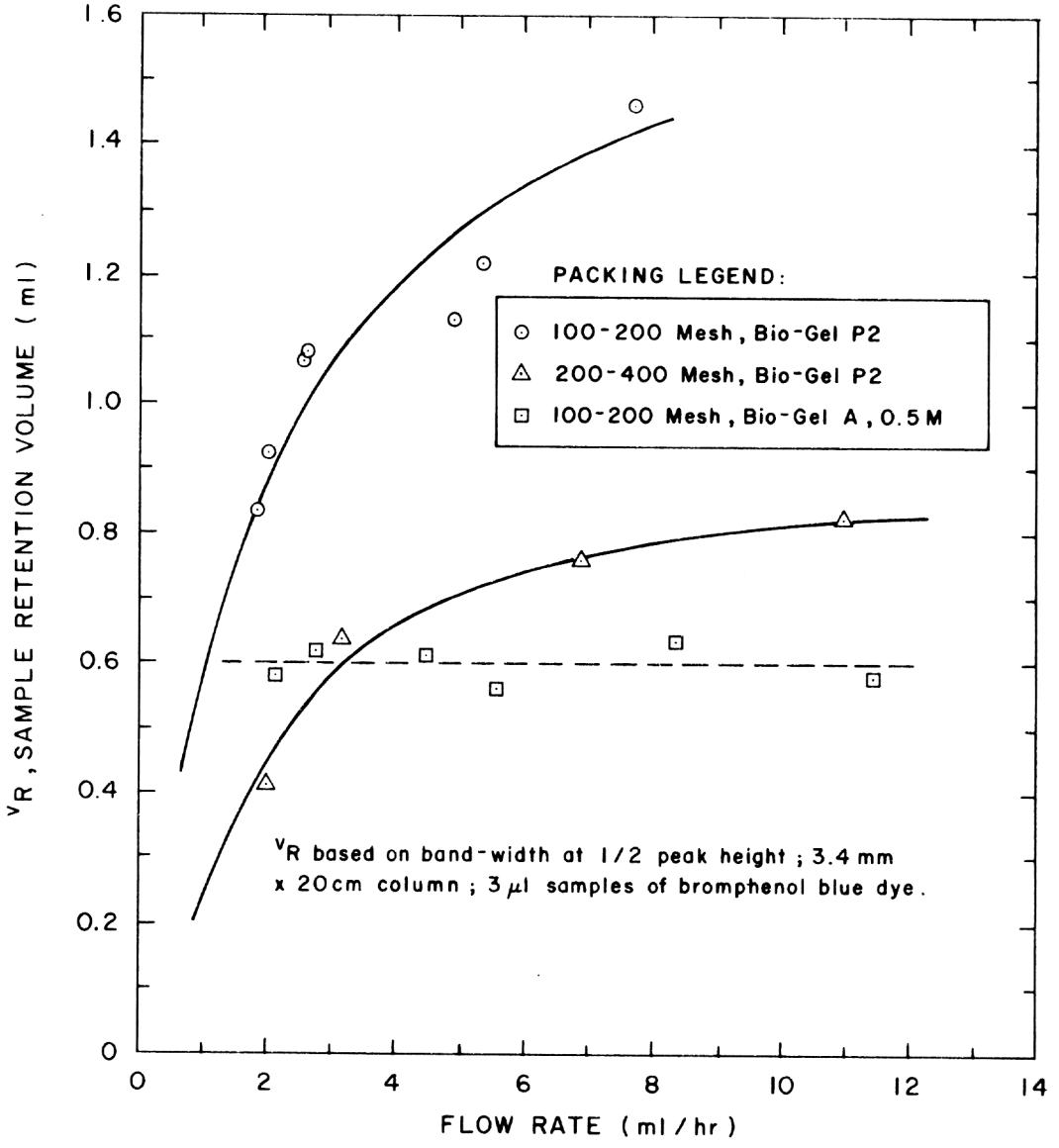

Fig. 3.15. Effect of particle size and column packing on chromatographic peak dispersion.

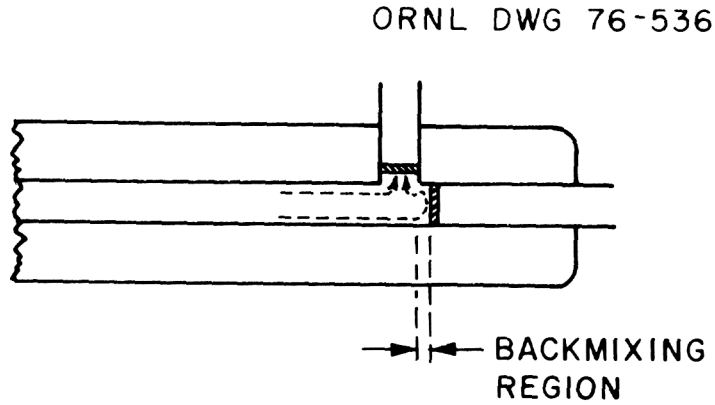

Fig. 3.16. Significant band spreading results from backmixing in a stagnant flow area at the column outlet to the detector.

addition to studies with serum proteins, some development work for hemolysate separations has been performed along the guidelines presented above. At present, creatinine phosphokinase (CPK) isoenzyme separations using elution electrophoresis are under study; preliminary work supports the feasibility study published earlier.[8] In all cases, useable systems and applications depend on further studies.

3.3.3 Alternate concepts for automated electrophoresis systems

The work on this automated elution electrophoresis system has resulted in certain other concepts which may be pursued as automated, high-resolution electrophoresis systems. These include:

(1) Optically monitoring a plane in the separations column which is perpendicular to the axial movement of the components without interrupting their motion. This may be achieved directly in a precast polyacrylamide gel or in a bed of particulate packing (if the monitored plane is maintained by membranes).

(2) Introducing a micro-scale collection chamber penpendicular to the direction of migration in a precast gel. The chamber would be faced on either side by membranes chosen to selectively entrap components of interest and would be continuously swept by a liquid flow removing components to a monitoring system.

(3) Optically scanning a precast gel along its axial direction by synchronized, translating optics. The time between axial scans could be adjusted, and the data from each run would define not only the final separation and resolution but also the rate of each resolved component during the run.

These concepts have been qualitatively demonstrated. The first case should produce high resolution without zone recovery. The possibility of a migrating zone crossing a thin liquid discontinuity without the loss of resolution was successfully demonstrated by the use of albumin stained with bromphenol blue dye. The second case allows zone recovery with high resolution on an analytical scale. System parameters must be adjusted so that the effective residence time of the collection chamber is less than the time corresponding to the distance between separated zones. The third case adds the advantage of rate data to the high resolution of the first case and could be employed as a research tool in addition to its diagnostic capability. The method used to demonstrate these concepts is indicated schematically in Fig. 3.17. Figure 3.18 shows possible modifications of this system. Qualitative results are presented in Figs. 3.19 and 3.20.

3.3.4 Summary

Both imparting electrophoretic mobility to protein components in particulate packing and the eluting of separated zones from such a packing are technically feasible; they have been documented to some extent on the system described in Sect. 3.3.1 and are commonly reported in the literature for preparative systems. The combination of these ideas for analytical separations and quantitation has proved technically difficult to date. Alternative processes for automated electrophoresis have been proposed for possible future study. These efforts can be performed in parallel with continued development of the original elution electrophoresis concept.

ORNL DWG 76-537

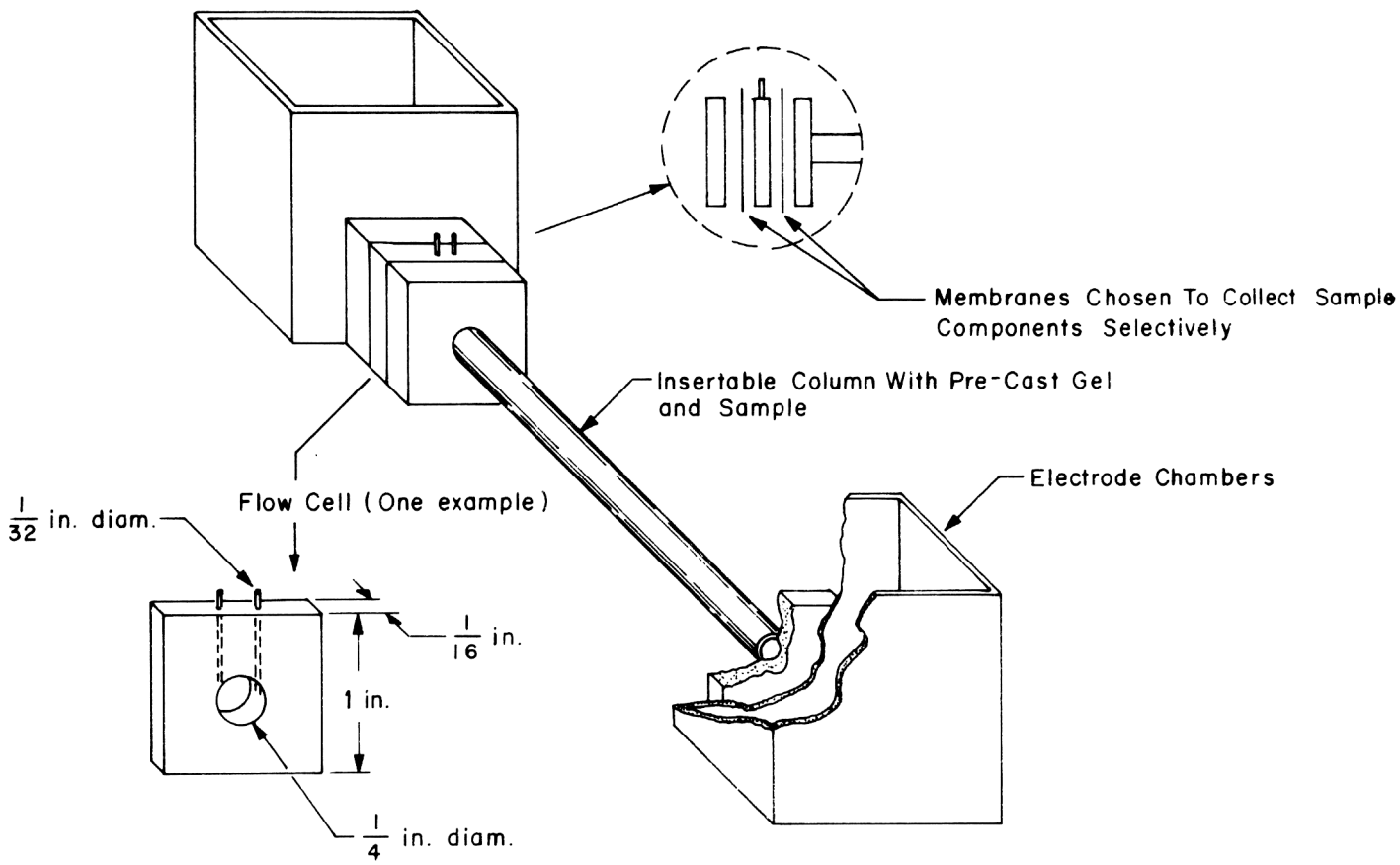

Fig. 3.17. Schematic design for an experimental system used to demonstrate concepts for zone-recovery electrophoresis.

ORNL DWG 76-540

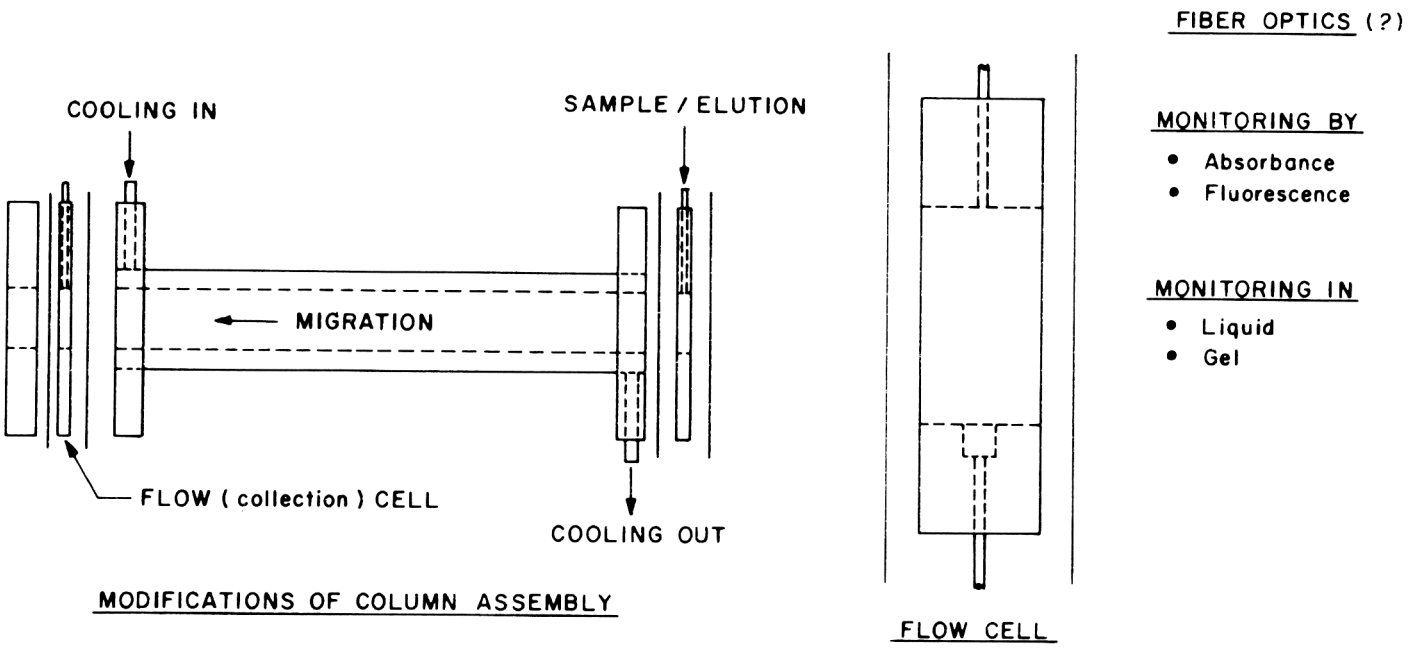

Fig. 3.18. Conceptual modifications to improve resolution of the zone-recovery electrophoresis system.

ORNL DWG 76-538

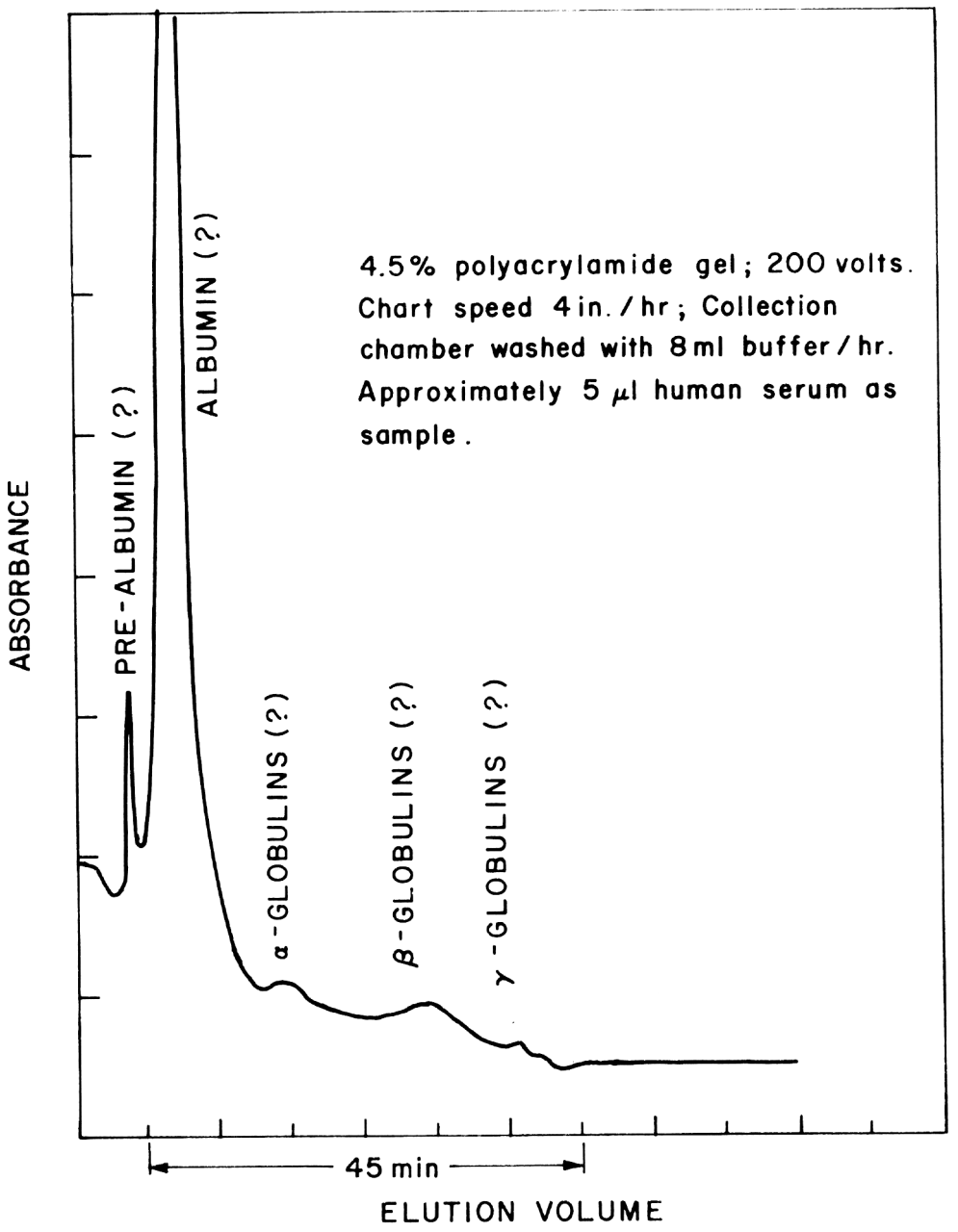

Fig. 3.19. Qualitative separation of serum proteins on zone-recovery electrophoresis system (based on electrophoretic rate).

ORNL DWG 76-539R1

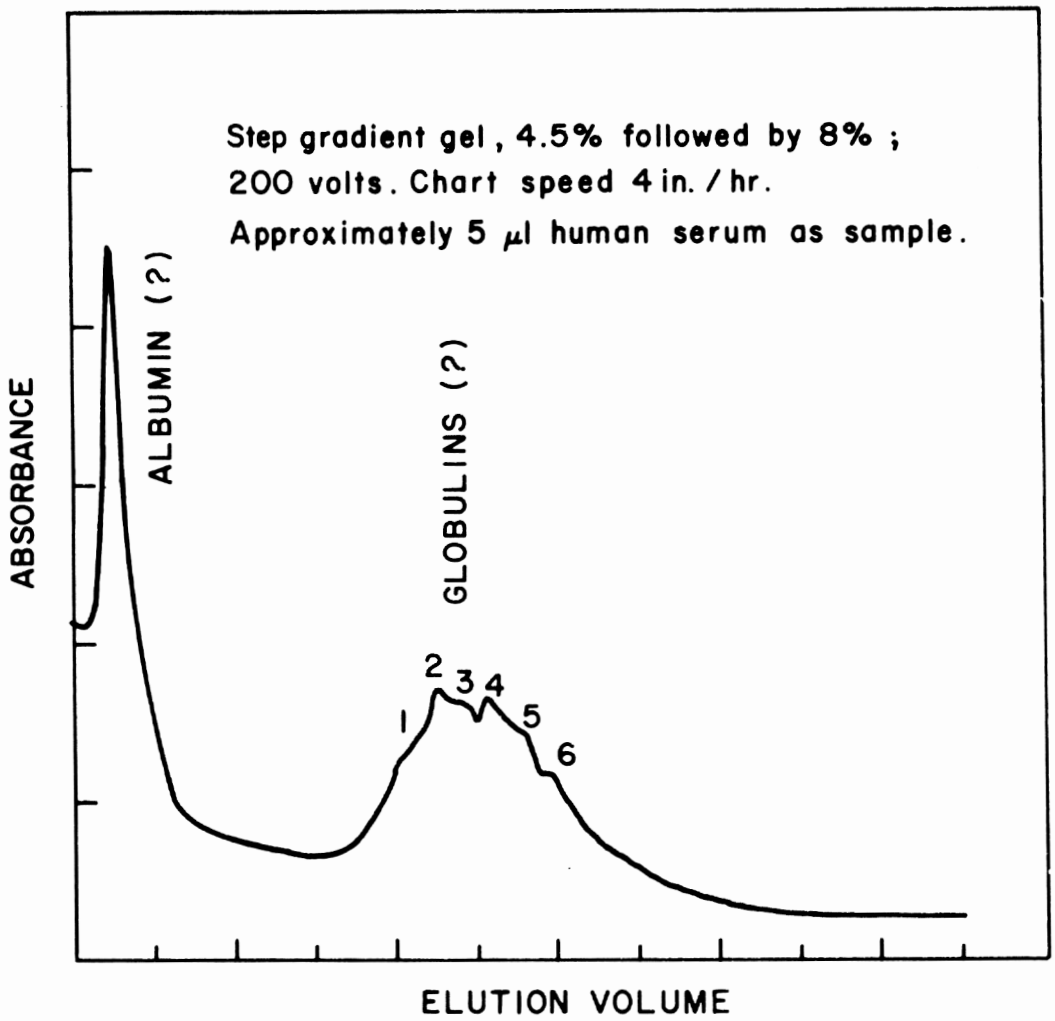

Fig. 3.20. Qualitative separation of serum proteins on zone-recovery electrophoresis system illustrating both electrophoretic rate and molecular-sieving effects.

3.4 References for Section 3

1. L. Svennerholm, "Quantitative Estimation of Sialic Acid. III. An Anion Exchange Method," Acta Chem. Scand. 12, 547 (1958).

2. L. Warren, "Sialic Acid in Human Semen and in the Male Genital Tract," J. Clin. Invest. 38, 775 (1959).

3. J. E. Mrochek, S. R. Dinsmore, and T. P. Waalkes, "Liquid-Chromatographic Analysis for Neutral Carbohydrates in Serum Glycoproteins," Clin. Chem. 21, 1314 (1975).

4. C. A. Burtis, J. E. Mrochek, and C. D. Scott, Biochem. Technol. Prog. Progr. Rep. for the Period July 1-Dec. 31, 1975, ORNL/TM-5167 (January 1976).

5. M. Tsuda, "Apparatus for Rapid Measurement of Optical Rotation Changes," Rev. Sci. Instrum. 46, 1419 (1975).

6. M. Morrow, H. Dovey, and R. Tanis, "Methods for Screening Red Cell and Serum Proteins," Department of Human Genetics, University of Michigan, Ann Arbor, personal communication, December 1973.

7. R. Tanis et al., "Starch Gel Electrophoresis," University of Michigan, Ann Arbor, personal communication, June 1975.

8. C. D. Scott et al., Experimental Engineering Sect. Semiannu. Progr. Rep. (Excluding Reactor Programs), Sept. 1, 1974 to Feb. 28, 1975, ORNL/TM-4961 (1975).

9. O. Levenspiel, Chemical Reaction Engineering, pp. 242-274, Wiley, New York, 1962.

4. PUBLICATIONS AND ORAL PRESENTATIONS

4.1 Publications

Bostick, W. D., Burtis, C. A., and Scott, C. D., "Simultaneous Determination of Silica and Phosphate in Water from a Single Experiment Using a Miniature Centrifugal Fast Analyzer," Anal. Lett. 9(1), 65 (1976).

Bostick, W. D., Lovelace, R. C., and Burtis, C. A., "Enzymatic Determination of Ammonia with a Miniature Centrifugal Fast Analyzer," in press, Water Research (1976).

Carr, P. W., Bostick, W. D., Canning, L. M., Jr., and Collicott, R. H., "Biochemical and Clinical Applications of the Temperature and Flow Sensitivity of Thermistors," Amer. Lab. 8, 45 (1976).

Ausmus, B. S., Witkamp, M., Shriner, C., and Bostick, W. D., "Evaluation of Extraction and Analysis of ATP and Its Interpretation as an Estimate of Microbial Activity," submitted to J. Env. Qual. (1976).

Burtis, C. A., et al., Biochemical Technology Program Progress Report for the Period July 1-December 31, 1975, ORNL/TM-5167 (January 1976).

Burtis, C. A., Begovich, J. M., and Watson, J. S., "Factors Influencing Evaporation from Sample Cups, and Assessment of Their Effect on Analytical Error," Clin. Chem. 21, 1907 (1975).

Lakings, D. B.,* Waalkes, T. P.,* and J. E. Mrochek, "High-Resolution Liquid Chromatographic Analysis of Methylated Purine and Pyrimidine Bases in Transfer RNA," J. Chromatog. 116, 83 (1976).

Mrochek, J. E., Dinsmore, S. R., Tormey, D. C.,* and Waalkes, T. P.,* "Protein-Bound Carbohydrates in Breast Cancer. Liquid Chromatographic Analysis for Mannose, Galactose, Fucose, and Sialic Acid in Serum," accepted for publication in Clin. Chem. 22 (1976).

Mrochek, J. E., Jolley, R. L., Young, D. S.,* and Turner, W. J.,** "Metabolic Response of Humans to the Ingestion of Nicotinic Acid and Nicotinamide," submitted to Clinical Chemistry (1976).

Shumate, S. E., II, and Scott, C. D., "A Centrifugal System for Affinity Chromatography with Eluate Monitoring," accepted for publication in Clin. Chem. 22 (1976).

---

*National Institutes of Health, Bethesda, Maryland.

**Central Islip State Hospital, Central Islip, New York.

4.2 Oral Presentations

W. D. Bostick

"Simultaneous Determination of Silica and Phosphate in Water from a Single Experiment Using a Miniature Centrifugal Fast Analyzer," 27th Southwestern Regional Meeting, American Chemical Society, October 29-31, 1975, Memphis, Tennessee.

C. A. Burtis

"Historical Development and Concept of the Centrifugal Analyzer," Centrifugal Analyzer Workshop, American Society of Clinical Pathologists, Chicago, Illinois, September 20, 1975.

"Recent Developments in Centrifugal Analyzer Technology," Centrifugal Analyzer Workshop, American Society of Clinical Pathologists, Chicago, Illinois, September 20, 1975.

"The Centrifugal Analyzer - A New Tool in the Clinical Laboratory," Continuing Education Program, Veterans Administration Hospital, Birmingham, Alabama, October 29, 1975.

"The Analytical Effect of Sample Evaporation in the Clinical Laboratory," The Florida Section of the American Association of Clinical Chemists, Miami, Florida, November 14-15, 1975.

R. K. Genung

"Kinetic Assay for Gamma-Glutamyl Transpeptidase with the Centrifugal Fast Analyzer," Southeastern Meeting of the American Association of Clinical Chemists, Atlanta, Georgia, April 1976.

N. E. Lee

"Automated, High-Resolution Elution Electrophoresis. A Fast, Efficient Technique with Potential in the Clinical Laboratory," Beckman Instruments Company, Inc., December 18, 1975, Fullerton, California.

J. E. Mrochek

"Protein-Bound Carbohydrates in Breast Cancer. Liquid Chromatographic Analysis for Mannose, Galactose, Fucose, and Sialic Acid in Serum," Eighth Annual Symposium on Advanced Analytical Concepts for the Clinical Laboratory, Oak Ridge National Laboratory, March 25-26, 1976.

"Isoenzyme Analysis Based on Differences in Kinetic Parameters," 171st National Meeting, American Chemical Society, New York City, April 1976.

C. D. Scott

C. D. Scott and R. S. Melville, "Introduction to 8th Annual Symposium on Advanced Analytical Concepts for the Clinical Laboratory," Oak Ridge National Laboratory, Oak Ridge, Tennessee, March 1976.

"Some Advanced Techniques in Liquid Chromatographic Separations for the Biomedical Sciences," Seminar, Department of Chemistry, University of Iowa, Iowa City, April 1976.

C. D. Scott and R. K. Genung, "Serum Isoenzyme Analysis by Elution Electrophoresis," ACS Spring Meeting, New York, New York, April 1976.

"Advanced Technology for Health Care Delivery," University of Tennessee Engineering Science Society, Knoxville, February 24, 1976.

S. E. Shumate, II

"A Centrifugal System for Affinity Chromatography with Eluate Monitoring," Eighth Annual Symposium on Advanced Analytical Concepts for the Clinical Laboratory, Oak Ridge National Laboratory, March 25-26, 1976 .

INTERNAL DISTRIBUTION

1. Biology Library
2-3. Central Research Library
4. Document Reference Section
5-7. Laboratory Records
8. Laboratory Records-RC
9. ORNL Patent Office
10. S. I. Auerbach
11. M. L. Bauer
12. W. D. Bostick
13. K. B. Brown
14. C. A. Burtis
15. F. L. Culler
16. S. R. Dinsmore
17. B. Z. Egan
18. D. E. Ferguson
19. R. K. Genung
20. C. W. Hancher
21. W. F. Johnson
22. R. L. Jolley
23. N. E. Lee
24. T. A. Lincoln
25. S. E. Lindberg
26. R. C. Lovelace
27-31. J. E. Mrochek
32. J. B. Overton
33. W. W. Pitt
34. H. Postma
35. C. R. Richmond
36-45. C. D. Scott
46. W. D. Shults
47. S. E. Shumate
48. J. B. Storer
49. D. A. Sundberg
50. L. H. Thacker
51. D. B. Trauger
52. R. G. Wymer
53. W. K. Davis (Consultant)
54. J. C. Frye (Consultant)
55. C. H. Ice (Consultant)
56. R. B. Richards (Consultant)

EXTERNAL DISTRIBUTION

57-83. TIC, Oak Ridge, Tenn. 37830.
84. Research and Technical Support Division, ERDA-ORO.
85. Justin Bloom, ERDA, Washington, D.C. 20545.
86. C. E. Carter, ERDA, Washington, D.C. 20545.
87. Dr. Morris Cranmer, NCTR, Jefferson, Ark. 72079.
88. Dr. James F. Dickson, NIGMS, NIH, Bethesda, Md. 20014.
89. C. W. Edington, ERDA, Washington, D.C. 20545.
90. J. L. Fasching, Dept. of Chemistry, U. of Rhode Island, Kingston, R.I. 02881.
91. C. R. Fisher, ERDA, ORO, Oak Ridge, Tenn. 37830
92. Dr. Arthur Karmen, Hospital of Albert Einstein College of Medicine, 1825 Eastchester Road, Bronx, N.Y. 10461.
93. Dr. T. D. Kinney, Dept. of Pathology, Duke Univ. Medical School, Durham, N.C. 27706.
94. Dr. Ruth Kirschstein, Director, NIGMS, NIH, Bethesda, Md. 20014.
95. D. G. Lakomy, 612 Hertel Avenue, Buffalo, N.Y. 14207.
96. Carl Larson, Office of Life Sciences, NASA Headquarters, 600 Independence Ave., Washington, D.C. 20546.
97-101. Dr. Carolyn Leach, NASA, Johnson Space Center, Houston, Tex. 77058.
102. Dr. J. L. Liverman, ERDA, Washington, D.C. 20545.

103-112. Dr. R. S. Melville, NIGMS, NIH, Bethesda, Md. 20014.
113-117. Dr. Harvey Mohrenweiser, NCTR, Jefferson, Ark. 72079.
118. Dr. James V. Neel, Dept. of Human Genetics, Univ. of Michigan Medical School, 1137 E. Catherine St., Ann Arbor, Mich. 48104.
119. W. Z. Penland, Jr., NCI, NIH, Bethesda, Md. 20014.
120. R. Rabin, ERDA, Washington, D.C. 20545.
121. S. P. Vinograd, Scientific and Technical Information Div., NASA, Washington, D.C. 20545.
122. Dr. T. P. Waalkes, NCI, NIH, Bethesda, Md. 20014.
123. R. W. Wood, ERDA, Washington, D.C. 20545.
124. Dr. D. S. Young, Clinical Center, NIH, Bethesda, Md. 20014.